

UNIVERSITY OF CAPETOWN
DEPARTMENT OF CIVIL ENGINEERING

*Considerations of Mineralogy and Permeability Testing of
selected Sand/Bentonite Mixes*

A thesis presented in partial fulfilment of the requirement for the degree of

Master of Science in Civil Engineering

by

Boné Makgekgenene

Supervisor: Dr. F Scheele

2008

The copyright of this thesis vests in the author. No quotation from it or information derived from it is to be published without full acknowledgement of the source. The thesis is to be used for private study or non-commercial research purposes only.

Published by the University of Cape Town (UCT) in terms of the non-exclusive license granted to UCT by the author.

DECLARATION

I, Boné Makgekgenene, declare that this thesis is my own work. It is submitted as a requirement towards the degree of Master of Science in Engineering to the University of Cape Town. All supporting information and data used in this thesis has been appropriately referenced and acknowledged.

Signed by candidate

.....

Boné Makgekgenene

Datedday of2008

DEDICATION

Letshopa...“just persevere you will get there”.

Ke a leboga Kgabo

Ntatemogolo: Rre Lemme Makgekgenene

Nekere e akolwa ke yo o emonang...I will remember that forever dad...

My Father: Rre Phenyo Ted Makgekgenene

SYNOPSIS

The disposal of municipal, commercial and industrial waste contained in near impervious lining systems still poses challenges in terms of sustainability and long-term durability.

This thesis assesses the engineering behaviour and chemical performance of selected Sand/Bentonite mixes to be used in the context of an environmentally inert landfill liner. Numerous test series in the laboratory focused on the permeability as a consequence of the physio-chemical characteristics of the selected mixes of two South African Bentonites and locally available sands. Several exploratory techniques (i.e. Cation Exchange Capacity; X-Ray Fluorescence; Scanning and Transmission Electron Microscopy) were employed to obtain the respective properties of the test materials.

A flexible membrane test setup in connection with the falling head principle was used to determine the permeability of the mixes. A wide variety of bentonite percentage mixes (by mass) and a range of confinement pressures were investigated. The testing schedule catered for high and low compaction energy levels, hence covering a wide range of densities of the barrier material.

The results of the exploratory techniques reveal valuable information on the quality and uniqueness of the two types of bentonites and allow comparative studies of their performance within a technical application.

In the context of permeability, the grain size distribution, all round pressure, compaction, hydraulic gradient, quantity and distribution of bentonite within a mix contribute immensely towards the coefficient of permeability of any sand/bentonite mix. A visual presentation of the interrelationship of bentonite content, density of the mixes, confinement and coefficient of permeability is presented.

ACKNOWLEDGEMENTS

Dr F Scheele: I would say it was the difficult times I experienced with my supervisor that I wish to treasure forever, the times when I could not see the complexity of a situation or problem at hand. I also have learnt that good times are rewards of what you have sacrificed during the year and a time to reflect what it is that you have achieved. I have had many good times with Doc, meaning I have worked hard for myself and achieved so many things. Also, the responsibility he bestowed unto me, as his student, to perform to the required standards. He has demonstrated that one confronts each problem in various ways and many of them are not easy to get by. He kept reminding me of why exactly I am here, why do I have to do this and that, without the slightest doubt in me, hence my confidence grew by the day. But it was at my quiet moments (alone), that I realise that his words shall echo in my mind forever. I pray to God and I wish I could have another chance to work under him, forever if possible because, I had great fun and at the same time I was able learn the best of Soil Mechanics. I would like to wish him and his family all the success and blessings in his retired life. Thank you Dr. Scheele.

My Parents: Dreams becomes true at the end, in between is a struggle that everyone experiences. Perhaps it was the hardships and sacrifice that has taught me to look far back into my life and realise that anything is possible. Keep moving forward and never give up the measures that God gives you. Thanks for being there, especially you mother... Kealeboga.

Dr J Rogers: I wish to thank him for the endless support in the geological research of my work. He has always been available for me and has given me wealth of information, guided by his continuous inspirational motive of deeper learning.

Lastly I wish to thank ***Jeffares and Green Consulting Engineers*** for their financial and technical support. Also I wish to thank ***Nuroo Ismail*** from the Knowledge Commons UCT Libraries, for her editorial assistance.

LIST OF FIGURES

Figure 1:	Three dimensional sketch of the structure of Smectite (Grim, 1968)	28
Figure 2:	Transmission electron micrograph of Smectite quasicrystals grouped together in a clay film (Laird, 2006).....	35
Figure 3:	High resolution transmission electron micrograph of individual layer within a Smectite quasi-crystal (Laird et al. 1989).....	36
Figure 4:	Schematic diagram depicting the break-up and formation of quasi-crystals (Laird et al., 1989).....	38
Figure 5:	Schematic diagram depicting demixing of Ca and Na (Laird, 2006).....	39
Figure 6:	Schematic diagrams depicting Co-volume swelling (Laird, 2006).....	40
Figure 7:	Flowchart of the mining process of Koppies Mine (Agnello, 2004).....	45
Figure 8:	Acid activation processing flow diagram (Agnello, 2004)	47
Figure 9:	Riversdale Geological Map: Mining locations of Cape Bentonite	51
Figure 10:	Illustration of X-ray Diffraction.....	58
Figure 11:	Schematic of Specimen Interaction in Transmission Electron Microscopy (Website: www.unl.edu).....	71
Figure 12:	Schematic of Technology of Electron Transmission Electron Microscopy (Website: www.unl.edu).....	72
Figure 13:	Schematic of configuration of Alkylammonium cations in the interlayer of 2:1 Phyllosilicates (Lagaly & Weiss, 1969)	73
Figure 14:	Initial Dry Density and Final Dry Density - Moisture Content of Phillipi Dune Sand/Envirobent mixes.....	106
Figure 15:	Initial Dry Density and Final Dry Density - Moisture Content of Klipheuwel Sand/Heidelberg Raw Bentonite mixes.....	107

LIST OF TABLES

Table 1: Landfill Size Classes (DWAF, 2008).....	7
Table 2: Relationship between Climate Water Balance, Site Specific Factors, Site Water Balance (DAWF, 2008).....	8
Table 3: Test Programme for Sand/Envirobent mixes regarding Compaction and Permeability	20
Table 4: Test Programme for Sand/Heidelberg Raw mixes regarding Compaction and Permeability	20
Table 5: Geotechnical properties of Philippi Dune Sand	24
Table 6: Geotechnical properties of Klipheuwel Sand.....	27
Table 7: Geotechnical properties of Envirobent.....	50
Table 8: Geotechnical properties of Heidelberg Raw Bentonite.....	56
Table 9: Chemical Composition of Natural Koppies Deposit Bentonite (Horn & Strydom, 2000)	65
Table 10: Chemical Composition of Envirobent (Reid, 2007).....	66
Table 11: Chemical Composition of Bentonite from the Heidelberg Deposit for Specific Applications (Horn & Strydom, 2000)	68
Table 12: Chemical Composition of Heidelberg Raw Bentonite (Reid, 2008).....	69
Table 13: Chemical Composition of Klipheuwel and Philippi Dune Sand (Reid, 2008).....	70
Table 14: Average basal spacing of Heidelberg Raw Bentonite and Envirobent.....	77
Table 15: Sand/Bentonite mixes for Cation Exchange Capacity testing	84
Table 16: Results of potential Cation Exchange Capacity	86
Table 17: Summary of Compaction of Mixes at 15 blows per layer.....	93
Table 18: Summary of Compaction of Mixes at 27 blows per layer.....	94

LIST OF IMAGES

Image 1: Map of Sand Dune Deposits on the West Coast (Compton, 2004)	22
Image 2: SEM image of Philippi Dune Sand, Magnification 10 000 (Waldron, 2008).....	23
Image 3: SEM of Klipheuwel Sand, Magnification 10 000 (Waldron, 2008)	25
Image 4: Scanning Electron Microscope of Envirobent, Magnification 3 000 (Waldron, 2006).	48
Image 5: Scanning Electron Microscope of Envirobent, Magnification 15 000 (Waldron, 2006)	49
Image 6: Scanning Electron Microscope of Heidelberg Raw Bentonite, Magnification 5 000 (Waldron, 2008)	55
Image 7: Scanning Electron Microscope of Heidelberg Raw Bentonite, Magnification 15 000 (Waldron, 2008)	55
Image 8: High resolution transmission electron micrograph of Envirobent (Jaffer, 2008) ..	78
Image 9: High resolution transmission electron micrograph of Envirobent after Hexal-Alkylammonium Cation treatment (Jaffer, 2008).....	79
Image 10: High resolution transmission electron micrograph of Heidelberg Raw Bentonite (Jaffer, 2008)	80
Image 11: High resolution transmission electron micrograph Heidelberg Raw Bentonite after Hexal-Alkylammonium cations (Jaffer, 2008).....	81
Image 12: SEM image of Klipheuwel Sand and Envirobent, Magnification 10 000 (Waldron, 2008)	89
Image 13: SEM image of Klipheuwel Sand/Heidelberg Raw bentonite mix, Magnification 10 000 (Waldron, 2008)	90

LIST OF GRAPHS

Graph 1: Grain Size Distribution of Philippi Dune Sand.....	24
Graph 2: Grain Size Distribution of Klipheuwel Sand	26
Graph 3: Grain Size Distribution of Envirobent (Divey, 2008).....	50
Graph 4: Grain Size Distribution of Heidelberg Raw Bentonite (Divey, 2008)	56
Graph 5: XRD Pattern of Envirobent.....	60
Graph 6: XRD Pattern of Heidelberg Raw Bentonite	60
Graph 7: Effect of sand type on compaction of mixes with Envirobent	91
Graph 8: Effect of sand type on compaction of mixes with Envirobent	91
Graph 9: Effect of sand type on compaction of mixed with Heidelberg Raw Bentonite	92
Graph 10: Effect of sand type on compaction of mixes with Heidelberg Raw Bentonite	92
Graph 11: Dry Density - Bentonite Content - Coefficient of Permeability of Philippi Dune Sand/Envirobent mixes.....	98
Graph 12: Dry Density - Bentonite Content - Coefficient of Permeability of Philippi Dune Sand/Envirobent mixes.....	98
Graph 13: Dry Density - Bentonite Content - Coefficient of Permeability of Klipheuwel Sand/Envirobent mixes.....	100
Graph 14: Dry Density - Bentonite Content - Coefficient of Permeability of Klipheuwel Sand/Envirobent mixes.....	100
Graph 15: Dry Density - Bentonite Content - Coefficient of Permeability of Philippi Dune Sand/Heidelberg Raw Bentonite mixes.....	102
Graph 16: Dry Density - Bentonite Content - Coefficient of Permeability of Philippi Dune Sand/Heidelberg Raw Bentonite mixes.....	102
Graph 17: Dry Density - Bentonite Content - Coefficient of Permeability of Klipheuwel Sand/Heidelberg Raw Bentonite mixes.....	104
Graph 18: Dry Density - Bentonite Content - Coefficient of Permeability of Klipheuwel Sand/Heidelberg Raw Bentonite mixes.....	104
Graph 19: Initial Dry Density and Final Dry Density - Moisture Content of Phillipi Dune Sand/Envirobent mixes.....	106
Graph 20: Initial Dry Density and Final Dry Density - Moisture Content of Klipheuwel Sand/Heidelberg Raw Bentonite mixes.....	107

LIST OF PHOTOS

Photo 1: Koppies Mine in the Free State (www.gwbase.co.za).....	43
Photo 2: Mining of the Heidelberg Raw Bentonite	54
Photo 3: Heidelberg Raw Bentonite	54
Photo 4: Pan Alytical PW 3830 X-Ray Diffractometer.....	59
Photo 5: Preparation of Briquette for X-Ray Fluorescence Analysis	64
Photo 6: Envirobent and Heidelberg Raw Bentonite samples embedded in resin.....	75
Photo 7: Diamond Cutter Machine	75
Photo 8: Transmission Electron Microscope	76
Photo 9: Atomic Absorption Spectrometer.....	84
Photo 10: Preparation of samples for CEC testing	85
Photo 11: Solutions of the different samples after centrifugation and filtration.....	85
Photo 12: Falling Head Permeability test apparatus	95

TABLE OF CONTENTS

DECLARATION.....	I
DEDICATION	II
SYNOPSIS.....	III
ACKNOWLEDGEMENTS	IV
1. INTRODUCTION	1
2. OBJECTIVE AND OUTLINE OF RESEARCH.....	4
3. LITERATURE REVIEW	5
4. RESEARCH MATERIALS.....	19
4.1 Philippi Dune Sand.....	21
4.1.1 Geotechnical properties and fabric.....	22
4.2 Klipheuwel Sand.....	25
4.2.1 Geotechnical properties and fabric.....	26
4.3 Bentonite	27
4.3.1 Smectite minerals.....	28
4.3.2 Montmorillonite	29
5. GEO-CHEMICAL CHARACTERISTICS OF BENTONITES.....	31
5.1 Electrolyte Systems and Cation Exchange.....	31
5.2 Exchange Capacities of the Clay Minerals	31
5.3 Swelling of Bentonite	34
6. SELECTED SOUTH AFRICAN BENTONITES	42
6.1 Koppies Bentonite.....	42
6.1.1 Geology of Koppies Bentonite Deposits.....	42
6.1.2 Mining Process.....	44
6.1.3 Geochemical Effects of Acid Activation	45

6.1.4 Geotechnical properties and fabric.....	48
6.2 Heidelberg Bentonite (Raw)	51
6.2.1 Geology of Heidelberg Bentonite Deposits	52
6.2.2 Mining Process.....	53
6.2.3 Geotechnical properties and fabric.....	55
7. GEOCHEMICAL INVESTIGATIONS OF RESEARCH MATERIALS....	57
7.1 X-Ray Diffraction	57
7.1.1 Theoretical background of X-Ray powder diffraction	57
7.1.2 Objectives of X-Ray diffraction of Bentonites	58
7.1.3 Sample preparation	59
7.1.4 Results of XRD analysis and discussion.....	60
7.2 X-Ray Fluorescence (XRF)	63
7.2.1 Theoretical background of X-ray Fluorescence	63
7.2.2 Objective of X-ray Fluorescence analysis.....	64
7.2.3 Sample preparation	64
7.2.4 Results of XRF analysis and discussion.....	65
7.3 Transmission Electron Microscopy (TEM)	71
7.3.1 Theoretical background of Transmission Electron Microscopy	71
7.3.2 Objective of Transmission Electron Microscopy.....	73
7.3.3 Alkylammonium method	73
7.3.4 Synthesis of Alkylamine Hydrochlorides	74
7.3.5 Preparation of Alkylammonium-saturated clay samples	74
7.3.4 Results of TEM and discussion.....	77
7.4 Cation Exchange Capacity (CEC)	82
7.4.1 Objective of Cation Exchange Capacity	82
7.4.2 Atomic Absorption Spectrometry (AAS).....	83
7.4.3 Procedure and characteristics	84
7.4.4 Results of CEC and discussion	86
8. GEOTECHNICAL INVESTIGATION OF SAND/BENTONITE MIXES	88
8.1 Compaction.....	88
8.2 Fabric of Sand / Bentonite Mixes.....	88
8.3 Summary of Compaction Results.....	90
8.4 Discussion and Analysis.....	93

9. HYDRAULIC CONDUCTIVITY.....	94
9.1 Hydraulic Conductivity and Gradient.....	94
9.2 Falling Head Permeability.....	95
9.3 Summary of Permeability Testing	97
9.4 Discussion and Analysis.....	105
10. CONCLUSIONS	108
REFERENCES	116
APPENDICES	123
Appendix 1.....	Error! Bookmark not defined.

1. Introduction

Traditional designs and construction of landfill repositories relied on the properties of the aquifer to ameliorate contaminates. However, with the ever growing production of potentially hazardous substances and their adverse impact on the receiving aquifers, the approach became environmentally unacceptable. The design and construction of modern landfills now focuses in mitigation and containment of leachate migration. Therefore, legislation in many countries around the world, have enforced a minimum requirement of a permissible separation of waste and aquifer founding landfills. The directives are to select cost effective materials, guided by the conditions on site, methods of construction and ultimate use of the landfill. This approach has triggered innovative research methods and exploratory techniques into the design and construction of landfills to suit modern life demands.

The aim of this research is to investigate the engineering behaviour and geo-mechanical properties of materials selected for the use of hydraulic barriers, which may be applied as hydraulic barriers. In the context of the objectives outlined by this research, the mineralogical properties and permeability Sand/Bentonite mixes are explored and presented.

The chemical composition and effects of leachate emanating from landfills have the potential and ability to undermine the integrity and performance any new age technological materials selected as hydraulic barriers. Therefore, many researchers in the classical field of Geotechnical Engineering have opted to extend their investigative parameters and expand their objectives, by exploitation of knowledge of Chemists, Physicists and Geochemists. The idea is to access and use their research techniques to strengthen their investigative methodologies. The combination of the information resulting from these diverse fields forms the fabric of the approach adopted in this research.

Bentonite is a highly sought after naturally occurring material, has been studied and applied in many technical scenarios over the years. Its popularity and selection revolved around its geological properties. These unique properties include swelling,

consistency, workability which constitute towards lowering the hydraulic conductivity of permeates to levels near imperviousness. This is mainly due to the morphology and layered structure of the clay mineral. The clay occurs in many parts of the world, namely North America, Europe and in Africa. In South Africa, deposits are found in the Free State Province and in Western Cape Province.

For the purposes of this research, two local bentonites were used, namely Envirobent and Heidelberg Raw Bentonite. Envirobent is a commercially available product from the Koppies deposit in the Free State Province whilst Heidelberg Raw Bentonite from the Heidelberg deposit in the Western Cape Province. The bentonites were mixed at various percentages (by mass), with local sands, namely Phillipi Dune Sand and a weathered Cape Granite, Klipheuwel Sand.

A flexible wall test setup in connection with the falling head principle was designed and implemented. The setup accommodated six permeameters running concurrently. The mixes were compacted at a higher energy level and lower energy levels to cover a wide range of densities similar to those obtained in major field works. Various all-around pressures were applied to simulate the in-situ stress conditions experienced by the sand/bentonite liners. The permeability test programme covered twenty eight different Sand/Bentonite mix samples, spanning over 14 months of continuous testing. Other parameters such as, hydraulic gradient, hydration periods, thermal conditions within laboratory conditions were monitored. Field conditions are very difficult to simulate and laboratory testing are challenging.

The results of the geotechnical testing programme, supported by the scientific findings from various laboratories of the University of Cape Town have revealed a wealth of information. These involved Scanning and Transmission Electron microscopy, X-Ray Diffraction, X-Ray Fluorescence, Cation Exchange Capacity. The results are discussed and summarised within this thesis.

In general, the hydraulic conductivity of a barrier depends on the grain size distribution, chemical composition and most importantly the quality of the bentonite for any combination of sand/bentonite mixes. The geo-physical properties of the sand

such as shape, surface texture and quantity of fines are characteristic properties which control the engineering behaviour of the selected Sand/Bentonite mixes.

2. Objective and Outline of Research

- To adopt exploratory investigative techniques to understand the geochemical properties and morphology of a commercially available treated Bentonite and a selected untreated Bentonite for the application as a landfill liner.
- To study the physico-mechanical properties and fabric of sands suitable for the selection of Sand/Bentonite mixes used in hydraulic barriers.
- To determine the coefficient of permeability of different Sand/Bentonite mixes using two geologically independent Bentonites mixed with local sands of various densities subjected to a wide range confinement stresses.

3. Literature Review

Waste Disposal and Lining Systems

Traditionally, landfills operated on the dilute and attenuate principle. This principle allowed leachate to leak from sites into the underlying strata where contaminants would be attenuated by a suite of physical, biological, and chemical processes. The principle relied on the exploitation of the properties of the aquifer to ameliorate the potential impact of leachate on nearby water resources. However, with the ever growing production of potentially hazardous substances and their adverse impact on the receiving aquifers, this principle becomes environmentally questionable as society realised the consequences of contamination of the environment and possible threats to their lives. This approach changed and the design and construction of landfills is now solely based on the concept of “concentrate and containing” of waste (Thornton et al., 1999). This idea solely relies on the physical separation between the waste body and the founding ground conditions.

Contamination of aquifers has led legislation to enforce minimum requirements of permissible separation of waste and aquifers founding landfills. This separation involves a technically designed lining system, approximately 2m thick, incorporating the use of multilayers of both natural and synthetic materials. The consequences of the approach, with the ever increasing construction cost, have imposed various challenges to the innovative applications and performance of the lining materials.

Lining systems are designed and implemented to act as impervious barriers to the migration of leachate into the ground water table and aquifer. The liner system must also meet the requirements stipulated by environmental conditions such as climate conditions, ground water tables and geological conditions on site. The liner system must also minimise the release of landfill gases and be resistant to the adverse effects of the variety of chemical properties of the leachate throughout the life time of the landfill.

Furthermore, the focus is on a sustainable society, municipalities, environmental frontiers and design engineers across the world have been pressured to look into new directives concerning the different classes of waste repositories, hence different leachate production resulting in various degrees of contamination. Allen (2000) suggests that construction of sustainable landfills and their operational life thereof should be guided by the principles postulated by this phrase:

Safe disposal of waste within a landfill and its subsequent degradation to the inert state in the shortest possible time-span, by the most financially efficient method available and with minimal damage to the environment.

In order to achieve this, Allen (2000) further stresses that a sustainable waste management philosophy should encompass a reduction in the generation of waste, waste streaming at source, recycling and reuse of waste, pre-treatment of waste to minimise quantity and volume. Sällfors et al. (2001) suggests that a possible strategy is to create waste repositories that will remain intact over a long period of time and which will not require any repairs or maintenance in the future.

Internationally, landfill regulators have made the installation of artificial lining systems and impermeable cappings mandatory for all landfills. An exception for sites possessing natural characteristic properties of these artificial lining systems can be granted. Artificial lining materials typically consists of sheets of synthetic membranes, such as High Density Polyethylene (HDPE) sheets of various textures and thickness, Geosynthetic Clay Liners (GCL) and Bentonite Enriched Soils. All these lining material are combined in layers of various thicknesses to form a base for receiving waste. With these ideas in mind, the design, construction and operation of modern lining system relies on solutions embracing technological research, social anthropology and environmental aspects.

Classification of Landfills

In South Africa, classification of landfills focuses on the amount of waste it receives and the consequent size of the operation. This relates to the size of the population served. The impacts of a landfill, i.e. the minimum requirements applicable to the site

and the resources required to control them, will be dictated by the size of the operation and lifetime of the landfill (DWAF, 2008).

Considering time and growth, landfills are classified using the Maximum Rate of Deposition (**MRD**). This is simply the projected maximum annual rate of waste deposition, expressed in tonnes per day during the expected life of a landfill (see Table 1).

Landfill Size Class		(MRD)* t/day
Communal	C	<25
Small	S	25 < x < 150
Medium	M	150 < x < 500
Large	L	> 500

* Maximum Rate of Deposition

Table 1: Landfill Size Classes (DWAF, 2008)

Based on international waste groups, waste is grouped into nine classes. These waste types are rated according to the toxicity of the generated leachate to humans, environmental degradation and other criteria. The wastes have different treatment, disposal requirements and are divided into two major categories. **H:H** landfills accept all waste rated extremely hazardous waste and **H:h** accept high hazard to low hazard waste (DWAF, 2008).

To avoid water pollution, it is essential that leachate generation from landfills be managed by means of leachate collection and treatment systems. DWAF, (2008) points out three factors that are used to determine potential leachate generation in landfills.

- Site Water Balance. This is affected by such factors as rainfall, evaporation, moisture content of incoming waste and water ingress into the waste body on account of poor landfill site selection, design and operation.
- Climatic Water Balance. This is used as the first step in determining the potential for significant leachate generation. This indicates whether the climate

in which a landfill is located will cause it to generate significant leachate or not, therefore it is a tool to alert the developer to the need to address leachate management in the landfill design and costing

- Site Specific Factors such as waste moisture content and ingress of runoff and ground water into the waste body must be taken into account.

A relationship between the Climatic Water Balance, Site Specific Factors and Site Water Balance is illustrated in Table 2.

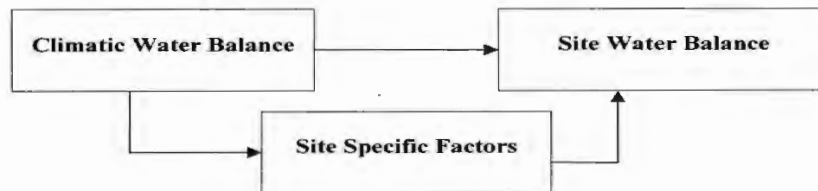


Table 2: Relationship between Climate Water Balance, Site Specific Factors, Site Water Balance (DAWF, 2008)

These parameters have led to the formation of ten classes of landfills. They are identified as follows: **G:C:B⁻**, **G:C:B⁺**, **G:S:B⁻**, **G:S:B⁺**, **G:M:B⁻**, **G:M:B⁺**, **G:L:B⁻**, **G:L:B⁺**, **H:h** and **H:H**. Of the ten landfill classes, eight cater for general waste and two cater for hazardous waste (DAAF, 2008).

In comparison to other countries e.g. Sweden, there are three main classes of landfills, grouped according to the type of waste they receive. Class 1 includes landfills with the highest risk to human health and the environment, whereas the classes 2 and 3 possess medium to low risk, respectively (Allen, 2000).

Bentonite

Bentonite is a name used to identify clays comprising the Montmorillonite mineral. The mineral is mostly valued for its crystalline structure responsible for swelling. It is a naturally occurring mineral that has been formed as a deposit of volcanic ashes at shallow wet sites in various locations around the world (Grim & Guven, 1978). These deposits are variable, depending on the nature of the volcanic ashes and the salinity of the water into which they were deposited. The swelling characteristics of bentonite

are essentially related to whether it is formed of Sodium Montmorillonite or Calcium Montmorillonite. In South Africa, both of these clays are available. Sodium Montmorillonite occurs in the Western Cape Province whilst, Calcium Montmorillonite occurs in the Free State Province. Across the world, in the USA, there is the Wyoming deposit, which is a highly swelling Sodium Montmorillonite and in parts of Europe e.g. Turkey there are deposits consisting mainly of Calcium Montmorillonite (Grim, 1968).

For the application of hydraulic barriers the selection of the bentonite that will be used as a mixture with the appropriate soil is based on several factors. These factors stem from the structure of the Montmorillonite mineral.

Montmorillonite is an aluminosilicate mineral with a 2:1 unit layer structure. Two structural units are involved in the atomic lattices of the clay minerals: one unit consists of two sheets of closely packed Oxygens or Hydroxyls in which Aluminium, Iron or Magnesium atoms embedded in octahedral coordination so that they are equidistant from six Oxygens. When Aluminium is present (dioctahedral), only two-thirds of the possible positions are filled to balance the structure, whilst if Magnesium is present (trioctahedral) all the positions are filled to balance the structure (Grim, 1968).

The second unit is built of Silica tetrahedrons. In each tetrahedron, a Silicon atom is equidistant from four Oxygens or Hydroxyls which balance the structure i.e. is arranged in the form of a tetrahedron with a Silicon atom at the centre. The resulting structure of the clay mineral (Smectite) is composed of units made up of two Silica tetrahedral sheets with a central Alumina octahedral sheet. All the tips of the tetrahedrons point in the same direction and are towards the centre of the unit. The tetrahedral and octahedral sheets are combined so that the tips of the tetrahedrons of each silica sheet and one of the Hydroxyl layers of the octahedral sheet form a common layer. The layers are continuous in the horizontal directions and are stacked one above each other in the vertical direction (Grim, 1968).

Grim (1968) states that oxygen layers are sandwiched in between the stacking of the Silica-Alumina-Silica units. Creating an outstanding feature where water and other polar molecules can enter causing the lattice expansion, i.e. swelling.

Laird (2006) describes swelling of bentonite as a complex process. Bentonites swell by allowing water or polar organic solvents between its quasi-crystals and between the individual layers within the clay. Swelling also occurs when small interlayer cations are replaced by larger organic cations or by larger polymeric hydroxyl-metal cations.

To fully understand the swelling of a specific Smectite it is necessary to know the entire system, including the amount of clay in the system relative to the liquid volume, properties of the clay (purity, surface area, layer charge) and morphology of the individual layers. The nature and distribution of exchangeable and non-exchangeable interlayer cations must also be known. The history of the sample, i.e. industrial treatment of the bentonite, mining process, storage, etc is equally important (Laird, 2006).

Discussions of theories addressing interlayer swelling and forces responsible for the behaviour of Smectites has been going on for years. These involve colloidal stability, electrostatic attractive and repulsion forces and clay-water interactions. The validity of the theories surrounding these concepts, especially the role of the van der Waals forces in colloidal systems, remains controversial (Low, 1980). Recently, several authors have suggested that osmotic swelling controlled by a long range Columbic attraction forces between the surfaces and counterions may be the fundamental explanation of Smectite swelling (Sogami & Ise, 1984; Smalley, 1994; Mc Bride, 1997; Mc Bride & Baveye, 2002).

However, Laird (2006) is of the opinion that, although there is a substantial body of evidence to support long-range double layer repulsion, the role of long range attractive forces is dubious for Smectite suspensions due to the challenges of propagating van der Waals interactions throughout an aqueous medium. Furthermore, the proposed long range Columbic attraction theory is also questionable because it does not appear to account for field electrostatic repulsions within the overlapping

diffuse regions of opposing double layers. This leaves unanswered questions into the nature of long-range attractive forces.

Six separate processes controlling swelling of Smectites in aqueous system are proposed by Laird, 2006. They are Crystalline Swelling, Double-Layer Swelling and Break-up of Quasi-crystals, Cation De-mixing, Co-volume Swelling and Brownian Swelling. It is believed that all these processes operate in concert towards the overall swelling of Smectites.

Geochemical Characteristic of Bentonite

The layer charge is also one of the criteria for the classifications of 2:1 clay minerals. Czimerová et al. (2006) suggested that layer charge is one of the most important parameters which determine material properties suited for industrial applications. These are related to the mineral structure and their composition is constant with reactive conditions over a wide pH range. There are few methods that are suitable for estimating layer charges.

Cation exchange capacity (CEC) is a measure of cations, which balance the negative charge sites of the clay (Tournassat et al., 2004; Czimerová et al., 2006). In pure Smectites, the CEC can accurately measure prominent permanent and variable charges, but admixtures may pose problems of consistency (Czimerová et al., 2006).

Layer charge may also be estimated from stoichiometric coefficients of structural formulae. The formulae are calculated from elemental analysis and are expressed as distributions of elements in the tetrahedral and octahedral sheets (Čičel & Komadel, 1994). The layer charge is estimated as the sum of non-equivalent substitutions occurring in the tetrahedral and octahedral sheets.

Unfortunately, this method is significantly influenced by relatively low deviations in the stoichiometric coefficients in the formula and may depend on approximations. Moreover, the coefficients of the structural formula are very sensitive to the presence of mineral admixtures and false assumptions (Laird et al., 1989, Czimerová et al., 2006)

Mermut and Lagaly (2001) have put forward the Alkylammonium method, which is based on the relationship between the arrangement of Alkylammonium cations intercalated in the interlayer spaces and the charge densities. The Alkylammonium method also provides information on the distribution of charges.

The method requires the preparation of a large set of samples and is insensitive to the presence of non-clay admixtures, but may be influenced by clay sized particles (Rühlicke & Kohler, 1981; Lagaly, 1994). Variations and modifications, as well as criticism of this method have been reported. It is concluded that this method requires further studies (Laird et al., 1989; Olis et al., 1990; Czimerová et al., 2006).

Bujdák & Komadel (1997) discovered a method that is based on molecular aggregation of cationic dyes for the characterisation of the layer charge. In this method, the charge density controls the distances between adsorbed dye cations. The amount and the type of dye molecular aggregates formed at the clay surface can be determined from ultraviolet spectra (Bujdák et al., 2002). The influence of the mineral admixture has not been observed, although the spectra may be very sensitive to the presence of some exchangeable cations (Czimerová et al., 2004).

Presently, the effects of other parameters on the accuracy of this method have not been evaluated. The dye spectra method is convenient and provides qualitative information but lacks in other aspects such as quantitative charge characterisations (Cenens & Schoonheydt, 1990; Czimerová et al., 2006).

South African Bentonites

In South Africa, the reserves of bentonite are in excess of 8Mt but not all of it is considered to be economically mineable (Agnello, 2004). Annual exploration and drilling programmes are typical of South African bentonite producers, although exploration is not pivotal to the success of the company. Cut-off grades are determined more so by overburden thickness than ore content and most operations work on a 10 year continuous mining plan. However, commercially available Bentonites in South Africa are treated either by soda ash addition or activation process so as to optimise swelling properties. A large proportion of the Koppies

Bentonite is acid-activated to enhance surficial properties. The activation process includes blunging, sulphuric activation and filtering (Agnello, 2004).

Acid-activation of clays refers to the controlled partial dissolution of the raw materials by mineral acids, resulting in clay protonation and amorphous hydrous silica phases (Komadel et al., 1996; Komadel, 1999; Tkáč et al., 1994; Gates et al., 2000). Treatment is required when clays are used in industry as catalysts during alkylation, dimerisation and polymerisation. This results in an increase in surface area and porosity. The most widely used acid-activated clays are the bleaching earths (Anderson & Williams, 1962; Siddiqui, 1968) which remove colours, odours and impurities from edible products (Gates et al., 2000).

Studies have shown that the type of Smectite and its composition influence dissolution rates during acid activation (Novák & Čičel, 1978). Typically, Magnesium rich trioctahedral Smectites dissolve much faster in inorganic acid than their Aluminium-rich dioctahedral counterparts (Komadel et al. 1996). Noyan et al. (2007) have shown that the crystallinity of the Smectite decreases when the mass-percentage of Sulphuric Acid in the acid treatment exceeds 10 percent. Furthermore, Madejová et al. (1998) used infrared spectroscopy to monitor the acid dissolution of various bentonites, with special reference to the effects of octahedral/tetrahedral substitution, the extent of dissolution and the nature of the reaction products.

Partial preservation of the original structure may result and the clay may perform to the desired characteristics but the effects are highly unpredictable and complex. Structures of non-clay minerals are not affected by activation process but may be present in the geological deposit of the clay mineral and, hence, further cause complications in the activated clay.

In conclusion, the exchangeable cations exchange sites and, to a lesser extent, structural cations of Smectites in a bentonite are removed by acid activation (Noyan et al., 2007; Komadel et al., 1997). The extent of structural decomposition is a function of length of treatment, temperature, type and concentration of the inorganic acid used. The mineralogy and chemical composition of the original is also crucial in the effects of acid treatment.

The application of acid treated clay minerals is highly popular in non-engineering applications such as pharmaceutical and edible products (Falaras et al., 1999; Morgan et al., 1985).

Sand/Bentonite Lining Systems

Research concerning the selection of the appropriate materials used in lining systems of landfills has been underway since the 1970's. Furthermore, a great deal of effort has been put into studying the performance of landfill liners constructed from synthetic materials especially Sand/bentonite mixtures. The general requirement of a material barrier is that the in-situ hydraulic conductivity should not exceed 1×10^{-9} m/s under 1m head of leachate (Cowland, 1990; Bremmer et al., 1992; Sällfors et al., 2001; Thornton et al., 1999). Due to various conditions stipulated by the site, population served and classification of the landfill in question this conductivity value may differ. In most cases, the maximum allowable hydraulic conductivity for a barrier material for a specific type of landfill is specified by the regulatory body or municipality.

The aim of this research is to investigate the engineering behaviour and geomechanical properties for the use of sand/bentonite mixtures as an appropriate lining system for hazardous waste landfills. Sand/bentonite mixtures are widely used as barriers to control the movement of liquids from waste disposal facilities because of their geomechanical properties. Stewart et al. (2003) states that sand/bentonite mixtures have high strength, low compressibility and very low hydraulic conductivities. This is achieved by using a mixture that contains competent sand particles that would ensure stability of the compacted mixture and bentonite to seal the voids between the sand particles. The sand accounts for the "skeleton" as it provides the mix strength and stability while the bentonite fills in the pores between the sand particles.

The sand is usually a local material and can vary from place to place within the area of interest. Some sands may contain high percentages of chemical components that effect the behaviour of the bentonite and hence the overall objective of the liner.

Other sands may be structurally unstable e.g. collapsible soils, and hence could introduce global differential instability within the lining system.

To design a sand/bentonite liner, it is necessary to firstly select a suitable soil and appropriate type of bentonite. Secondly, series of permeability tests must be performed to find the bentonite content yielding an adequate degree of imperviousness. A higher percentage of bentonite, by mass, tends to form around the sand grains, resulting in highly plastic mixtures, possessing difficulties during compaction (Sällfors et al., 2001). Kenney et al. (1992) reports that the hydraulic conductivity decreases rapidly as the bentonite content increases from 0 to 8%. Mixes with more than 8% bentonite content thereafter, the hydraulic conductivity becomes comparable to the hydraulic conductivity of bentonite, in view of the number of assumptions and conditions surrounding permeability testing.

Several investigators have studied how water content and compactive effort affects the hydraulic conductivity of sand/bentonite mixtures. Haug & Wong (1992) claimed that the moulding water content is not a critical factor in design and construction of sand/bentonite barrier layers because water is not required to break down lumps and facilitate remoulding as is required for clayey soils. Kenny et al. (1992) pointed out that the effects of bentonite distribution and hydration rates of a soil/bentonite mix are crucially important to the final hydraulic conductivity of any soil/bentonite mix.

Although a sand/bentonite mixture is mostly assumed to be a two phase material consisting of sand and bentonite gel, predictive models generally assume that the mixture is an “ideal mixture”. This assumption is based on the fact that bentonite particles have effectively embedded the sand particles as a homogeneous, continuous film and hence the final hydraulic conductivity is controlled by the properties of the bentonite (Chapuis, 1990; Kenney et al., 1992; Mollins et al., 1996).

“Ideal mixtures” depend on several physical factors such as mixing, gradation of the bentonite type and quality of bentonite. Sand/bentonite mixtures in a laboratory situation can be taken as “ideal mixes” but in practice this assumption remains questionable. Mostly, it is the uniform distribution of bentonite and the variation of the type of sand on site that causes concern. Chapuis et al. (2006) points out that, powder bentonites performs much better than granular bentonites because its finer,

dry particles provide a better coating efficiency. But in practice, finer bentonite particles can escape to the atmosphere and cause dust pollution, which can be environmentally problematic. Nowadays, ready mix sand/bentonite mixtures are available and are produced in automated pug mill plants (Webber & Williams, 1993).

Researchers have also noted that at high bentonite contents, the hydraulic conductivity of sand/bentonite mixes are fully controlled by the bentonite. Chapuis et al. (2006) confirm that once the bentonite exceeds a certain threshold there is little or no contact between sand particles, as the swelling capacity of the mixture is increased at the expense of the friction angle of the mixture. Greater amounts of bentonite tend to cause compaction difficulties which leads to instability of a liner (Sällfors, 2000). Mitchell (1993) suggests that a consistent fabric contributes immensely to the final hydraulic conductivity of a sand/bentonite mix.

Sällfors (2000) proposed that a theoretical hydraulic conductivity for sand/bentonite mixtures can be predicted. These theoretical values would augment experimental values and assist in understanding the variation of experimental hydraulic conductivity data. A parameter (k_f) which reflects the amount of bentonite per pore volume was introduced. The concept is based on the relative amount of bentonite in the voids between the sand particles and depicts the degree of compactibility of the mix. Different degrees of compaction drastically change the concentration of bentonite in the pore volume while the measured percentage of bentonite in the mix remains unchanged.

However, theoretical and experimental results will always differ in some respects. A conceivable explanation for the difference is that confinement stresses control the degree of saturation of mixes. Higher confinement pressures cause extended experimentation periods, whilst lower confinement stress could introduce experimental defects such as piping and flushing of fines from the compacted mould. The hydraulic gradients of permeability testing contributes to the flow of permeate within the mix, which depends on the experimental set-up and laboratory constraints.

In the theoretical model by Sällfors (2000), the mixture is assumed to be fully saturated, i.e. maximum swelling of bentonite and the distribution of the bentonite is

uniform within the mix. According to Kenny et al. (1992), there is a threshold value of bentonite content characteristic of the bentonite and sand used. Over 10% of bentonite (by mass), the hydraulic conductivity of sand/bentonite approaches theoretical conductivity values. However, this depends on the sand and most importantly the quality of bentonite. The final conductivity depends on the initial water content at compaction, compaction method, quality and amount of bentonite and grain size distribution of the sand (Sällfors, 2000).

In this research work laboratory permeability testing of sand/bentonite mixes are performed in flexible wall triaxial permeameters. Two sets of equations are used to determine the coefficient of permeability, the inflow permeability, k_{in} and the outflow permeability, k_{out} . The equations assume laminar flow of the permeate through the fully saturated sample and can be expressed as:

$$k_{in} = \frac{aL \ln\left(\frac{h_1}{h_2}\right)}{A(t_2 - t_1)} \quad 1$$

where h_i = head difference at any time t_i

A = cross-sectional area of specimen

a = cross-sectional area of standpipe

L = length of specimen

Using Darcy's law the outflow (Q) coefficient of permeability, k_{out} , is given by:

$$k_{out} = \frac{Q}{(iA)} \quad 2$$

where A = area of specimen

i = hydraulic gradient

Q = the measured outflow in time Δt

In summary, the hydraulic conductivity of a sand/bentonite mix relies on a number of variables. These are based on the specifications and desired level of performance. In practice, the magnitudes of variables are infinite because of the vast number of considerations and extent of different factors involved. These may include site conditions, design specifications, construction techniques and costs.

Within a research environment, many variables can be accommodated. The information gathered from them can be used to understand the intricacies of permeability testing of sand/bentonite liners. The emphasis of research is to explore, and predict the hydraulic conductivity of local sand/bentonite mixes and their engineering behaviour for practical applications.

4. Research Materials

The objective of this thesis is to investigate the geochemical and geotechnical properties of the following materials; the bentonites Envirobent, Heidelberg Raw and the two types of sand Philippi Dune Sand and Klipheuwel Sand. The geochemical tests were performed in various laboratories of the University of CapeTown i.e. the Department of Physics (Electron Microscopy Unit), the Department of Geological Sciences and the Department of Chemical Engineering. The prescribed procedures for the respective tests were followed during testing. However, a short summary of each test would be beyond the scope of this write-up. Only procedures which are more complex are briefly provided in the thesis.

The geotechnical tests were performed in the Geotechnical Laboratory of the Department of Civil Engineering at the University of Cape Town. In Table 3 and 4, the test programmes of the compaction and permeability series for this research are shown. Compaction tests were done according to AASHTO T-99 and ASTM D698. Falling Head permeability tests were performed according to ASTM D5084.

Complimentary tests such as Atterberg Limits (ASTM D4318), Free Swell test (ASTM D5890), Sieve Analysis (ASTM C117) and Specific Gravity test (ASTM D854-06) on the various materials were carried out concurrently during the research.

Scanning Electron Microscope (SEM)

The scanning electron microscope is a technique used extensively for the study of soil fabrics, particle shape, textures and to some extent the identification of minerals in soils. The technique provides an opportunity to give images at various and continuous ranges of magnifications (20× to 20000×). In this thesis, the SEM images were used as a tool to study all the different soil fabrics, the fabrics of Sand/Bentonite mixes, the surface textures, particle shapes and particles sizes and most importantly, a visual interpretation of the research materials could be undertaken. Electron microscopy was performed by the Electron Microscope Unit of the Physics Department.

Bentonite Type	Sand Type	Compaction Effort	Bentonite Content by mass (%)
Envirobent	Philippi Dune Sand	27Blows/ 3 layers	5
			7
			9
		15Blows/ 3 layers	5
			7
			9
Envirobent	Klipheuwel	27Blows/ 3 layers	3
			5
			7
		15Blows/ 3 layers	9
			3
			5
			7
			9

Table 3: Test Programme for Sand/Envirobent mixes regarding Compaction and Permeability

Bentonite Type	Sand Type	Compaction Effort	Bentonite Content by mass (%)
Heidelberg Raw Bentonite	Philippi Dune Sand	27Blows/ 3 layers	5
			7
			9
		15Blows/ 3 layers	5
			7
			9
Heidelberg Raw Bentonite	Klipheuwel	27Blows/ 3 layers	3
			5
			7
		15Blows/ 3 layers	9
			3
			5
			7
			9

Table 4: Test Programme for Sand/Heidelberg Raw mixes regarding Compaction and Permeability

4.1 Philippi Dune Sand

Coastal dunes and dune fields form areas where there is an adequate sand supply and sufficient wind energy to move the sand. The coastline of southern Africa possesses both these attributes and hosts many impressive coastal aeolian deposits (Compton & Franceschini, 2006).

As the waves of the predominant southwest swell break on Cape Town's beaches, the sand travels up the beach face in a skewed trajectory. The net effect is to send the sand northward in what is called longshore or littoral drift. This moving body of sand along the coast is in turn fed by rivers, as well as by coastal erosion and the breakdown of shells in the surf zone. Strong southeaster winds pick up fine sand exposed on the dried-out upper reaches of beaches and carry it inland to form sand dunes. These winds can carry, approximately one-third of the beach sand to form dunes, which in turn return sand back onto the land.

The dune sand is primarily composed of quartz grains and carbonatous shell fragments and white mussel (*Donax Serra*). The carbonate shell content reduces in quantity as most if it reacts with the acidic content in winter rains. The variation in grain size of the beach sand along a beach reflects the amount of wave energy received from the predominant swell (Compton & Franceschini, 2006). In Image 1 a map of sand dune deposits on the west coast is shown. The dune sand used in this research work was collected from an area called Philippi in the Cape Flats.

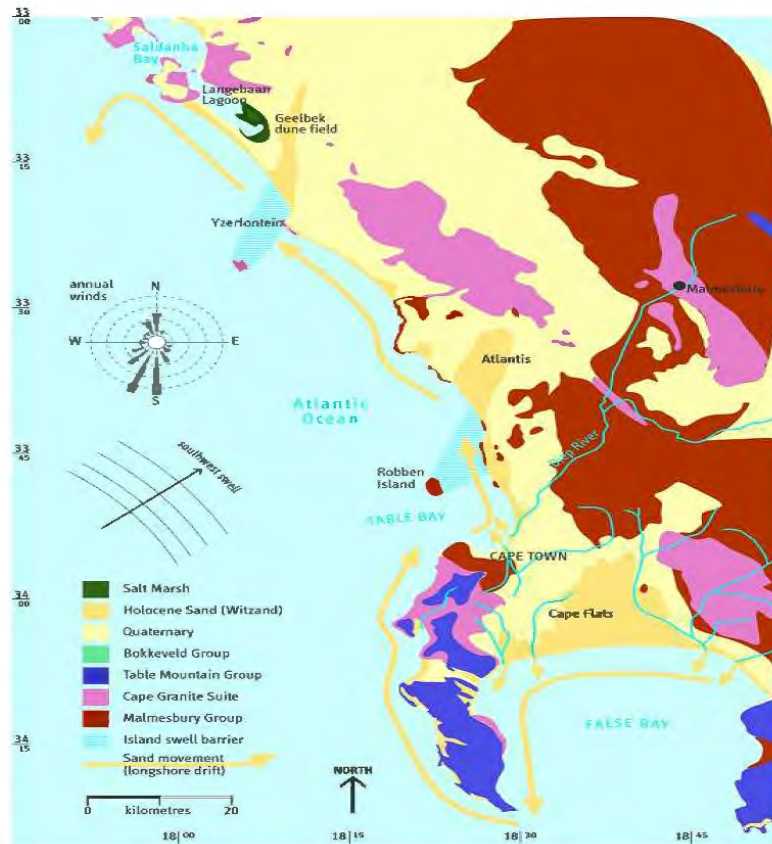


Image 1: Map of Sand Dune Deposits on the West Coast (Compton, 2004)

4.1.1 Geotechnical properties and fabric

An SEM image of Philippi Dune sand, is generally displaying the surface of the Quartz as shown in Image 2. The mineral particles appear smooth and well rounded, small pieces of broken shell fragments are seen to be hanging on to the surfaces of the larger particles. The grain size distribution is shown in Graph 1. The fabric of Philippi Dune sand consists of single grains with round shaped, smooth particles and scattered shell fragments. In Table 5 the geotechnical properties of Philippi Dune sand are listed.

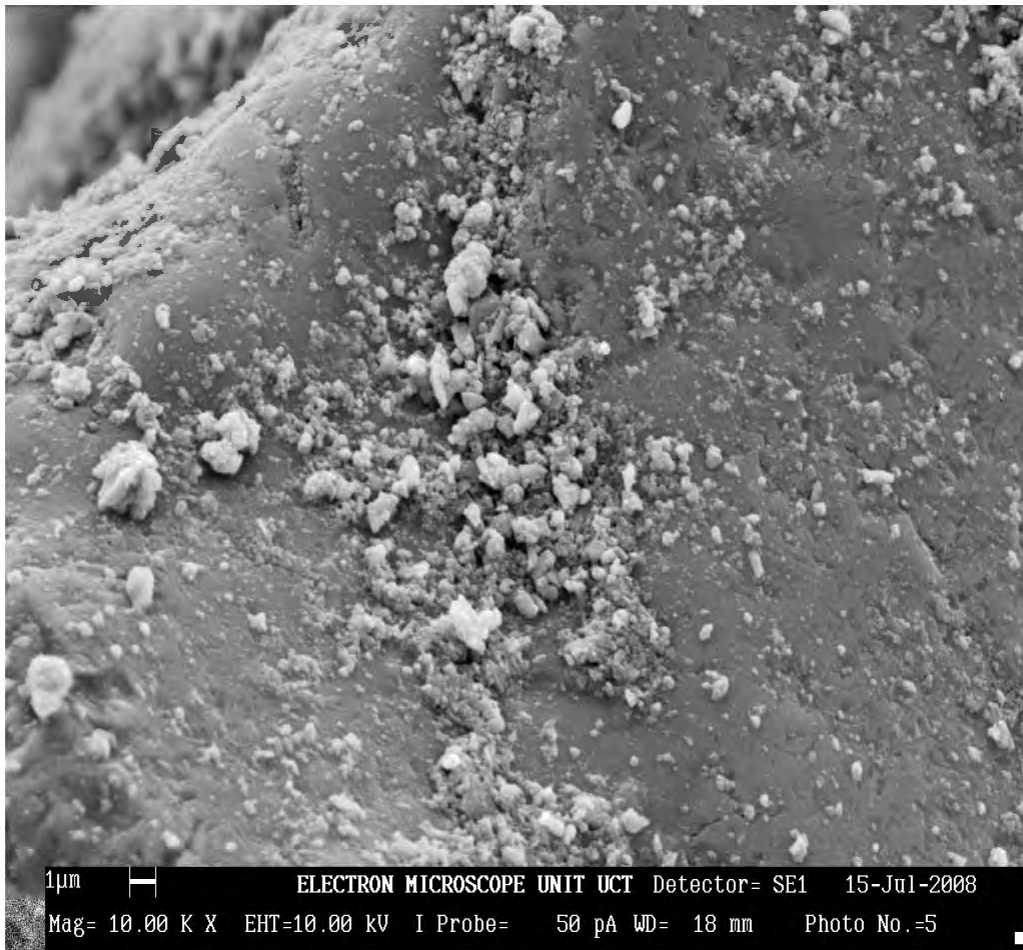
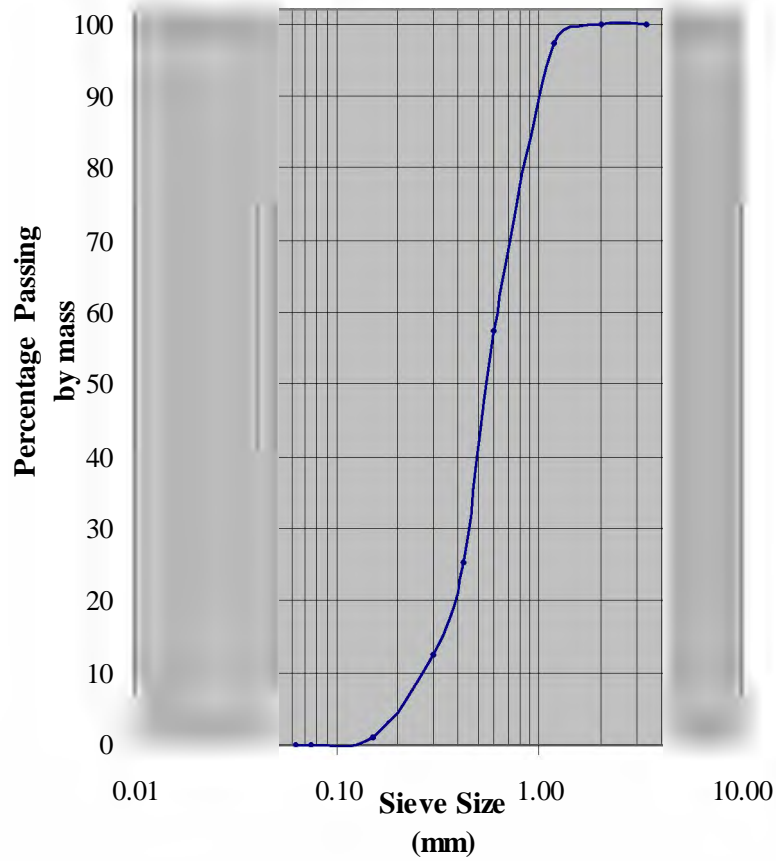


Image 2: SEM image of Philippi Dune Sand, Magnification 10 000 (Waldron, 2008)

Grain Size Distribution Curve of Philippi Dune Sand



Graph 1: Grain Size Distribution of Philippi Dune Sand

Property	Unit
Specific Gravity	2.67
Natural moisture content	3.1 %
Optimum moisture content	7.0 %
Maximum Dry density	1660 kg/m ³
Particle Range	0.063 - 3.35 mm
Mean Grain Size	0.53 mm
Coefficient of Uniformity	2.3
Coefficient of Gradation	1.16

Table 5: Geotechnical properties of Philippi Dune Sand

4.2 Klipheuwel Sand

Magma that is thought to have originated from the partial melting of ancient ocean (Adamastor) amalgamated into subsurface blobs that rose up buoyantly toward the surface, partially melting deep continental rocks along the way. This rising magma eventually intruded into and displaced Malmesbury rocks and accumulated along the edge of the continent. The magma began to cool and crystallise below the surface into a variety of different igneous rock types from Cape Agulhas north to Cape Columbine. Collectively, these are known as the Cape Granite Suite (Compton, 2004).

Klipheuwel sand is weathered Cape Granite. The sand appears as a colourless with pinkish and smoky gray particles of various grain sizes, shapes, surface textures and form. The mineralogy of Klipheuwel sand reveals a high Quartz content. This mineral is vitreous and exhibits no cleavage planes.

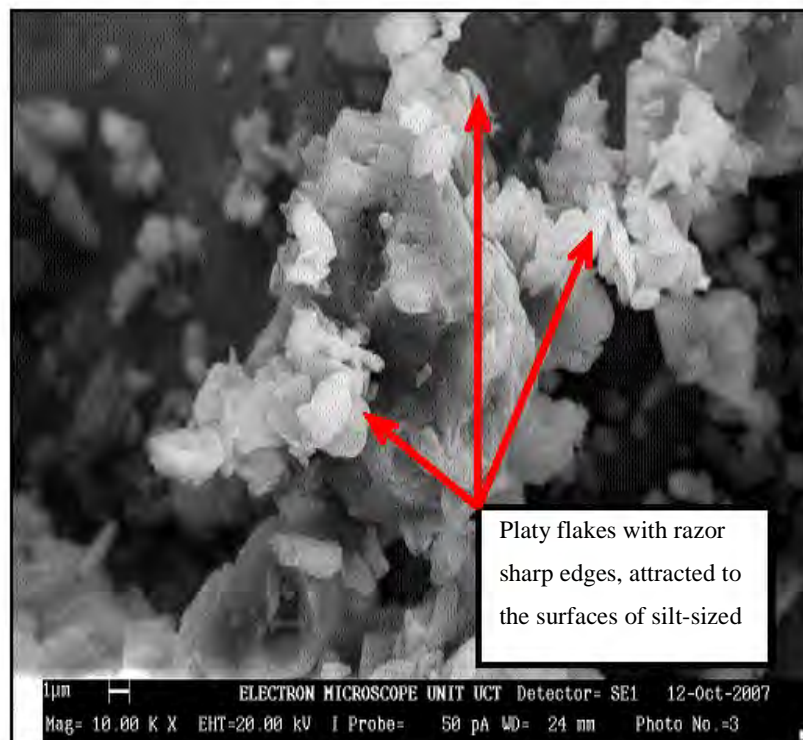
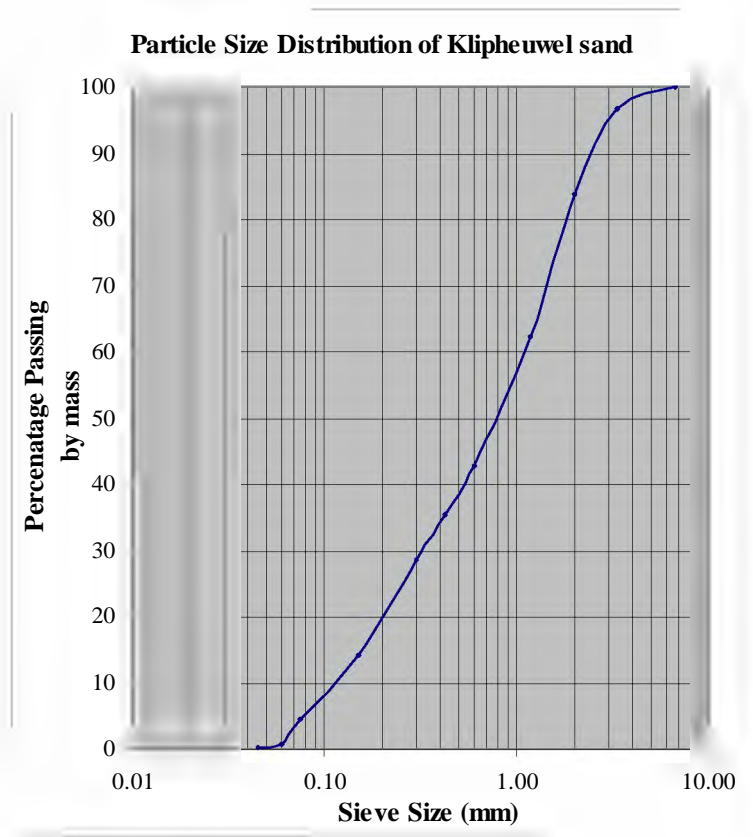


Image 3: SEM of Klipheuwel Sand, Magnification 10 000 (Waldron, 2008)

Image 3 is an SEM image of Klipheuvel sand, displaying sub-angular to irregular shaped particles. Ultra thin smaller fragments of Quartz cling to the surfaces of larger pieces. Mitchell (1993) suggests that surface attraction is mainly due to surface forces on the larger particles. The grain size distribution of Klipheuvel sand shows that there is a considerable amount of silt, particles in the range 20 μ m to 75 μ m and a small portion of clay sized particles which are less than 75 μ m.

Visually, Klipheuvel sand appears like a distribution of broken pieces of a larger particle to a finer particle grain size. This may also suggest that Klipheuvel sand has a multigrain fabric but multigrain arrangements form from silt-sized particles during sedimentation (Mitchell, 1993). It is concluded that Klipheuvel sand has a single grain fabric with considerable quantities of silt-clay sized particles. It is mined in a quarry near Malmesbury in the Western Cape.

4.2.1 Geotechnical properties and fabric



Graph 2: Grain Size Distribution of Klipheuvel Sand

Property	Unit
Specific Gravity	2.60
Natural moisture content	2.7 %
Optimum moisture content	9 %
Maximum Dry density	2100 kg/m ³
Particle Range	0.06-7 mm
Mean Grain Size	0.80 mm
Coefficient of Uniformity	10
Coefficient of Gradation	0.794

Table 6: Geotechnical properties of Klipheuwel Sand

4.3 Bentonite

The nomenclature and classification of clay minerals have been discussed for many years. Komadel (1999) suggests that clay minerals are microcrystalline materials of very fine particle sizes ($< 2\mu\text{m}$). Grim (1968) further explains that these naturally occurring crystallines can be divided into chain and layer structures and that their layer structures be divided into 2:1 and 1:1 families, with the names Triphormic and Diphormic.

In this thesis, the 2:1 type of clay mineral is investigated i.e. Smectite bearing mineral. Smectites are expandable layer silicates and are composed of two tetrahedral sheets separated by an octahedral sheet (Komadel, 1999). The Smectite minerals differ from Pyrophyllites as there is extensive isomorphous substitution for Silicon and Aluminium by other cations.

Aluminium in the octahedral sheet may be replaced by Magnesium, Iron, Zinc, Nickel, Lithium or other cations. Aluminium may replace up to 15 % of the Silicon ions in the tetrahedral sheet. Possibly some of the Silicon positions can be occupied by Phosphor (Grim, 1968). Furthermore substitution for Aluminium in the octahedral sheet may be one for one or three for two (since Aluminium occupies only two thirds

of the available octahedral sites) or in any combination from a few to complete replacement. The resulting structure, however, is either almost exactly dioctahedral or trioctahedral or a Saponite subgroup (Mitchell, 1993; Komadel, 1999; Grim, 1968).

Montmorillonite, the most common mineral of the group possesses a chemical composition as described below. The charge deficiencies that result from the isomorphous substitutions are balanced by exchangeable cations located between the unit cell layers and on the surfaces of particles (Mitchell, 1993). The negative charge of the layers, arising from the partial non-equivalent substitution of the central atom in the tetrahedral or in the octahedral e.g. Mg^{2+} for Al^{3+} in the dioctahedral or Li^+ for Mg^{2+} in the trioctahedral sheets is compensated by interlayer cations.

4.3.1 Smectite minerals

The minerals of the Smectite group have a prototype structure similar to that of Pyrophyllites, thus consisting of an octahedral sheet sandwiched between two Silica sheets, as shown diagrammatically in Figure 1.

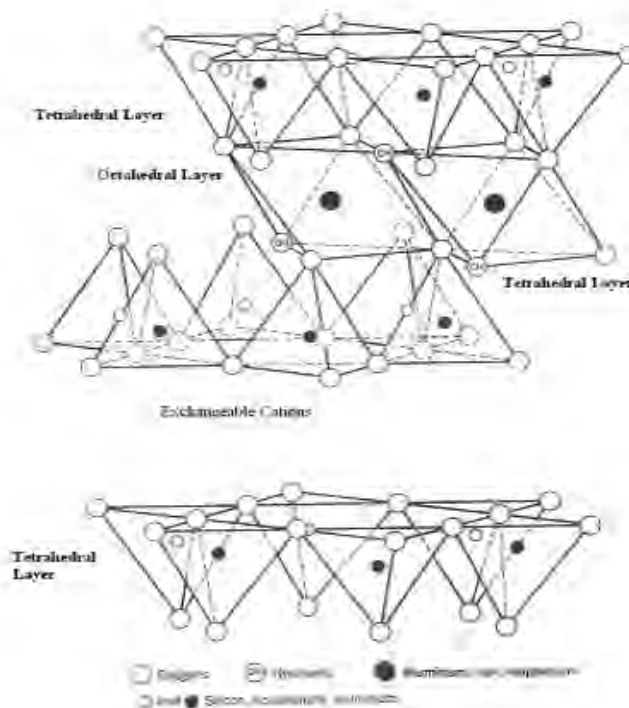


Figure 1: Three dimensional sketch of the structure of Smectite (Grim, 1968)

All the tips of the tetrahedron point towards the centre of the unit cell. The Oxygen forming the tips of the tetrahedra is shared by octahedral sheet as well. The anions in the octahedral sheet that fall directly above and below the hexagonal holes formed by the bases of the Silica tetrahedra are Hydroxyls (Mitchell, 1993).

The layers formed in this way are continuous and stacked one above the other. Bonding between successive layers is by van der Waals forces and by cations that are present to balance charge deficiencies in the structure. These bonds are weak and are easily separated by cleavage or adsorption of water or other polar liquids (Mitchell, 1993). The basal spacing in the vertical direction is variable ranging from about 9.6Å to complete separation. The structural configuration is stable and the corresponding charge distributions are electrically neutral. The name Montmorillonite is used for all clay minerals with an expanding lattice.

4.3.2 Montmorillonite

Individual layers or lamellae are about 10Å thick, but up to several orders of magnitude larger in the other directions. The long axes of the layers are usually less than 1µm or 2µm (Grim, 1968; Mitchell, 1993). Stable Montmorillonite unit particles are stacks of 1 to 16 lamellae (Sposito, 1984), although 2 to 3 lamellae is typical of Sodium Montmorillonite (van Olphen, 1991).

These unit particles can aggregate together to form clusters i.e. alignments caused by the platy nature of the unit particles (Pusch, 1999). Pusch (1999) suggests that Montmorillonite clusters can consist of possibly 10^7 to 10^9 particles Mitchell (1993) and Noyan et al (2007) suggest that the structural elements of Montmorillonite exist at several scales and can be arranged in the size order:

Unit layers (Lamellae) < Unit particle < Particle clusters

A representative volume of Bentonite consists of particles and voids which, arranged in the size order:

Interlayer pores < Interparticle pores (micropores)
<2nm) < Intercluster pores (mesopores 2 to 50nm and macropores >50nm)

Bentonite is a popular name of all clay mineral that consist mainly of the Montmorillonite mineral. Minor trace mineral such as quartz can exist in a sample. Exposure of Bentonite to water or even water vapour, results in surface hydration due to the attraction of water molecules to the clay surface (Steward et al., 2003). This is primarily an interlayer process due to the relative amounts of interlayer and external surface. Water uptake beyond this required to facilitate interlayer separation of about 1.2\AA results from diffuse double layer forces between the hydrated Montmorillonite unit layers (Yong, 1999; Steward et al., 2003).

The thickness of the water layer between the silicate units depends on the nature of the exchangeable cation at a given water-vapour pressure (Grim, 1968). Under ordinary conditions, Smectites with Sodium as the exchange ion frequently has one molecular water layer and a spacing of about 12.5\AA . With Calcium as the exchange ion, there are frequently two molecular water layers and spacing from about 14.5\AA to 15.5\AA . Therefore, Sodium possesses larger layer expansion properties. The expansion properties are reversible, although once the structure is completely collapsed by removal of all the interlayer polar molecules, re-expansion may be difficult (Grim, 1968).

In a Sodium Montmorillonite unrestrained double layer swelling can occur. The dispersion of the unit layers and formation of a gel phase is a homogeneous system with some rigidity and elasticity (Steward et al., 2003; van Olphen, 1991). However, complete dispersion of lamellae is sometimes prevented by the formation of stable regions where the lamellae are orientated essentially parallel to one another at a distance of about 100\AA possibly due to van der Waal forces or edge-face bonding of occasional non-aligned layers.

5. Geo-Chemical Characteristics of Bentonites

5.1 Electrolyte Systems and Cation Exchange

In dry clay, adsorbed cations are tightly held by the negatively charged clay particles. Cation in excess of those needed to neutralize the electronegativity of the clay particles and associated anions are present as salt precipitates. When the clay is placed in water, the precipitated salts go into an aqueous environment which supports cationic activity. The adsorbed cations produce higher concentrations near the surfaces of particles and try to diffuse away in order to equalise concentrations throughout. Mobility of the cations is restricted by the negative electric field originating at the particle surfaces. These movements of cations lead to ion distributions round the clay particles (Mitchell, 1993).

Grim (1968) suggests that in Calcium Montmorillonites, the adsorbed water is packed octahedrally about the Calcium cations and the addition of water results in the development of double layers of water which are superimposed as successive layers follow. In Sodium Montmorillonites increasing amounts of water develop successive layers of superimposed water molecules. However, it is the cation exchange capacity of the clay mineral that controls the role of cation activity, hence overall performance of the clay.

5.2 Exchange Capacities of the Clay Minerals

Cation exchange capacity (CEC) refers to the quantity of negative charges existing on the surfaces of clay. Clay minerals do not have a single fixed cation exchange capacity value. The typical values for different clay minerals fall within the range 1 to 150 meq/100g, whereas the range for montmorillonite bearing clay minerals is 80 to 150 meq/100g. These values of exchange capacity represent the amount of readily exchangeable cations that can be replaced easily by leaching with a solution containing other dissolved cations of higher replacing power than the absorbed cation (Mitchell, 1993).

Mechanisms of cation adsorption on a silicate surface of clay minerals have been described and illustrated by Sposito (1989). Inner sphere cations are ions that are held within the hexagonal 'hole' in the silicate surface with no water molecule between the surface and the cation. This is referred to as Ion Fixation. The outer sphere cations are in dissolution and are electro-statically absorbed on the surface. The outer sphere complex of the silicate surface houses readily exchangeable ions which control expansion of the layers (Mitchell, 1993).

Cation exchange occurs on the basal surfaces and along the edges of the broken flakes and elongations of the clays sheet layers. In Smectites and Vermiculate about 80% of the cation exchange occurs in the basal plane surfaces and the remainder is taking place on the edges (Grim, 1968).

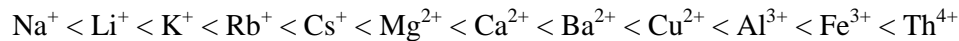
The rate of exchange varies within the clay mineral as a function of the nature and concentration of the cations and anions. In general, for non expandable clay minerals, e.g. Kaolinite, the exchange occurs rapidly and it is slower for Smectites and for Attapulgite as the penetration of dissolved cations between the layers of the Smectites or into the channels of Attapulgite requires more time (Grim, 1968). Cation replaceability also plays a major role in the capacity at which cations are exchanged.

A great deal of research on this problem has been reported, the idea is not yet completely understood (Grim, 1968). However, factors influencing replaceability of cations involve the following:

- Effect of concentration
- Population of exchange positions
- Nature of dissolved anions
- Temperature effects

Nonetheless, ions of one type can be replaced by ions of another type. For instance, Na^+ may replace Ca^{2+} and Fe^{3+} may replace Mg^{2+} , and so on. The ease of replacement depends mainly on the valence, relative abundance of the different ion types and ion size (Mitchell, 1993). Trivalent cations are held more tightly than divalent and

divalent cations are held more tightly than monovalent. A typical replaceability series is as follows:



Although there is no single universal replaceability series, it is possible to displace cations of high replacing power such as Al^{3+} by one of low replacing power such as Na^+ by mass action and, if there are differences in concentration of the ions of low replacing power relative to the ions of high replacing power (Mitchell, 1993).

Causes of cation exchange

Grim (1968) outlines the causes of the cation-exchange capacity of Montmorillonite, bearing clay minerals, addressing three processes:

- Broken bonds around the edges of the silica-alumina units gives rise to unsatisfied charges, which would be balanced by absorbed cations. The number of broken bonds and hence the exchange capacity due to this cause, would increase as the particle size decreased. In Smectites and Vermiculites, broken bonds are responsible for a relatively small portion ($\pm 20\%$) of the cation-exchange capacity. The remainder probably is resulting from substitutions within the lattice. Numerous investigations have studied in detail the character of the broken bonds on clay-minerals units (Grim, 1968).
- Substitutions within the lattice structure of the trivalent Aluminium for quadrivalent Silicon in the tetrahedral sheet and of ions of lower valence. Particularly Magnesium, for trivalent Aluminium in the octahedral sheet results in unbalanced charges in the structural units of some clay minerals. Sometimes such substitutions are balanced by other lattice exchanges i.e. OH for O, or by filling more than two thirds of the possible octahedral positions. However, frequently they are balanced by adsorbed cations. Exchangeable cations resulting from lattice substitutions are to be found mostly on cleavage surfaces, e.g. the basal cleavage surfaces of the layer clay mineral. Since the charges resulting from substitutions in the octahedral sheet would act through a greater distance than the charges resulting from substitutions in the

tetrahedral sheet, it would be expected that cations held because of the latter substitutions would be bonded by a stronger force than those held by forces resulting from substitutions in the octahedral sheet. In some cases, cations held by forces due to substitutions of Aluminium for Silicon seem to be substantially non-exchangeable e.g. the Potassium in the Micas. In the clay minerals, replacements in the octahedral layer are probably the major substitute causing cation-exchange capacity.

- The hydrogen of exposed hydroxyls may be replaced by a cation which might be exchangeable.

5.3 Swelling of Bentonite

Swelling of Smectites is a complex process (Laird, 2006). Smectites swell by taking in water or organic solvents between Smectites quasicrystals and/or between the individual layers within quasicrystals. Swelling also occurs when small interlayer cations are replaced by larger organic cations or larger polymeric hydroxyl-metal cations (Laird, 2006). Although this swelling of the lattice during hydration takes place in a step-wise fashion, each of the forms of swelling represents different processes and is controlled by different forces (Grim, 1968).

To fully understand the swelling of a specific Smectite sample it is necessary to know the entire system, including the amount of clay in the system relative to the liquid phase mass or volume, properties of the clay such as purity, surface area, layer charge and morphology of the individual layers. Furthermore, the nature and distributions of exchangeable, non-exchangeable interlayer cations within the clay, the quantity and activity of all solvents in the equilibrating solution should be determined. Literature further, points out that some phases of Smectites swelling are inherently hysteretic; hence the history of the sample is of vital importance (Laird, 2006).

In order to achieve this, the mechanisms supporting Smectite swelling, the nature and morphology of the quasicrystals must be studied and understood. In Figure 2, a transmission electron micrograph (TEM) of Smectite quasicrystals is shown.

Interpreting the micrograph, Laird (2006) suggests that the dark electron dense regions, seen in the micrograph, are the Smectite quasicrystals. The light regions are holes or micropores. Three important observations are derived from this image:

- The individual quasicrystals are generally curved, suggesting that they are flexible.
- Individual quasicrystals are joined together forming a continuous film of fabric.
- Joints between quasicrystals are both face-to-face and edge-to-edge.

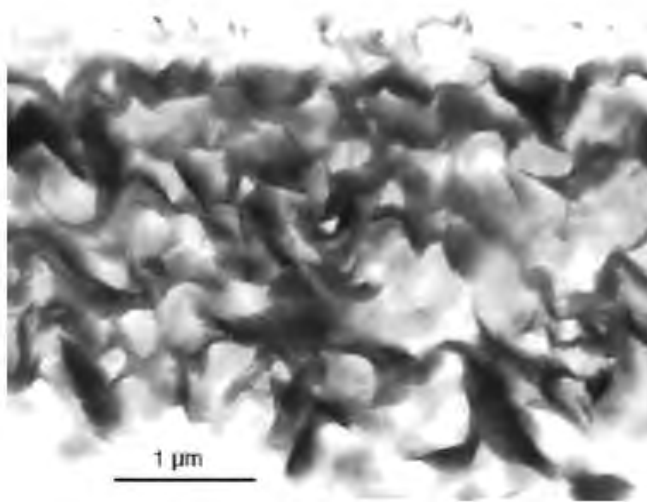


Figure 2: Transmission electron micrograph of Smectite quasicrystals grouped together in a clay film (Laird, 2006)

In Figure 3 a high-resolution TEM micrograph of the arrangement of individual layers within a quasicrystal is displayed. The layers appear to be slightly to moderately curved, again suggesting that the individual layers are flexible. Furthermore, some layers appear to terminate within the middle of a quasicrystal, while others extend beyond the main body of the quasicrystals. This observation suggests that the individual layers have been randomly stacked. Furthermore, it appears that some layers have peeled off of the main body of the quasicrystal hinting that quasicrystals are dynamic constantly moving around forming clusters and breaking up (Laird, 2006).

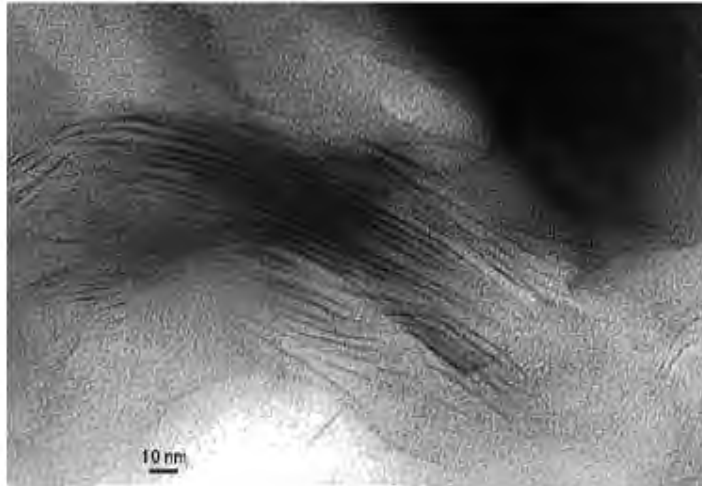


Figure 3: High resolution transmission electron micrograph of individual layer within a Smectite quasi-crystal (Laird et al. 1989)

With the help of electron microscopy, Laird (2006) suggests that there are six separate processes that control the swelling of Smectites in aqueous systems. These processes are summarised as:

Crystalline swelling

Crystalline swelling is a process whereby discrete layers of water molecules are drawn in within the individual 2:1 layers of the Smectite quasicrystal. The process is controlled by a balance between strong forces of attraction and repulsion.

The attractive potential energies are electrostatic and dominantly arise from the attractions between the negative surface charge sites and positively charged interlayer cations. On the other hand, repulsion potential energies are highly sensitive to changes in electrolyte chemistry. These forces emanate from the partial hydration of the interlayer cations found in the water molecules.

As more is intercalated into the layer of the Smectite, hydrated cations causes changes in the existing repulsive potential energies. As this sequence continues the repulsive forces overcome the attractive forces and energy is released during hydration. The resulting effect is a separation of the layers, i.e. swelling occurs.

During drying of the Smectite layer the opposite occurs, where the electrostatic attractive forces become dominant and pull the layers together (Norrish, 1954; Kittrick, 1969; Laird, 2006).

Double-layer swelling

Double-layer swelling is a process that occurs between quasicrystals (Laird, 2006). Most of the total surface charge on Smectites is expressed within the interlayers of quasi-crystals and does not participate in the formation of diffuse double layers (DDL).

However, a smaller portion of the total charge is expressed on the external surfaces of a quasi-crystal. The negative charge on an external surface forms one half of the electric double layer. The positive charge develops because exchangeable cations are weakly held by the external surfaces and tend to diffuse from regions of high concentration in the bulk solution. The diffusion of the cations is opposed by the electrostatic attraction between the positive charge of the cations and the negative surface charge. At the same time, anions from the bulk solution diffuse toward the regions of low anion concentration near the surface but are retarded by the electrostatic repulsion from the negatively charged surfaces. The separation of negative surface charges from the positive charge of the compensating cations in the diffuse portion of the double layer is responsible for the colloidal behaviour of Smectites in suspension (Laird, 2006).

Formation and break-up of quasi-crystals

When two Smectite quasicrystals approach each other in an aqueous suspension with sufficient kinetic energy to overcome the double layer repulsion, the diffuse portions of their layers fusion occurs (Laird, 2006).

As this occurs, anions, excess cations and water are expelled from the region between the two approaching surfaces. If the two surfaces approach close enough and have sufficient anions, the excess cations are expelled. During this process the electrostatic

forces will undergo a complete reversal from being repulsive to attractive. The result is that two quasicrystals join together to form large quasi-crystal.

On the other hand shaking or stirring may break a large quasi-crystal. These effects are more significant in Sodium and Lithium Smectites as complete delamination may occur. The resulting layers of Smectite may behave as separate colloids. In Figure 4 a schematic illustrating this concept is shown.

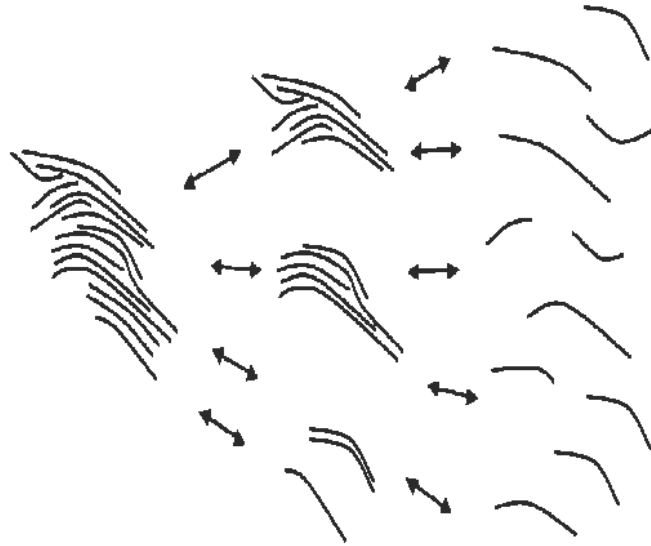


Figure 4: Schematic diagram depicting the break-up and formation of quasi-crystals (Laird et al., 1989)

Cation de-mixing

The nature of the exchangeable cation adsorbed on Smectite surfaces has a dominating influence on Smectite swelling behaviour. Smectites saturated with strongly hydrated monovalent cations like Sodium and Lithium readily swell.

When placed in distilled water or a dilute electrolyte solution, most quasi-crystals of low-charge in Na-Smectites will spontaneously break-up such that diffuse double layers form and separate the individual Smectite layers. For high-charge Na-Smectite, some quasicrystals will remain intact but most will at least partially break-up. The addition of kinetic energy i.e. stirring is usually all that is required to disperse a Na or Li-Smectite in distilled water. Calcium and Magnesium saturated Smectites when

placed in distilled water, typically expand from 15Å (air dry) to 19Å (distilled water), but the quasi-crystals do not spontaneously delaminate. Stirring will cause some quasicrystals to break up forming a suspension of smaller Calcium or Magnesium Smectite quasicrystals, although Calcium Smectites cannot be delaminated even by vigorous shaking (Laird, 2006).

When two different types of cation, for example Na and Ca, are present in an aqueous Smectite system, the Smectite may exhibit distinct preference for one cation over the other. Such cation exchange selectivity is governed by a complex feed back process, whereby the extent of crystalline swelling controls selectivity for one cation relative to another. Selectivity as well as the composition of the equilibrating solution controls the mix of cations in the interlayers. The mix of cations in the interlayers and the other clay cations and solution properties control the extent of crystalline swelling (Laird & Shang, 1997). For instance, in a Na and Ca-Smectite system, the demixing means that Na-ion will tend to be segregated in certain interlayers while the competing Ca-ions are segregated into other interlayers. When the clay is shaken, the quasi-crystals will readily break apart at interlayers dominated by Na. In Figure 5 an illustration of this concept is schematically shown.

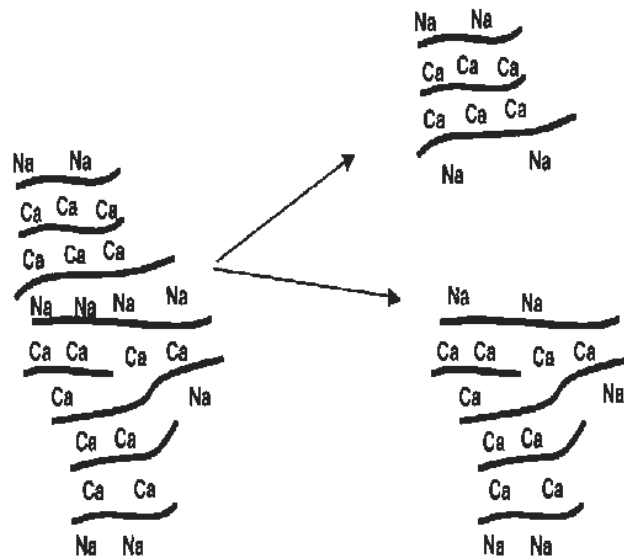


Figure 5: Schematic diagram depicting demixing of Ca and Na (Laird, 2006)

Co - volume swelling

Water molecules are constantly colliding with colloid particles in aqueous suspension. Each collision transfers kinetic energy from the water molecule to the colloid or vice-versa, resulting in colloid being in constant motion. If the collisions are unbalanced, a colloid will have net movement in one direction, thus diffusion occurs (Laird, 2006). However, colloids are also in constant rotational motion but because individual Smectite layers are anisometric, their longest dimension determines their minimum free rotating volume as seen in Figure 6 (A).

Furthermore, when two freely rotating Smectite layers approach each other, their first interaction will be due to the intersection of the diffuse portions of their double layers, which will result in a repulsive force before the layers actually touch. The effective rotational volume is determined by the longest dimension of the layer plus twice the length of the double layer as shown in Figure 6 (B).

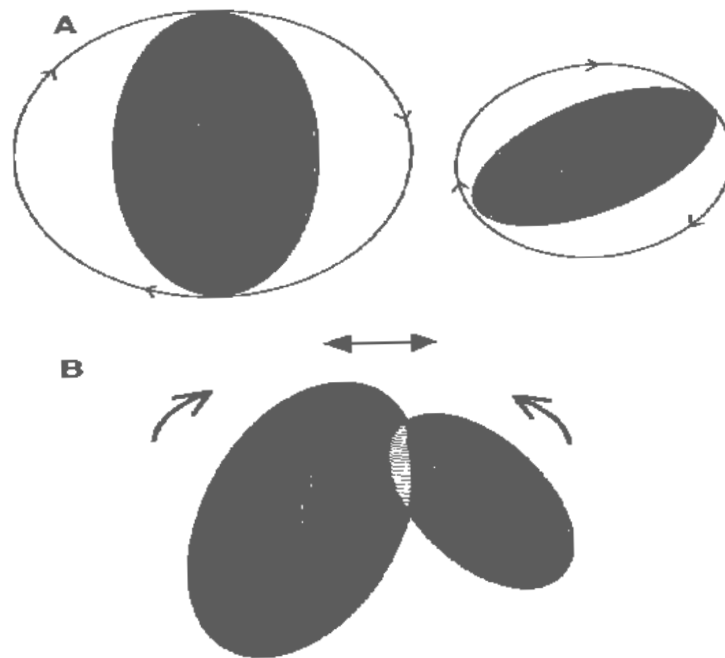


Figure 6: Schematic diagrams depicting Co-volume swelling (Laird, 2006)

Brownian swelling

Brownian swelling is the ultimate state of dispersion or delamination for a Smectite. In this process individual layers (in an aqueous suspension) are so widely dispersed that there is no interaction between the neighbouring layers. Due to random thermal motion individual layers are most likely to diffuse away from a zone of relatively high concentration to zones of low concentration. Brownian swelling of Smectites is an entropy driven process, which is not influenced by layer charge (Laird, 2006).

6. Selected South African Bentonites

In South Africa there are deposits of relatively pure Bentonite. These are found in Koppies in the Free State and in the Western Cape, near Heidelberg and Plettenberg Bay. Impure deposits are found in Mkuze in Northern Kwazulu Natal and in Wodehouse, near Jamestown, Eastern Cape (Agnello, 2004). For the purposes of this research samples of Bentonite from the Koppies deposit and Heidelberg deposit were studied.

6.1 Koppies Bentonite

Envirobent is a product name of a Calcium Montmorillonite bearing Smectite in the Koppies area. This product is a chemically modified natural clay mineral which is mined and distributed commercially. This product is used in important Civil Engineering (industrial) such as dam liners, wall barriers, etc and to a minor extent pharmaceutical applications

6.1.1 Geology of Koppies Bentonite Deposits

The largest deposits in South Africa occur in the Koppies District of the Northern Free State Province. Bentonite is currently being mined by G&W Base and Industrial Minerals (Pty) Ltd on Oceaan 64, Oceaan 99 and Blaauwboschpoort 13, located 6 km west-northwest of Greenlands siding near Koppies (Horn & Strydom, 2000). Boreholes drilled on Oceaan 64, Kronenbloem 513, Hattingh's Rus 68, the southern portions of Benshoop 22 and Zwartlaagte 321 as well as on Broodkop 30, intersected Bentonite deposits. Clay also occurs in palaeobasins around an inliner, which is reported to consist of Swazian-aged rocks, on Wittekoppies 169 and Bakenkop 415, 16 km south-southwest of Vredefort, also near Koppies.

Much of the Koppies area is overlain by a thick overburden of black, humic-rich Smectite-bearing topsoils. Schmidt (1976) mentioned four ore bodies in the area. During the 1950's when mining activity started in the Koppies area, Bentonite occurred at the ground surface. However, the Bentonite in the currently exploited

deposits is overlain by topsoil and micaceous shale of the Volksrust Formation of the Karoo Super Group in which lenses of fine grained sandstone are found in places (Purbrick, 1993).

The total thickness of overburden is variable, but rarely exceeds 12m. In general, the ore bodies are tabular to lenticular. The ore body on Oceaan 64 in the north of the field has a near - horizontal horizon while on Blaauwboschpoort 13, in the southern part, the dip is towards the west-southwest. The colour of the Oceaan Montmorillonite varies between very light yellowish grey to light olive brown (Horn & Strydom, 2000). A view of the Koppies mine in the Free State is shown in Photo 1.

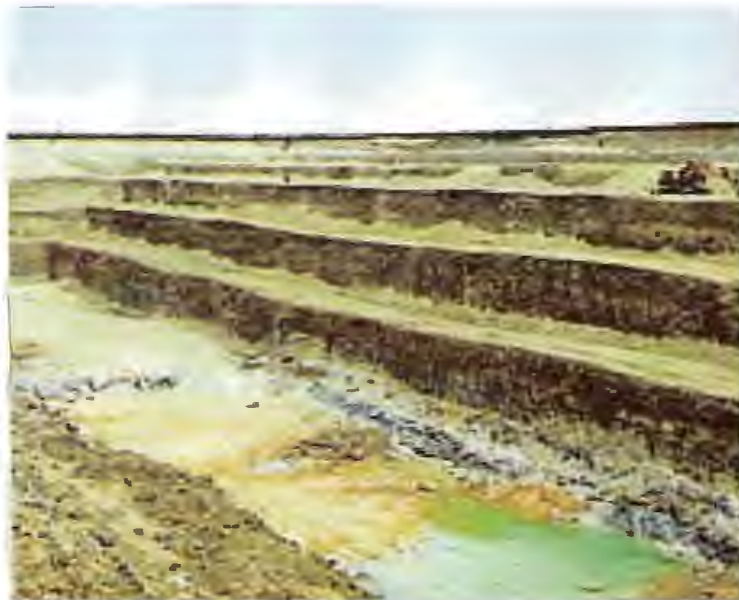


Photo 1: Koppies Mine in the Free State (www.gwbase.co.za)

The shales occurring above and below the deposit are typical Ecca shales and consist mainly of Montmorillonite, some Illite and Quartz. The Bentonite from occurrences in this field contains between 60% and 85 % Montmorillonite, with accessory Quartz and Illite and traces of other minerals. In most parts of the mining area the footwall of the Bentonite consists of shale and mudstone of the Ecca Group, or basement Granite Gneiss, while in some localities it is Swazian-aged greenstone rocks of the Blaauwboschpoort Formation. Silica, which is probably derived from the Bentonite, has resulted in resification of the host rock immediately bordering the contact zone.

Two possible modes of formation have been proposed for the Bentonite on Oceaan. The first suggests that the Bentonite resulted from direct weathering of the Achaeen Schists, while the second suggests that the clays resulted from in-situ alteration of volcanic ash that was deposited in a shallow sea under brackish water conditions, the ash having accumulated in channels and embayments on a pre-existing palaeo-erosion surface consisting of Achaeen rocks. The latter mode of formation is currently supported by most researchers. Petrographic studies of Bentonite revealed a volcanic-ash fabric with larger grains displaying typical Shard grain morphology, while the matrix is very fine grained and highly altered (Horn & Strydom, 2000).

Natural Oceaan Bentonite contains between 20% and 30% moisture and has a pH between 8.2 and 9.0, inactivated, and 9.5 and 11 in activated form. The cation exchange capacity varies between 94meq/100g and 99meq/100g of dry clay. The exchangeable cations are essentially Ca^{++} and Mg^{++} in equal proportions of about 50 meq/100g each, which makes it very similar to the so-called Southern Bentonites occurring in the USA, in States bordering the Gulf of Mexico (Le Fond, 1989). Differential thermal analysis (DTA) shows a conspicuous high-temperature endotherm at between 700°C and 720°C, indicating the permanent loss of crystalline water after which the structure of the bentonitic clay collapses and is therefore permanently altered (Horn & Strydom, 2000).

6.1.2 Mining Process

The ore body shape and general topography of the area determines what style of mining would be appropriate. Minimal overburden and extensive nature of the ore body promotes extraction via front-end loader, dozers and articulated dumper trucks. Agnello (2004) state, that at least 60% of the beneficiation is done in or next to the site plant. This includes primary crushing, soda activation and washing, in no specific order, as well as drying and screening. Additional processing would include milling and granulation either done on-site or at a nearby plant, followed by either selling of individual Calcium and Sodium Bentonites products, blending of both bentonites, acid activation of Calcium Bentonite and fine milling of the processed product. Figure 7

illustrates a flow diagram of the mining process of the Koppies mining process after Agnello (2004).

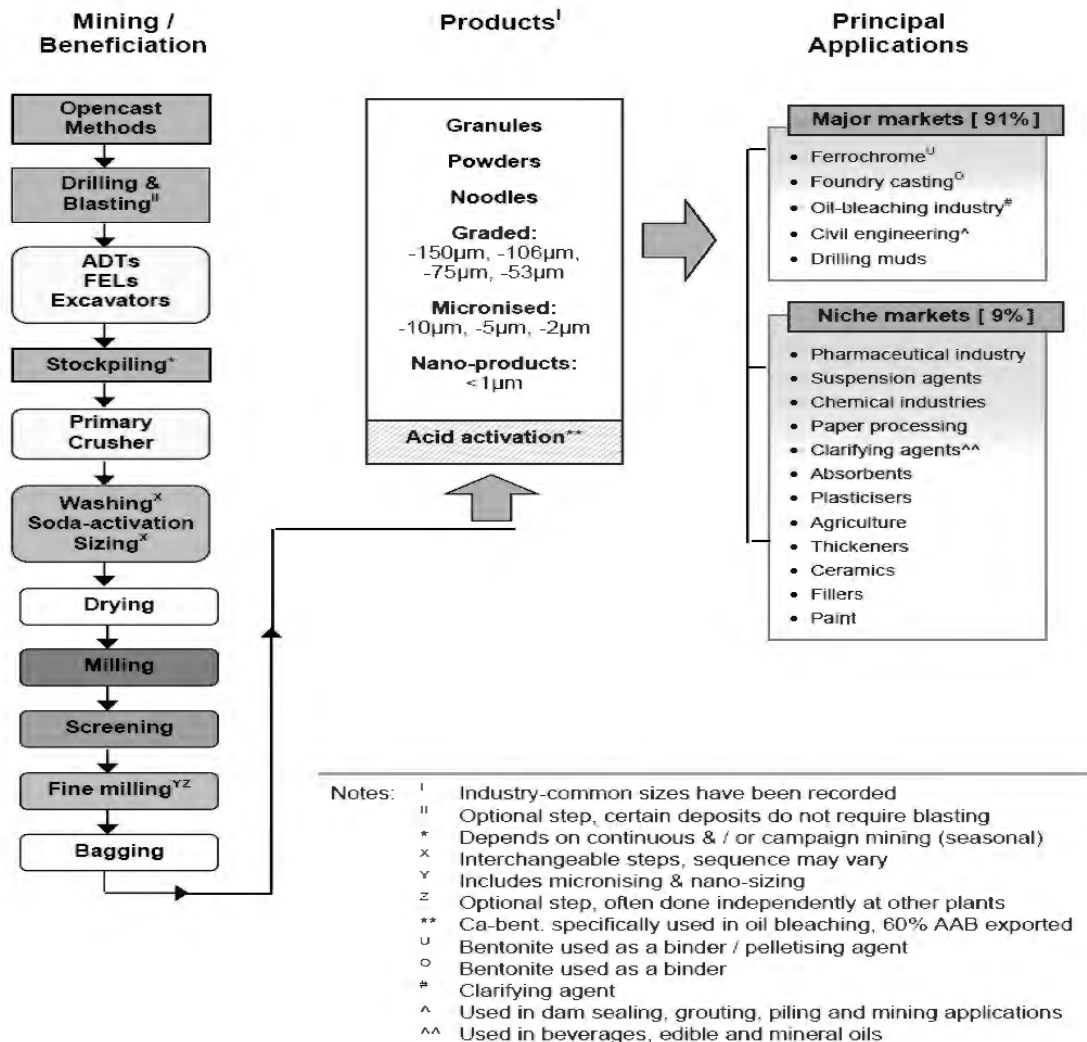


Figure 7: Flowchart of the mining process of Koppies Mine (Agnello, 2004)

6.1.3 Geochemical Effects of Acid Activation

Technological advances of Bentonites depend on quality and quantity of Smectites and other minerals within it. The valence of exchangeable cations, cation exchange capacity (CEC), adsorption capacity and most importantly water uptake tendency are crucial qualities of bentonite hence, the performance and application of bentonite (Luckham & Rossi, 1999; Murray, 2000).

Physicochemical and geotechnical properties such as CEC, swelling, pore structure, structure area, surface acidity, decolouring power, catalytic activity, strength, plasticity and compression as well as the chemical and mineralogical composition change considerably depending on the mining process.

Activation is the chemical treatment applied to certain types of clays to develop a capacity to absorb colouring matter and other impurities in oils and solutions. The term of activity denotes chemical and physicochemical reactivity whose increase is traceable to an increase in surface area of solids (Daglioglu et al., 2002, Franciso et al., 2001; Christidis et al., 1997; Babaki et al., 2007).

Önal et al. (2002) reveal that, activation of bentonite is carried out in a continuous stirred tank reactor at low temperatures between 70°C and 120°C in the presence of activation agents, mostly sulphuric acid. During the reaction, the surface area of bentonite increases due to decomposition of the Smectite structure (Franciso et al., 2001).

This structural change i.e. surface area increase, results because acid replaces exchangeable cations Na^+ , Ca^{2+} , Mg^{2+} , Fe^{3+} with Hydrogen ions and leach Aluminium and other cations out of both the tetrahedral and octahedral sites, leaving the Silicon Oxide (SiO_4) groups largely intact (Theocharis et al., 1988; Ravichandran & Sivasankar, 1997; Gates et al., 2002).

The mechanism of decomposition of the Smectite structure is also facilitated by the pores found in the bentonite. Bentonites contain natural mesopores ($\approx 2\text{nm}$ to 50 nm) and small amounts of micropores ($<2\text{ nm}$). Although the micropores and mesopores lie within the particles, the macropores lie between the particles.

The adsorption capacity of the macropores is negligible compared to that of the micropores and mesopores. The physicochemical properties of bentonites such as absorption and catalytic activity depend extensively on the micro and mesopores within the particles of the Bentonite. As the activation process progresses the empty spaces that were occupied by the exchangeable cations, Na^+ , Ca^{2+} , Mg^{2+} , Fe^{3+} , grow larger and larger, therefore micropores are transformed into mesopores. Furthermore,

as the rate of activation increases, possibly due to increases in concentration of the acid, some locations of the mesopores disappear, leading to an increase in surface area of the bentonite (Bakaki et al., 2008). Depending on the type of bentonite, a surface area of $70\text{m}^2/\text{g}$ may increase to $120\text{m}^2/\text{g}$ to $300\text{m}^2/\text{g}$ after activation.

Noyan et al. (2007); Yildiz et al. (2002); Babaki et al. (2007) further point out that it is not only the surface area of the bentonite that increases, the micro-mesopore volume, mesopore size distribution, surface acidity and overall swelling of a bentonite are greatly affected from acid activation. These properties are of vital importance to the performance and uniqueness of bentonite as an innovative application in civil engineering designs such as hydraulic barriers, where the properties of the raw bentonite are harnessed.

Acid-activated clays are however, essentially used in the refining of edible oils and fats, industrial lubricants and waxes. They are also used in pharmaceutical applications (Agnello, 2004; Noyan et al., 2007, Komadel, 1999, Babaki et al, 2007). In Figure 8 a flow diagram of the acid activation of the Koppies Bentonite is shown (Agnello, 2004).

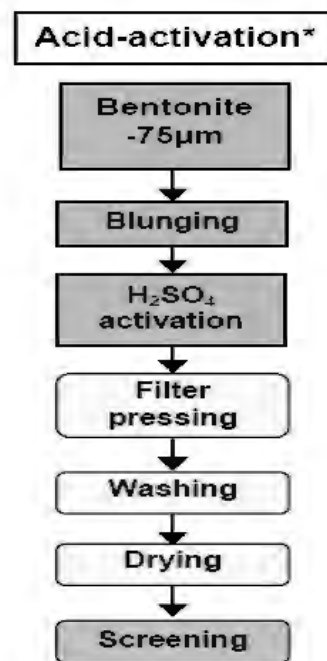


Figure 8: Acid activation processing flow diagram (Agnello, 2004)

6.1.4 Geotechnical properties and fabric

In Image 4, the SEM image of Envirobent, reveals individual silt sized particles ranging from about 2 μm to 30 μm in length. The particles appear to have been torn out from a continuous sheet. The edges are angular with large voids and trans-assembly pores. Some of the particles remain intact and bonded with other particles. The particle shape may be due to the mechanical processes of the milling machines during the production of Envirobent.

In Image 5, the SEM image of Envirobent at a much higher magnification (15 000) displays a flaky and layered form of particles. This arrangement of particles has several descriptions and is referred to as “domain” or “packet” by Aylmore and Quirk, (1960); Mitchell, (1993). An array of such fabrics is termed a turbostratic fabric (Mitchell, 1993).

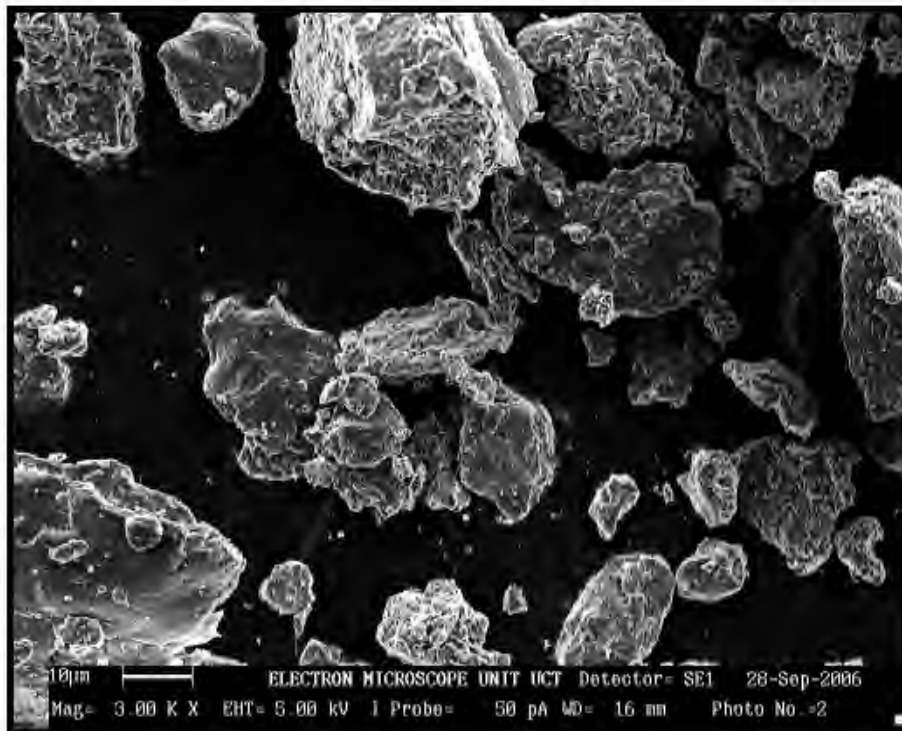


Image 4: Scanning Electron Microscope of Envirobent, Magnification 3 000 (Waldron, 2006).

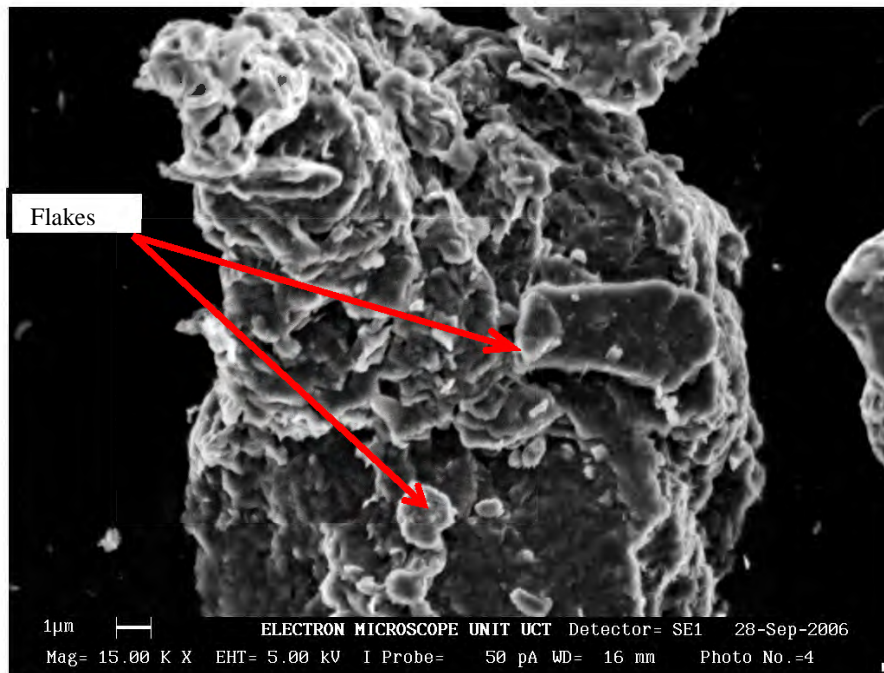
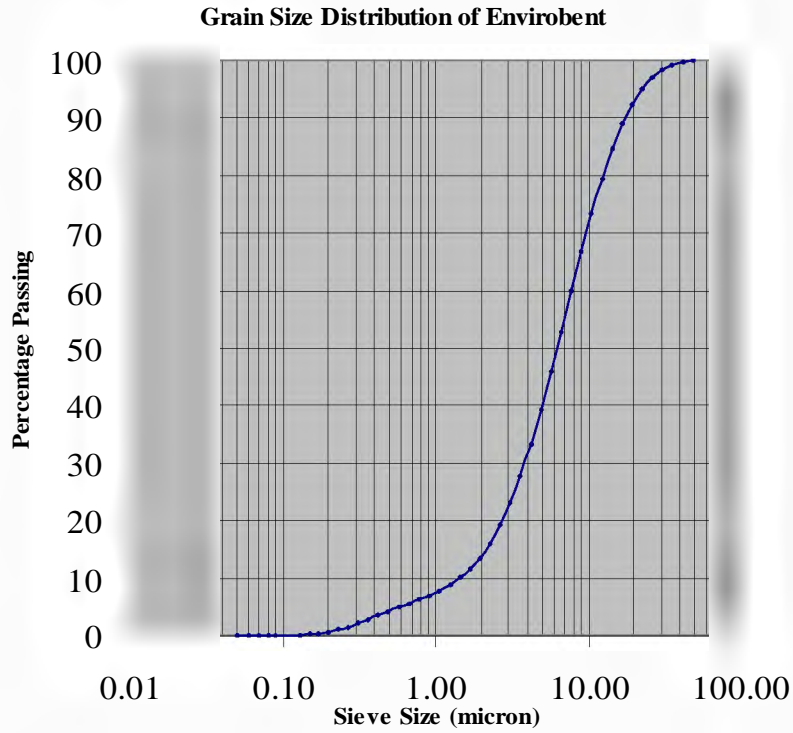


Image 5: Scanning Electron Microscope of Envirobent, Magnification 15 000 (Waldron, 2006)

Dry bentonite (5g) was mixed with sodium pentaphosphate and fed into a Malvern Mastersizer analysis. The grain size distribution of Envirobent is given in Graph 3. In Table 7 the geotechnical properties of Envirobent are listed.



Graph 3: Grain Size Distribution of Envirobent (Divey, 2008)

Property	Unit
Specific Gravity Gs	2.60
Moisture content	4%
Particle range	0.05 - 48.27 μ m
Grain size D50	6.24 μ m
Coefficient of uniformity, Cu	5.26
Coefficient of curvature, Cz	1.03
Plastic Limit	39%
Liquid Limit	142%
Plasticity Index	103
Free Swell	100%

Table 7: Geotechnical properties of Envirobent

6.2 Heidelberg Bentonite (Raw)

Heidelberg Raw Bentonite is an in-house name given to the second type of bentonite investigated in this research work. This bentonite was hand collected at the Heidelberg mine in May 2008. The Bentonite is mined by a subsidiary of the South African Minerals Resource Committee (SAMREC), called Cape Bentonite Mine. The mine is situated eastward towards Riversdale, also shown on the geological map in Figure 9. Along the route, toward the mining fields, which are privately owned farms, the clayey nature of the strata in the Heidelberg basin can be seen in the road cuttings, (Roger & Schwarz, 1902; Viljoen et al., 1990).

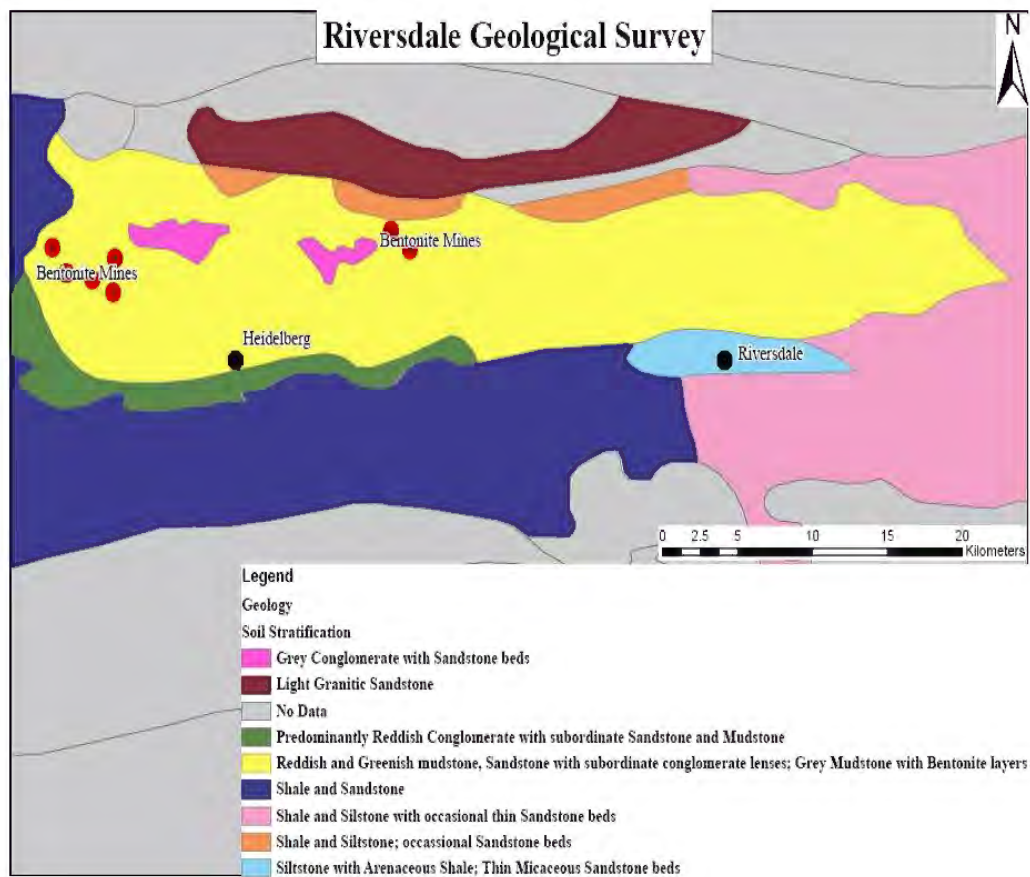


Figure 9: Riversdale Geological Map: Mining locations of Cape Bentonite

6.2.1 Geology of Heidelberg Bentonite Deposits

Cape Bentonite Mine (Pty) Ltd presently operates 10 bentonite quarries intermittently in the Heidelberg-Riversdale Cretaceous basin. These quarries occur on the remainder of the farm De Doorn River 300 approximately 13 km west-northwest of Heidelberg on Erf 1412 of Heidelberg Townlands, about 2 km west-northwest of Heidelberg and on the farm Spiegel Rivier 246, which is 9 km northeast of Heidelberg.

Old rehabilitated mine workings are mostly located on the farm De Doorn River. The workings follow the strike of the lowermost of two tuff-rich zones, which dip to the south, then southeast and eventually east towards the currently active mines on Heidelberg Townlands. The working mine on Spiegel River 246 is located on the uppermost tuff zone while a currently dormant quarry lies about 2 km south of the Spiegel Rivier deposit on the lower tuff zone and is located less than 1 km from the farm boundary with Kragga Kraal 244.

The bentonite mines in the Heidelberg area are all located within the 60 km long and 10 km wide Mesozoic onshore Heidelberg-Riversdale half graben (Dingle et al., 1983). This graben is bordered on the northern side by the Tradouw and Worcester mega faults and is surrounded on all sides by argillaceous rocks of the Bokkeveld Group. The Bentonite-Zeolite bearing Kirkwood Formation is divided into units, i.e., an upper, probably fluvial zone consisting of multicoloured, pale greyish yellow and reddish Sandstone and Mudstone with dispersed conglomerate lenses that probably represent proximal fluvial plain deposits and a lower zone comprising olive-green and greenish grey lacustrine mud and Sandstone beds (Viljoen, 1992&1996). Bentonite is associated with two tuffaceous zones and underlies Zeolite-bearing horizons. The lacustrine-derived lower Bentonite-Zeolite-bearing zones of the Kirkwood Formation can be up to 10 m thick consisting of several bentonite horizons directly overlain by Zeolite-bearing, altered and often reworked tuff (Viljoen, 1996).

The contact between and overlying Zeolite is generally very sharp though Zeolite seems to be absent, not only in the upper multicoloured fluvial zone, but also near the rim of the basin. There is a number of bentonite layers associated with the upper tuffaceous zones and are mined selectively. The colour of the clay varies from pale

reddish grey to greyish green. The two tuffaceous beds occur intermittently over a strike distance of 20km to 30 km with dips varying between 15° and 30° towards the north, on Spiegel Rivier 246 and the Heidelberg townlands.

However, the dip directions varies between northeast and east on De Doorn Rivier 300, while according to Viljoen (1996), individual dip measurements towards the south have been recorded where the bentonite bearing horizons have been influenced by local north-south striking faults (Horn & Strydom, 2000).

If the dips, potential strike length and thickness of the bentonite layers are considered, inferred resources are substantial. However, the economically viable bentonite resources could be increased if the associated Zeolite bearing horizons were exploited simultaneously.

6.2.2 Mining Process

The undulating topography and lenticular nature of deposits have forced Cape Bentonite Mining Company to mine up to 8 ore bodies simultaneously. The mining process is mainly by excavators and dumpers as the bentonite has to be hollowed out or scraped from rock faces, as shown in Photo 2. In Photo 3 a close-up photo of the Heidelberg Raw Bentonite. The material appeared cool, soapy and smooth due to the preserved moisture content.

Presently, Cape Bentonite Mine (Pty) Ltd is mining approximately 180 tones of bentonite per day. This figure is derived from the amount of orders received. Due to the current construction boom in South Africa, the mine is working long hours to meet demands. The mining process is done in sequences depending on the type of bentonite found in each farm (locations are shown in Figure 9). Since most of the mining of the Bentonite is carried out on private farms, land rehabilitation and restoration of the land is the mining company's highest priority. The established plant in Heidelberg includes crushing, drying, and soda-ash activation. Their clientele covers civil engineering construction companies, food processing industry such as wine makers, chocolate factories, and fruit-juice refining companies (Personal Communication: Cape Bentonite Mine Manager, Hannes Kleinhans, 2008).



Photo 2 : Mining of the Heidelberg Raw Bentonite



Photo 3: Heidelberg Raw Bentonite

6.2.3 Geotechnical properties and fabric

In Image 6, the SEM of Heidelberg Raw Bentonite displays an undulating 'mosaic' sheet of a continuous layer. In Image 7 reveals irregular flake-shaped layers stacked together depicting the distinct fabric of classical Montmorillonite bearing clay mineral.

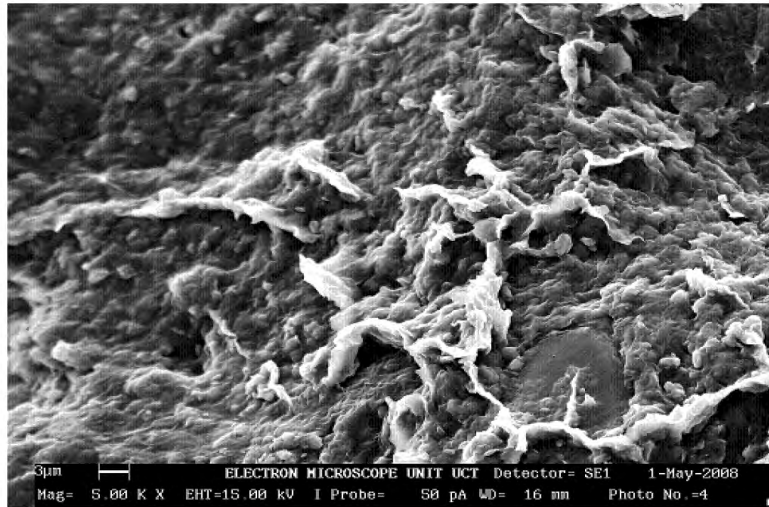


Image 6: Scanning Electron Microscope of Heidelberg Raw Bentonite, Magnification 5 000 (Waldron, 2008)

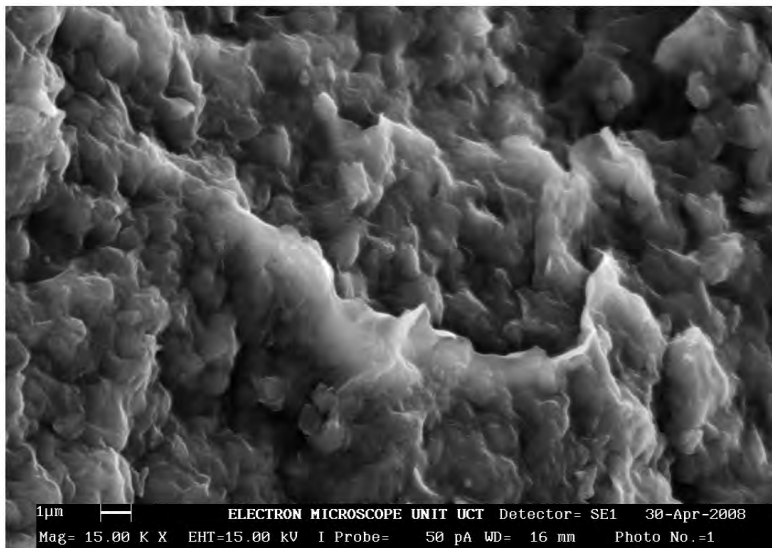
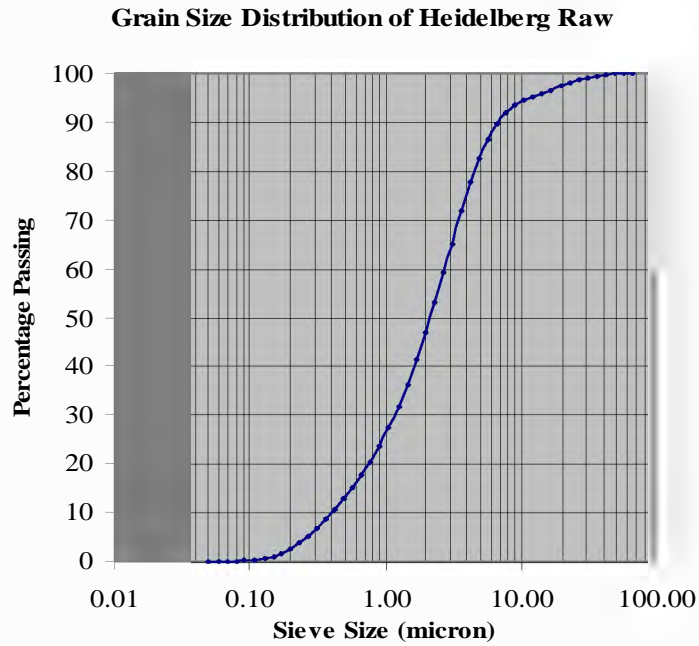


Image 7: Scanning Electron Microscope of Heidelberg Raw Bentonite, Magnification 15 000 (Waldron, 2008)



Graph 4: Grain Size Distribution of Heidelberg Raw Bentonite (Divey, 2008)

Property	Unit
Specific Gravity, Gs	2.50
Natural moisture content, w	39%
Particle range	0.05 - 76.32 μ m
Mean grain size, D50	2.46 μ m
Coefficient of uniformity, Cu	5.11
Coefficient of curvature, Cz	0.20
Plastic Limit	41%
Liquid Limit	160%
Plasticity Index	119
Free swell	110%

Table 8: Geotechnical properties of Heidelberg Raw Bentonite

7. Geochemical Investigations of Research Materials

Introduction

Material specification and their performance in Civil Engineering projects is based solely on the knowledge emanating from investigative research results that follow from material testing and analysis. The following is a series of geochemical tests undertaken in various laboratories within the University of Cape Town.

7.1 X-Ray Diffraction

When X-rays interact with a crystalline substance, a diffraction pattern is formed. Each crystalline substance gives a pattern. The same substance always gives the same pattern and in a mixture of substances, each produces its unique pattern independently of the others (Hull, 1919). In a way, an X-ray diffraction pattern of a pure substance is like a ‘finger print’ of the substance.

Diffraction patterns are represented in a diffractogram (see Appendix D). In diffractograms the diffraction angle ($^{\circ}2\theta$), and the intensities of the peaks (counts/s) of the sample are displayed. Print-outs of the investigated minerals are also provided showing the d -spacing in Ångstroms, the relative intensity, the mineral name, and other relevant information such as wave length, running time, the make of XRD machine, etc.

7.1.1 Theoretical background of X-Ray powder diffraction

Powder X-ray Diffraction (XRD) is one of the primary techniques used by mineralogists and solid-state chemists to examine the physico-chemical make-up of unknown solids. The schematic in Figure 10 illustrates the sample’s position, within the device, the X-Ray tube, the detector diaphragm, the scattered-radiation diaphragm and aperture diaphragm. Collectively, these components make up the Goniometer.

When an X-ray beam hits an atom, the electrons around the atom start to oscillate with the same frequency as the incoming beam. In almost all directions, destructive interference will occur. No resultant energy is leaving the solid sample. However, since the atoms in a crystal are arranged in a regular pattern, only in very few directions destructive interference will occur. Thus, in most directions the combining waves are in phase and there will be well-defined X-ray beams leaving the sample in various directions. Hence, a diffracted beam may be described as a beam composed of a large number of scattered rays mutually reinforcing one another in a so-called constructive interference. This will be picked up by the diaphragm detector. The intensity of the diffraction is expressed in Bragg's law as:

$$N(\lambda) = 2d \sin \theta \quad 3$$

θ = diffraction angle (degrees)

d = interatomic spacing (Å)

$N(\lambda)$ = intensity (µm)

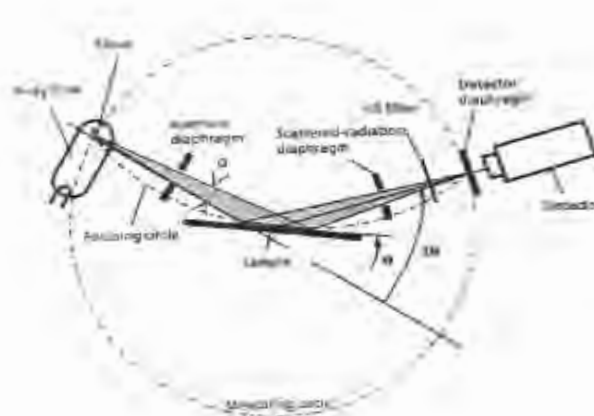


Figure 10: Illustration of X-ray Diffraction Ronel (2008)

7.1.2 Objectives of X-Ray diffraction of Bentonites

The main objective of the XRD analysis in this research work is to identify the minerals present in Envirobent and Heidelberg Raw Bentonite.

7.1.3 Sample preparation

To prepare a soil sample for a powder diffraction analysis, the sample is pressed into a slot in the sample holder. It is then trimmed flush across the slot before being inserted into the machine. The investigation was done using a Pan Alytical PW 3830 X- Ray Generator (see Photo 4). The generator is run at 40kV with 25mA and the test takes about 30 min to 45 min to complete. A computer is connected to the X-Ray machine which uses a software package called Phillips X'Pert Software, X'Pert Graphics & Identify Properties (Personal Communication: XRD Technician, Ronel 2008).

This software offers many functions such as a search match, a mineral identification function that uses powder diffraction file numbers (PDF #), a colour coded mineral check lists (a list of possible minerals found in sample), etc .



Front view

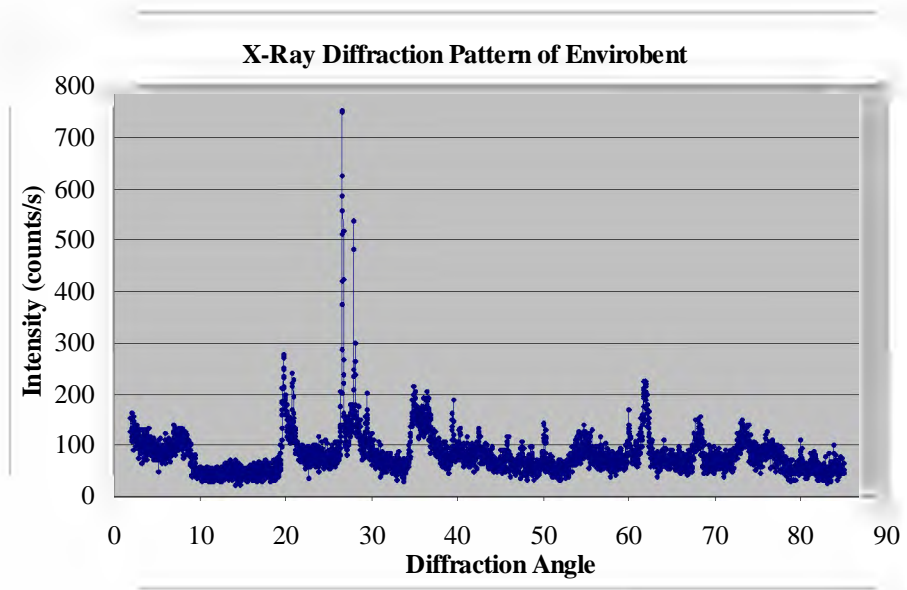


Side view

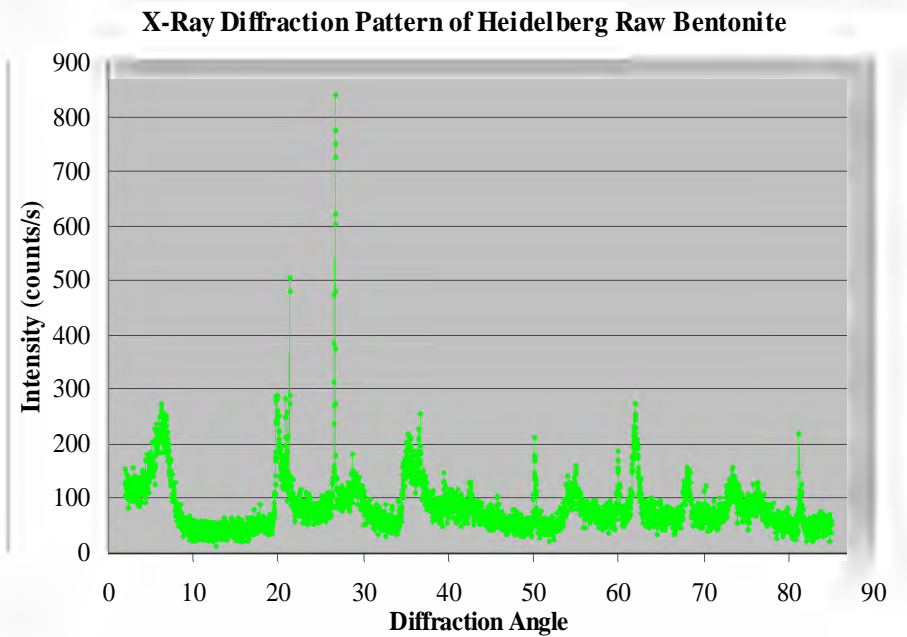
Photo 4: Pan Alytical PW 3830 X-Ray Diffractometer

7.1.4 Results of XRD analysis and discussion

The diffraction patterns of Envirobent and Heidelberg Raw Bentonite are shown in Graphs 5 and 6.



Graph 5: XRD Pattern of Envirobent



Graph 6: XRD Pattern of Heidelberg Raw Bentonite

7.1.4.1 Envirobent

The XRD results of the Envirobent are shown in Graph 5. The graph reveals that Illite, Illite 2M2, Biotite, Calcite are present. Illite is also a three-layered structured clay mineral. However, this structure is non-expansive, as of the same type found in Montmorillonite.

Birch (1975) and Gates et al. (2000) show that patterns of bentonite containing Ca-rich Montmorillonite peak at around 6° with a d -spacing of 13.6 \AA and also at 7° , with a d -spacing of 14 \AA . According to the diffractogram of Envirobent, the Illite and Biotite peak from (8° to 20°). The diffraction pattern of Envirobent also displays more changes in the diffraction angle range of 8° to 20° . These findings suggest that in Envirobent the characteristic mineral is Illite.

However, Gates et al. (2000) reveal samples of acid treated and untreated diffraction patterns of bentonite. The effects, caused by acid concentration, are evident in a reduction of the peaks nearer to the diffraction angle of the Montmorillonite mineral.

The diffraction pattern of Envirobent does not show any presence of Montmorillonite although this product originates from a deposit which contains 60 % to 85 % Montmorillonite (Strydom & Horn, 2000). Therefore this product is beyond the scope of geological investigations and falls in the category of industrial treatment of raw materials.

The consequence of acid activation affects many properties of the clay. For instance, the swelling of clay occurs in the interparticles of the face-to-face arrangement of the 2:1 tetrahedral and octahedral sheet layers of the Montmorillonite mineral within the clay (Önal, 2007). Horn et al.,(2000), confirm the chemical formation of this Montmorillonite as $\text{Ca}(\text{Ca}_3\text{Al}_2)\text{Si}_5\text{O}_{10}(\text{OH})_8$, where the essential elements are Ca, Al, Si, H, and O however Calcium Montmorillonite cannot be found in Envirobent. These elements are responsible for isomorphous substitutions within the layers of the Montmorillonite, which results in permanent charges that are responsible for the swelling characteristics of the bentonite (Grim, 1968). The charges are also related to the mineral structure and composition of the bentonite (Czimerová, 2006).

Furthermore, in the atomic structure of pure Montmorillonite, Aluminium ions in the octahedral structure are substituted by Magnesium and Iron cations or there is replacement of Silicon by Aluminium. This results in charge imbalances in the octahedrons of clay. The imbalance of charges is then filled by water and Sodium or Calcium ions. The resulting effects as well as a concert of various chemical reactions, within the layers allow water to seep into the exchangeable layers of the Montmorillonite structure and cause swelling.

Since Envirobent is an acid activated Calcium Montmorillonite, which is filtered off, washed thoroughly and dried (Agnello, 2004). Önal et al., (2002); Babaki et al. (2007) points out that, in most cases, the activation of bentonite is carried out in a continuous stirred tank at low temperatures between 70°C to 120°C in the presence of activation agents. During the reaction, the surface area of bentonite increases due to decomposition of the Smectite structure. The activation process causes a considerable amount of cations to be substituted by hydrogen cations which increases the specific surface area of the bentonite (Babaki et al. 2007; Yildiz et al. 2004).

The increase in surface area is a result of the combination of the smaller pores which bind together to create larger ones as a function of the acid concentration. Therefore, higher acid concentrations cause greater alterations in the morphology of the clay. In a similar activation process, an Australian bentonite showed an increase in SiO₂ content at the expense of exchangeable octahedral cations as a function of the duration and concentration of the acid (Gates et al., 2002).

These transformations of the Montmorillonite structure introduce undesirable changes in other physicochemical properties such as cation exchange capacity (CEC), swelling capacities and the overall behaviour of the bentonite.

7.1.4.2 Heidelberg Raw Bentonite

The diffraction pattern of the Heidelberg Raw bentonite (shown in Graph 6) has identified only one mineral i.e. Sodium Montmorillonite, with the chemical formula $\text{Na}_{0.3}(\text{Al, Mg})_2\text{Si}_4\text{O}_{10}(\text{OH})_2 \cdot 4\text{H}_2\text{O}$, with a *d*-spacing of 13.6Å and a diffraction angle of 6.49°. Other mineral such as Mica, Feldspar, Quartz and the other

Montmorillonite minerals were checked but none peaked sufficiently to consider their presence within the sample. Therefore, the main mineral of Heidelberg Raw Bentonite is a pure Sodium Montmorillonite clay mineral.

7.2 X-Ray Fluorescence (XRF)

X-Ray Fluorescence Spectrometry is a method that determines the total percentages of major and minor elements by measuring secondary X-ray emission after a solid sample is bombarded with primary X-ray beams.

7.2.1 Theoretical background of X-ray Fluorescence

X-ray fluorescence (XRF) is the emission of characteristic "secondary" (or fluorescent) X-rays from a material that has been excited by the bombardment of high-energy X-rays or gamma rays. The phenomenon is widely used for elemental analysis and chemical analysis, particularly in the investigation of metals, glass, ceramics and building materials applied in the research fields of geochemistry, forensic science and archaeology. Each of the atomic elements, present in a sample, produces a unique set of characteristic X-rays that is a fingerprint for that specific element. XRF analyzes determine the chemistry of a sample by measuring the spectrum of the characteristic X-rays emitted by the different elements in the sample when illuminated by high energy photons. A fluorescent X-ray is created when a photon of sufficient energy strikes an atom in the sample, dislodging an electron from one of the atom's inner orbital shells of lower quantum energy states.

The atom regains stability, filling the vacancy left in the inner orbital shell with an electron from one of the atom's higher quantum energy state. The electron drops to the lower energy states by releasing a fluorescent X-ray. The energy of this fluorescent X-ray (typically measured in electron Volts, eV) is equal to the specific difference in energies between two quantum energy states experienced by the dropping electron. Each element present in the sample emits its own unique fluorescent X-ray energy spectrum.

7.2.2 Objective of X-ray Fluorescence analysis

The objective is the determination of the chemical composition of the research materials and of the quantity of the respective chemicals within each sample.

7.2.3 Sample preparation

The sample is formed into a briquette, as shown in Photo 5. The briquette is then loaded face down into the XRF Spectrometer for analysis, (Personal communication XRF Technician: Stout 2008).



Photo 5: Preparation of Briquette for X-Ray Fluorescence Analysis

7.2.4 Results of XRF analysis and discussion

Horn & Strydom (2000) published the chemical compositions and the quantities of the natural and acid activated bentonites of Koppies Deposit which are listed in Table 9.

Composition	Natural Bentonite* (%)	Average of Natural Bentonite Samples** (%)	Activated Bentonite*** (%)
SiO ₂	61.58	58.05	59.1
TiO ₂	0.23	0.21	0.2
Fe ₂ O ₃ (total)	3.58	1.41	4.4
Al ₂ O ₃	18.89	12.06	18.6
CaO	1.32	0.87	2.2
MgO	4.54	3.23	4.2
K ₂ O	0.43	0.37	0.3
Na ₂ O	0.25	0.23	1.8
H ₂ O ⁻	-	16.73	-
H ₂ O ⁺	-	6.51	-
CO ₂	-	0.07	-
LOI (total)	8.80	-	8.9
Total	99.62	99.74	99.7

*Schmidt, (1976), ** Natural bentonite samples, ***Acid Activated samples (Horn & Strydom,2000).

Table 9: Chemical Composition of Natural Koppies Deposit Bentonite (Horn & Strydom, 2000)

7.2.4.1 Envirobent

The results of the X-ray fluorescent analysis of Envirobent are listed in Table 10.

Composition	Envirobent (%)
SiO ₂	56.65
TiO ₂	0.39
Al ₂ O ₃	16.73
Fe ₂ O ₃	5.63
MnO	0.19
MgO	3.61
CaO	3.42
Na ₂ O	3.05
K ₂ O	1.28
P ₂ O ₅	0.35
SO ₃	0.11
Cr ₂ O ₃	0.04
NiO	0.004
H ₂ O-	-
LOI	8.12
Total	99.57

Table 10: Chemical Composition of Envirobent (Reid, 2007)

With reference to the chemical composition of the natural Koppies Bentonite taken by Schmidt (1976), and those of Envirobent, investigated in this work, it is evident that there is a reduction in the amount of Silicon dioxide (SiO₂) of about 4% and a reduction in the Aluminium Oxide (Al₂O₃) by about 2%. An increase in the original Calcium Oxide (CaO) content of about 2.1% is noted.

Komadel (1999) reveals that the physiochemical properties of a bentonite changes considerably due the activation treatment. It is pointed out that the product of an acid activated natural clay mineral is independent of the initial clay mineral content used. The extent of chemical decompositions of clay minerals depends on the type of

Smectite mineral within the bentonite. Madejová et al. (1997) point out that, if a Smectite is of a dioctahedral type, the octahedral sites are occupied mainly by Al^{3+} ions and if the Smectite is of a trioctahedral type, the octahedral sites are occupied mainly by Mg^{2+} ion. Horn & Strydom (2000) have identified Ca^+ and Mg^{2+} as the major cations within the Koppies Bentonite. Therefore, Envirobent is a Trioctahedral Smectite. Noyan et al. (2007), Madejová et al. (1997), Komadel, (1999) and Babaki et al. (2007) suggest that the effects of acid activation for this type of smectite are more significant than those of a dioctahedral type.

Furthermore, the dissolution rate of Al by Mg in Montmorillonites increases the acidic conditions as a function of concentration of the acid, volume and time to which the clay mineral is exposed (Komadel, 1999). Gates et al (2002), points out that the mechanism of structural changes due to acid activation in bentonite matrixes are different, depending on the length of treatment, content of impurities and presence of other mineral such as Illite, Feldspars, Mica and Quartz.

Horn & Strydom (2000) published the chemical composition and the quantities of the various bentonites of the Heidelberg Deposit which is listed in Table 11.

Composition	Soil Sealants (Soda-ash activated) (%)	Foundry (Soda-ash activated) (%)	Drilling mud (Soda-ash activated) (%)	Thermally treated and palletised (%)
SiO ₂	66.8	65.9	64.9	66
TiO ₂	0.24	0.32	0.4	0.1
Fe ₂ O ₃ (total)	3.13	2.84	5.4	2.5
Al ₂ O ₃	17	18	17.6	17
CaO	0.47	0.33	0.36	1
MgO	3.4	4	2.13	3
K ₂ O	0.47	0.38	1.07	0.4
Na ₂ O	2.97	2.55	1.55	2.5
LOI	6.55	5.44	6.59	7.5
Total	101.03	99.76	100	100

Table 11: Chemical Composition of Bentonite from the Heidelberg Deposit for Specific Applications (Horn & Strydom, 2000)

7.2.4.2 Heidelberg Raw Bentonite

In Table 12, the chemical composition and quantities of Heidelberg Raw Bentonite samples collected at the Heidelberg mine are listed.

Composition	Heidelberg Raw $\overline{\text{II}}$ (%)	Heidelberg Raw $\overline{\text{III}}$ (%)
SiO ₂	57.52	63.20
TiO ₂	0.12	0.13
Al ₂ O ₃	14.54	15.98
Fe ₂ O ₃	5.61	6.17
MnO	0.02	0.02
MgO	4.55	5.00
CaO	0.45	0.50
Na ₂ O	1.14	1.25
K ₂ O	0.42	0.46
P ₂ O ₅	0.03	0.04

SO ₃	0.07	0.08
Cr ₂ O ₃	0.00	0.00
NiO	0.00	0.00
H ₂ O-	8.34	-
LOI	6.57	6.57
Total	99.38	99.38

(∏ Heidelberg Raw Bentonite at natural moisture content,

∏ Heidelberg Raw Bentonite after moisture loss, dried at 110 °C)

Table 12: Chemical Composition of Heidelberg Raw Bentonite (Reid, 2008)

The X-ray florescence results of Heidelberg Raw Bentonite appear to be consistent with the soda-ash activated drilling mud published by Horn & Strydom (2000) in Table 11. The percentage differences of the major elements in are in the order 1% to 2%.

7.2.4.3 Klipheuwel and Philippi Dune Sand

In Table 13, the chemical composition and quantities of the selected local sands i.e. Klipheuwel and Philippi Dune Sand are listed.

Sample (%)	Philippi Dune Sand (%)	Klipheuwel Sand (%)
SiO ₂	77.72	87.74
Al ₂ O ₃	0.022	5.70
TiO ₂	0.259	0.13
Fe ₂ O ₃	0.232	0.56
MnO	0.006	0.02
MgO	0.039	0.15
CaO	13.457	0.03
Na ₂ O	0.075	0.35
K ₂ O	0.167	3.75
P ₂ O ₅	0.025	0.004
SO ₃	0.001	0.014
Cr ₂ O ₃	0.001	0.011
NiO	0.001	0.001
LOI	7.760	0.69
H ₂ O	0.091	-
Total	99.851	99.162

Table 13: Chemical Composition of Klipheuwel and Philippi Dune Sand (Reid, 2008)

Both Klipheuwel and Philippi Dune sand show a high SiO₂ content, although the Philippi Dune sand is signified by a high loss of ignition (LOI) of the sample. This suggests that there is a considerable amount of carbonaceous substances within the sample. Compton and Franceschini (2007) confirm that dune sands contain a considerable amount of an Aeolian shells, namely Donax Serra.

7.3 Transmission Electron Microscopy (TEM)

A transmission electron microscope (TEM) works in principle like a slide projector. A two dimensional morphology of a sample is detected as beams of light are transmitted through the sample. This technique allows a certain part of the light beam being transmitted through certain parts of the slide. The transmitted beam is then projected onto a viewing screen, forming an enlarged image of the slide.

The energetic electrons in the microscope strike the sample and various reactions occur. Ultra thin sections of the specimen have to be prepared so that electrons can be transmitted as illustrated in Figure 11

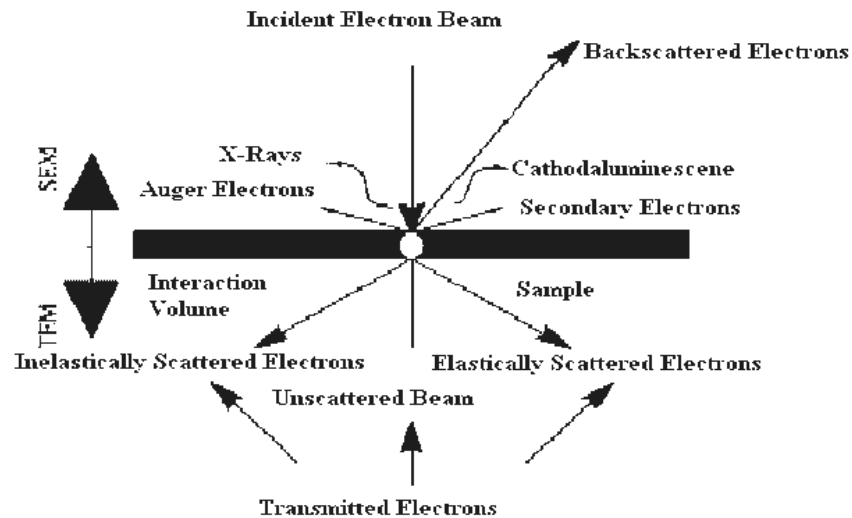


Figure 11: Schematic of Specimen Interaction in Transmission Electron Microscopy

(Website: www.unl.edu)

7.3.1 Theoretical background of Transmission Electron Microscopy

The "Virtual Source" at the top as shown schematically in Figure 12 represents the electron gun. This produces a stream of monochromatic electrons. The electrons are bundled and focused to a small thin coherent beam by the use of the first Condenser lens. This determines the general size range of the final spot that strikes the sample. The second lens changes the size of the spot on the sample, changing it from a wide

dispersed spot to a pinpoint beam. The beam is restricted by the condenser aperture, by knocking out high angle electrons so that the beam strikes the specimen and parts of it are transmitted.

The transmitted portion is focused by the objective lens onto an image. This image is passed through the intermediate and projector lenses, enlarging the image all the way. Once the image strikes the phosphor image screen light is generated, allowing the user to see the image.

Dark areas of the image represent those areas of the sample where only a few electrons were transmitted through. The lighter areas of the image represent those areas of the sample where electrons were transmitted through, i.e. thus they are thinner or less dense.

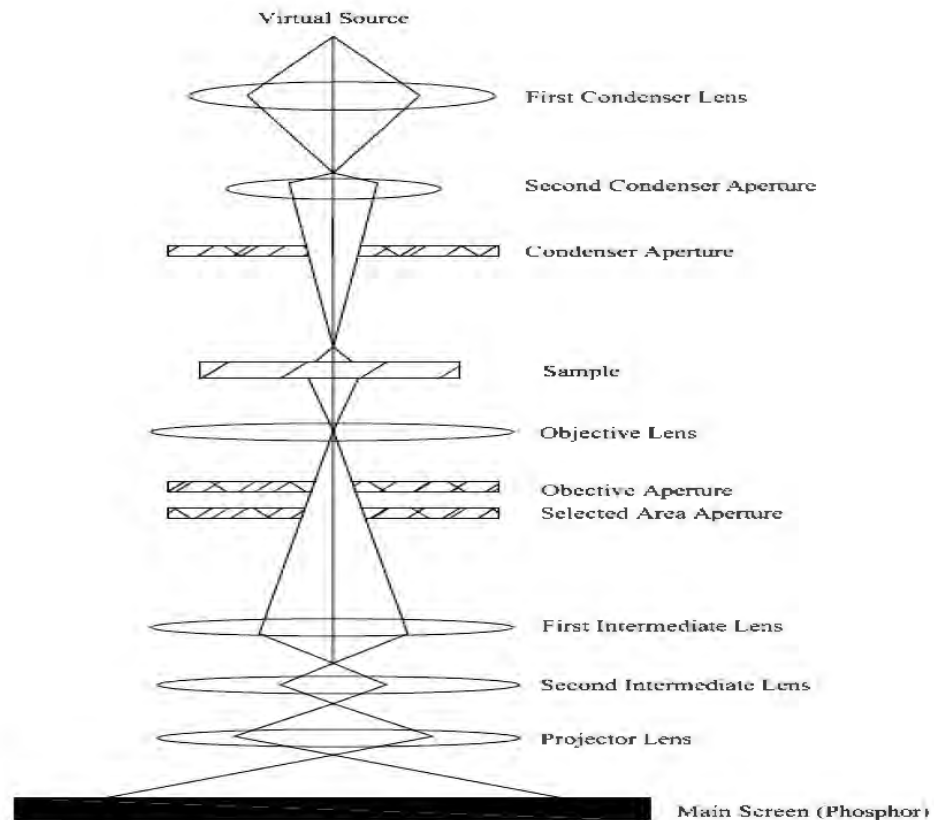


Figure 12: Schematic of Technology of Electron Transmission Electron Microscopy
(Website: www.unl.edu)

7.3.2 Objective of Transmission Electron Microscopy

The purpose of this investigation is to gain knowledge of the microscopic mechanisms underlying the swelling behaviour of the Bentonites used in this research. This, in turn involves the investigation of the layer structure of the ultra thin section of Montmorillonites layers before and after n-Alkylammonium ion treatment.

7.3.3 Alkylammonium method

Lagaly and Weiss (1969) observed that Alkylammonium cations assume monolayer, bilayer, pseudotrilyer or paraffin-type configurations in the interlayer space of 2:1 Phyllosilicates, as shown schematically in Figure 13. In Figure 13, the horizontal-striped polygons represent the 2:1 Phyllosilicate layers, the “zigzag” lines represent the alkyl tails of the Alkylammonium cations and the small circles represent the positively charged Ammonium head group of the Alkylammonium cations (Laird and Fleming, 2008). Depending on the chain length (n_c) and the layer charge of the clay the characteristic basal spacing of Phyllosilicates are 13.6Å, 17.6Å and 22Å. These configurations increase linearly with the chain length of the Alkylammonium solution.

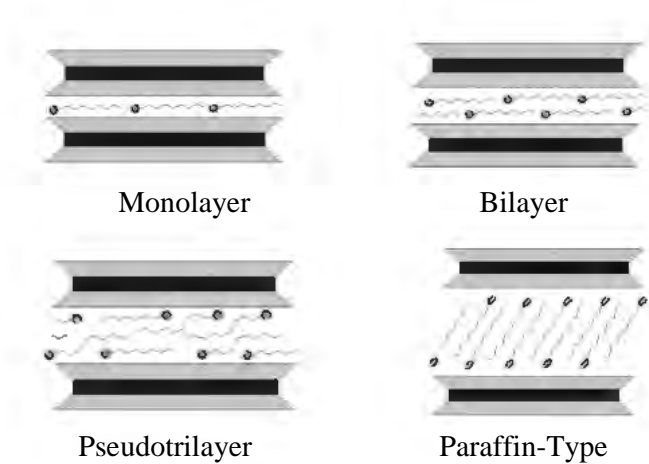
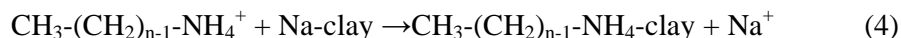


Figure 13: Schematic of configuration of Alkylammonium cations in the interlayer of 2:1 Phyllosilicates (Lagaly & Weiss, 1969)

Significant sample preparation is required for the Alkylammonium method. The first step is the stoichiometric exchange of inorganic interlayer cation with various straight chain *n*-Alkylammonium cations expressed in Equation 4.



Typically samples are prepared using Alkylammonium cation with a chain length (n_c) ranging from 6 (Hexylammonium) to 18 (Octadecylammonium) carbons.

7.3.4 Synthesis of Alkylamine Hydrochlorides

Most of the Alkylammonium Chlorides are not commercially available and must be prepared by protonation of their respective Alkylamines, which are commercially available. The reaction, shown in Equation 5, proceeds spontaneously whenever acid is added to an alcoholic solution of an Alkylamine.



Preparation of the Alkylammonium chloride solution used for this research was done according to the procedure described in Laird & Fleming, (2008).

7.3.5 Preparation of Alkylammonium-saturated clay samples

The preparation of Alkylammonium-saturated clays involves treating the clay sample with sufficient Alkylammonium cations to replace all of the exchangeable inorganic cations, washing excess Alkylammonium cations out of the sample, preparing an oriented sample on a glass slide, drying the sample and then analyzing the sample (Laird & Fleming 2008). To avoid rehydration of the treated clays, Lagaly (1981) recommended to seal the samples in glass capillaries and then to analyze the samples using a Debye-Scherrer camera. Samples prepared for this research were embedded in an epoxy resin and let to set overnight at 60°C, as shown in Photo 6. Thereafter the samples were stored in a desiccator at room temperature.

The embedded samples were then sectioned to about 700Å to 800Å in thickness with an ultra microtome using a Diatome diamond knife, (as shown in Photo 7). The Transmission Electron Microscope was a Leon 912, shown in Photo 8



Photo 6: Envirobent and Heidelberg Raw Bentonite samples embedded in resin



Photo 7: Diamond Cutter Machine



Photo 8: Transmission Electron Microscope

Basal Spacing of Measurement

A JEOL 1200 EX II microscope, operating at 120 KV, was then used to measure the average basal spacing of the negatives of the TEM images. In Table 14, the average of basal spaces, measured at 15 different locations of each the negatives of the TEM images are given. For comparative purposes the basal spacing of Heidelberg Raw Bentonite and Hexal-Alkylammonium treated using XRD analyses is also listed. For the Hexal-Alkylammonium cation treated Envirobent, only five locations were visible to be measured.

Bentonite Type	d-spacing (JEOL 1200 EX II Microscope)	d-spacing (XRD Machine)
Heidelberg Raw	10.78 ± 0.5 Å	13.6Å
n-Alkylammonium treated Heidelberg Raw	12.22 Å	-
Envirobent	10.78 Å ± 0.5 Å	-
Hexal-Alkylammonium treated Envirobent	10.83 Å	-

Table 14: Average basal spacing of Heidelberg Raw Bentonite and Envirobent

7.3.4 Results of TEM and discussion

Images were taken of untreated bentonites (no prior *n*-alkylammonium cations within the sample) and of treated samples with Hexa-alkylammonium cations. The following are images from a high resolution transmission electron micrograph showing the arrangement of individual layers within a Smectite quasicrystal of Envirobent and Heidelberg Raw Bentonite prior and after treatment.

7.3.4.1 Envirobent



Scale 1:20nm

Image 8: High resolution transmission electron micrograph of Envirobent (Jaffer, 2008)

In Image 8, the arrangement of individual layers of the quasicrystal structure of untreated Hexa-allylammonium Envirobent is shown. It appears that there are areas of non-expandable layers within the images, i.e. the electrons could not pass through certain layers. The average measured basal spacing using the JEOL 1200 EX II microscope is about 10.83Å. The individual layers appear broken, hence confirming the described fabric as observed in SEM image 5 in Chapter 6.

These measured basal spacings were variable, hence indicating some kind of mixed layer type of 2:1 structure within Envirobent. Vali et al. (1994) explained that mixed-layer structures have a particular pattern in TEM images. Comparing the images of Alkylammonium treated Envirobent and those studied by Vali et al. (1994), it was observed that in general, clay minerals exhibit such characteristics.

The XRD analysis of Envirobent has identified Illite, Biotite and Calcite as opposed to a Calcium Montmorillonite mineral. It was noticed that Illite also has a 2:1 layer Silicate structure similar to that of Montmorillonite but has no expandable layer.



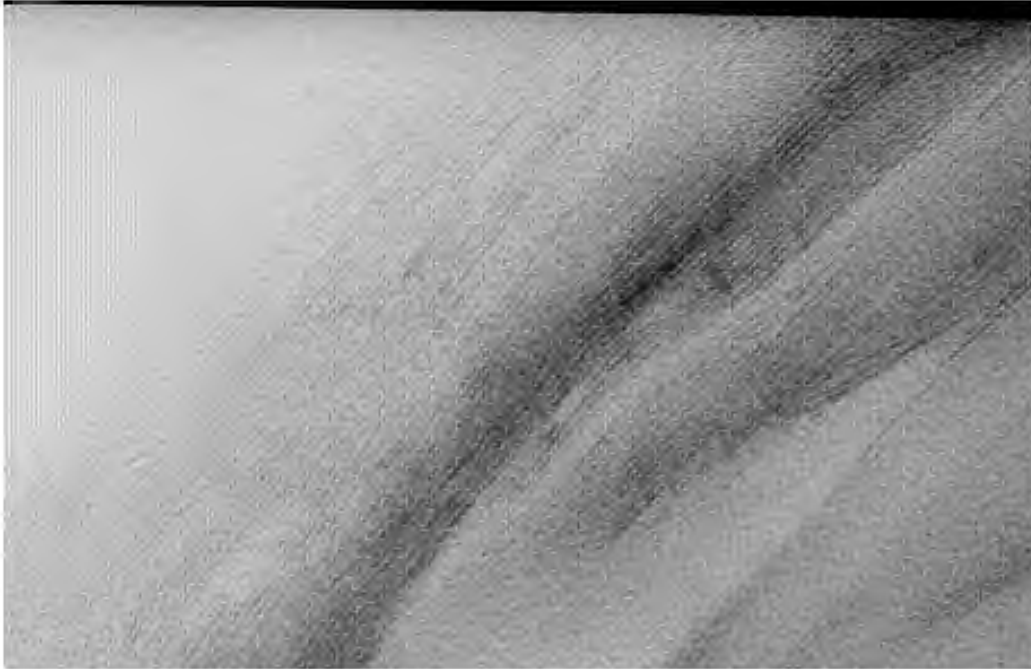
Scale 1:20nm

Image 9: High resolution transmission electron micrograph of Envirobent after Hexal-Alkylammonium Cation treatment (Jaffer, 2008)

In Image 9, the arrangement of individual layers of the quasicrystal structure of treated with Hexal-Alkylammonium Envirobent is shown. The image appears blurred and presents very few measurable basal spaces of individual layers. Some parts of the images appear as solid non transmissible layers. Only 5 locations were measurable and resulted in an average of about 10.78 Å.

Vali & Hasse (1990) point out that Illitic structures are not affected by after n-Alkylammonium treatment. Since there is no measurable expansion, it is believed that indeed, Envirobent contains a considerable amount of Illite. This sample dispersed uncontrollably during preparation, hence it is felt that the Hexal-Alkylammonium treatment and the remaining acidic content may have reacted and hence further destroyed the layers of the sample.

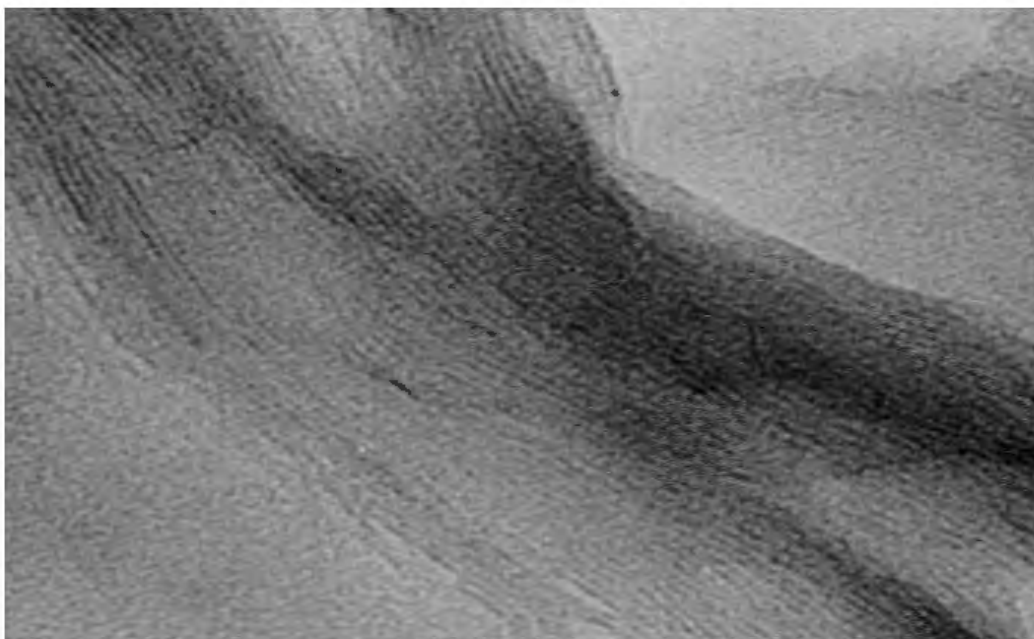
7.3.4.2 Heidelberg (Raw)



Scale 1: 20nm

Image 10: High resolution transmission electron micrograph of Heidelberg Raw Bentonite (Jaffer, 2008)

In Image 10, the arrangement individual layers of the quasicrystal structure of natural Heidelberg Raw Bentonite are shown. The Heidelberg Raw Bentonite displays dark fringes representing the 2:1 layers of the bentonite. These layers appear to be curvy suggesting they are flexible and continuous, representing a “mosaic morphology” as described by Grim (1968). The clear fringes represent the expandable interlayers. This appears to coincide with the description of the SEM images (Image 6&7) of Heidelberg Raw Bentonite in Chapter 6.



Scale 1:20nm

Image 11: High resolution transmission electron micrograph Heidelberg Raw Bentonite after Hexal-Alkylammonium cations (Jaffer, 2008)

In Image 11, the arrangement of individual layers of the quasicrystal structure of natural Heidelberg Bentonite treated with Hexal-Alkylammonium cations is shown. Hexal-Alkylammonium treatment of Heidelberg Raw Bentonite has an expanded basal spacing of 12.22\AA . This is an additional expansion of 1.44\AA from the original basal spacing of untreated Heidelberg Raw Bentonite.

The main objective of these test were achieved. The images also show continuity in the sheets of the Bentonite. There are no areas of broken layers, no areas of non-expandable layers and most importantly, the measured basal spacing showed consistent layer separation between the individual layers.

During the basal measurement of layers of the Heidelberg Raw Bentonite, a difference of about 0.5\AA was noted. However, if compared with the basal spacing measured in the XRD machine. The slight difference may be due to radiation damage of the sample caused by the electron beams.

The sample preparation of n-Alkylammonium treated sample is very cumbersome and time consuming. The results concerning the expandability behaviour of 2:1 layer Silicates, obtained in this investigation, agree with the results obtained using the procedure described in Laird & Fleming, (2008).

7.4 Cation Exchange Capacity (CEC)

There are a few methods that are suitable for measuring the cation exchange capacity of clays. The methods are based on the relationship between the layer charge and the properties of the mineral. Both, permanent and variable charges are determined in CEC (Czimerová et al., 2006).

7.4.1 Objective of Cation Exchange Capacity

The objective of the test is to determine the potential cation exchange capacity of the research materials using Lithium Chloride as an extraction solution.

Lithium chloride solution method

The concentrations of soluble and adsorbed cations are important characteristics for soil functions and potentials. Adsorbed cations may pose extraction difficulties. Therefore the selection of the exchange solution is crucial. The amount adsorbed is often not equivalent to the amount exchanged. Divalent ions are usually held more strongly than monovalent ions, i.e. they will be exchanged with more difficulty.

Various methods are available each exhibiting their uniqueness and shortfalls (Tan, 1989). Furthermore, the available technology for cation identification is unique to a selected few. In this research work, Lithium Chloride solution was used as an extraction agent.

Lithium Chloride is a neutral salt and does not change the pH- value of the soil unlike other extraction solutions such as NH₄-acetate. The solution must be adjusted to pH = 8.2 by means of Triethanolamine and Hydrochloric acid. The extraction permits the

analysis of nearly all relevant ions and facilitates the interpretation of ion relationships (St. Husz, 2000).

7.4.2 Atomic Absorption Spectrometry (AAS)

Atomic absorption spectrometry (AAS) is an analytical technique that measures the concentrations of elements. The process provides accurate quantitative analyses for metals in water, sedimentary soils or rocks. Samples are analysed in solution form, i.e. solid samples must be leached or dissolved prior to the analysis.

The technique makes use of the wavelengths of light specially absorbed by an element. To analyze any given element, a lamp is chosen that produces a wavelength of light that is absorbed by that element. The sample solutions are aspirated into the flame. If any ions of the given element are present in the flame, they will absorb light produced by a lamp before it reaches the detector. The amount of light absorbed depends on the amount of the element present in the sample. Absorbance values for unknown samples are compared with calibration curves of known samples. A more detailed description of this technique is published by the Royal Society of Chemistry, (Website; <http://www.chemsoc.org>). The spectrometer used in this research is shown in Photo 9.

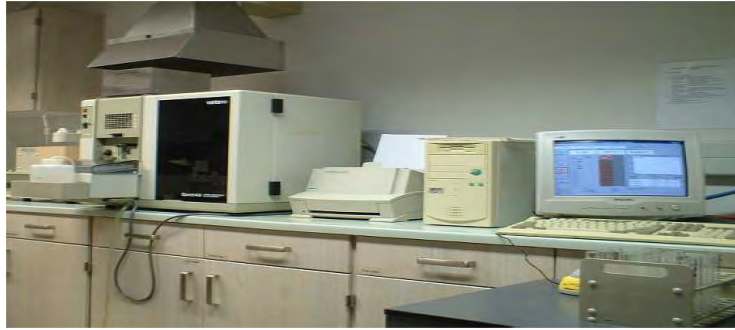


Photo 9: Atomic Absorption Spectrometer

7.4.3 Procedure and characteristics

In Table 15 samples that were investigated for cation exchange capacity (CEC) are listed. The samples were ground to a fine power (less than $63\mu\text{m}$) prior to cation extraction. The element concentrations from the supernatant were then analysed using the described technique. The saturation extract was produced in accordance to St. Husz, (2000).

Sand/Bentonite mixes for CEC Test		
Sample	Bentonite	Mix
		% by mass
Klipheuwel Sand	Envirobent	5
	Envirobent	7
	Envirobent	9
Philippi Dune Sand	Envirobent	5
	Envirobent	7
	Envirobent	9
Klipheuwel Sand	Heidelberg Raw Bentonite	5
	Heidelberg Raw Bentonite	7
	Heidelberg Raw Bentonite	9
Philippi Dune Sand	Heidelberg Raw Bentonite	5
	Heidelberg Raw Bentonite	7
	Heidelberg Raw Bentonite	9

Table 15: Sand/Bentonite mixes for Cation Exchange Capacity testing

In Photo 10 an array of polystyrene test tubes containing various samples mixed with Lithium Chloride solution are shown. The sample were shaken for two hours, centrifuged for 15 minutes and then filtered. The supernatant is extracted and prepared for the analysis, (shown in Photo 11).

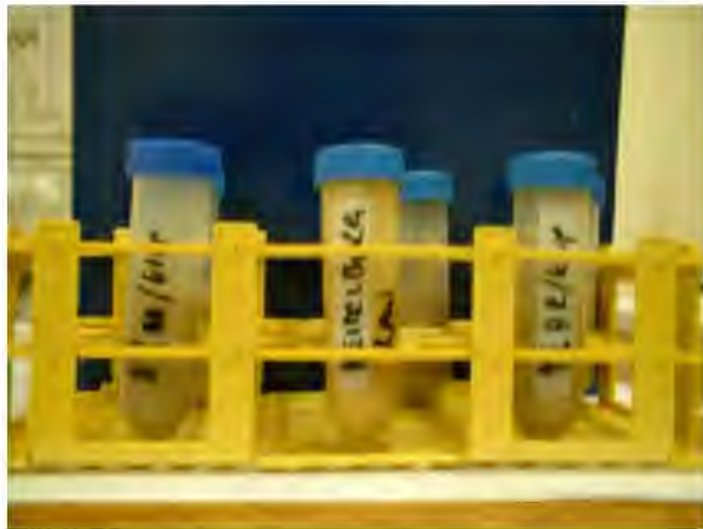


Photo 10: Preparation of samples for CEC testing



Photo 11: Solutions of the different samples after centrifugation and filtration

7.4.4 Results of CEC and discussion

The results of the potential cation exchange capacity of the various samples are shown in Table 16. In this research, the potential exchange capacity was calculated from the sum of all cations found in the sample. The cations consisted of Calcium, Magnesium, Potassium and Sodium ions (Saku, 2008).

Sample	Cation Exchange Capacity (meq/100g)
Klipheuwel Sand	5-9
Philippi Dune Sand	2-3*
Sand/Envirobent mixes	5-9.3
Sand/Heidelberg Raw mixes	5.3-13
Heidelberg Raw	125
Envirobent	48

* High shell content

Table 16: Results of potential Cation Exchange Capacity

7.4.4.1 Envirobent

The exchange capacity of Envirobent is similar to that of Illite as opposed to Montmorillonite. Illites have the exchange capacities in the order 10 to 40 meq/100g and Montmorillonites have an exchange capacities in the order 80 to 150 meq/100g (Grim, 1969; Mitchell 1993).

Horn & Strydom (2000) state, that the clay from the Koppies deposit has a total exchange capacity between 94 and 99 meq/100g, with the essential cations Ca^{++} and Mg^{++} contributing about 50 meq/100g to the total exchange capacity in equal proportions. However, in Envirobent each cation contributed concentrations of about 10 to 15 meq/100g. It is evident that the potential exchange capacity of Envirobent is closer to that of Illite as opposed to Montmorillonite.

Acid activation increases the surface area of the clay minerals by breaking down the continuous sheet structure of the clay. Grim (1968) points out that 80% of cationic

activity occurs in the basal surfaces of a Smectites. This activity includes cation exchanges. The remaining percentage of cationic activity occurs on the edges of the broken layers of the clay. Therefore, in Envirobent, preferential surfaces of cation activity, i.e. basal surfaces, are highly reduced by the increase of the surface area because the surfaces at which exchange occur are reduced in size and some lost due to the break down of the sheets of clay mineral. The cation exchange capacity of the clay is very low compared to those of (Horn & Strydom (2000) findings.

7.4.4.2 Heidelberg Raw

The potential cation exchange capacity of Heidelberg Raw Bentonite coincides with the cation exchange capacity value of 80 to 150 meq/100g published by Grim, (1969) and Mitchell, (1993). The Sodium cation alone contributed 100 meq/100g towards the overall CEC value.

7.4.4.3 Sand/Bentonite Mixes

The cation exchange capacity for the sand/bentonite mixes was found to be very low. All test values ranged between 2 to 14 meq/100g of mix. This is due to the high quantity of Quartz, which is a common mineral of the base sand. Also, minor clay mineral percentages within the matrix contribute minimally to the total cation exchange capacity value.

Cation exchange capacity depends on the grain size, the amount of organic matter, the amount of the clay coatings of the grains and the mineralogy of the mix. The results for Klipheuvel and Philippi Dune Sand, which consist primarily of Quartz, showed similar low exchange capacity values.

8. Geotechnical Investigation of Sand/Bentonite Mixes

8.1 Compaction

Mechanical energy is required for compaction and the energy input into the soil has a significant effect on the resulting compaction of the respective soil. Generally higher compaction energies increase in the maximum dry density of a soil and at the same time decrease the optimum moisture content. An increase in the maximum dry density is not proportional to the compaction effort because the resistance of the soil to further compaction depend on the physico-mechanical properties of the soil particles (Mitchell, 1993). These properties are the grain-size distribution, grain shape, specific gravity, amount and type of clay mineral present and pore water chemistry.

Two levels of compaction were investigated on the sand/bentonite mixes i.e., 27 blows/3 layers and 15 blows/3 layers in a Proctor pot of 100mm in diameter. This was done in order to achieve a wide range of possible dry densities, i.e. a high and a low dry density for a particular mix. Compaction in the laboratory is usually of the tamping type, while field compaction, different rollers imparts various kneading actions to the soil hence resulting in various dry densities. Therefore a need to cover a wider range of dry densities of the mixes was envisaged.

8.2 Fabric of Sand / Bentonite Mixes

The adopted compaction method and the initial state of the soil can have profound effect on both, the fabrics of the sands and the bentonite and the properties of the compacted mix. The water content is important as it controls the ease with which particles and particle groups can be rearranged under the compactive effort. If the hammer does not penetrate the soil, as is usual for compaction on the dry side of the optimum water content, then there may be a general alignment of particles or particle groups in horizontal planes. If the soil is sufficiently wet of the optimum moisture content, then the compaction hammer penetrates the soil surface hence, as a result of a bearing capacity failure under the hammer face. There is an alignment of particles along the failure surfaces. On the macroscopic scale, effects of compaction at constant

water content are to break down flocculated aggregations, destroy shear planes, eliminate large pores and produce a more homogeneous fabric (Mitchell, 1993).

Images 12 and 13 are scanning electron microscope images of typical Klipheuwel Sand/Bentonite mixes, where the fabrics of the two different materials are combined. The magnification is the same, i.e. 10 000. Image 12 shows a Klipheuwel sand mixed with 9 % Envirobent at a moisture content of 8%. In Image 13 a Klipheuwel sand mixed with 9% Heidelberg Raw Bentonite at a moisture content of 13% is shown.

In Image 12, the two different fabrics are visible: Envirobent showing a stacked “broken sheet morphology”, with Klipheuwel particles trapped in between the layers. In some regions only clay-sized Quartz particles are assembled. A Quartz particle and a layer of Bentonite lay separately in the top right corner of the image. It is believed that, upon hydration of the bentonite, the layers of the clay will swell and possibly close all the pores

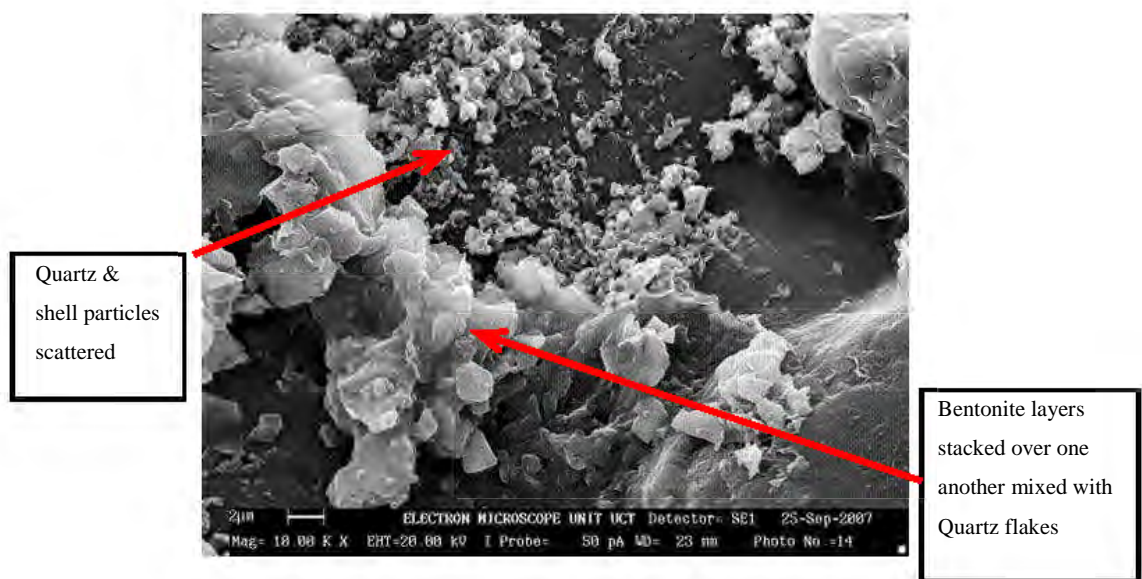


Image 12: SEM image of Klipheuwel Sand and Envirobent, Magnification 10 000 (Waldron, 2008)

In Image 13, there appears to be a continuous “blanket” of the Heidelberg Raw Bentonite embedding the sand particles. Therefore, in a Klipheuwel sand/bentonite mixture containing 9% Heidelberg Raw, the fine particles of the sand are actually coated together by the highly active bentonite.

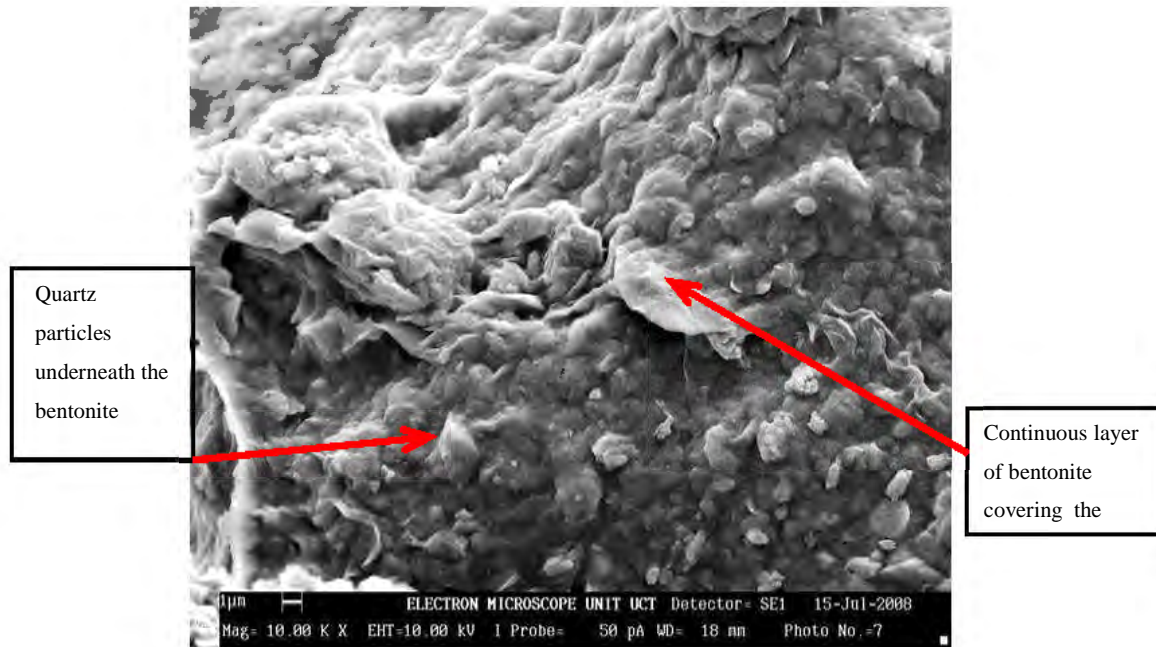


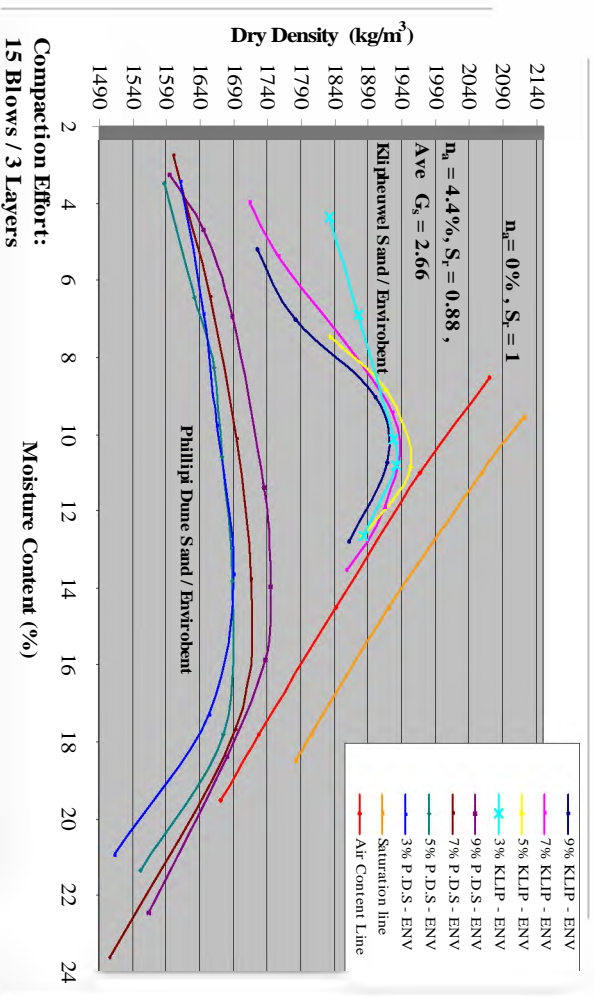
Image 13: SEM image of Klipheuwel Sand/Heidelberg Raw bentonite mix, Magnification 10 000 (Waldron, 2008)

The images suggest that, after compaction of a mix containing the Heidelberg Raw Bentonite (here 9%), a continuous layer forms and embeds the sand particles, therefore, the possible voids within mixture are completely covered by the layers of the bentonite. As hydration commences, pores within the matrix are being closed off, suggesting lowering of the hydraulic conductivity of the mixture.

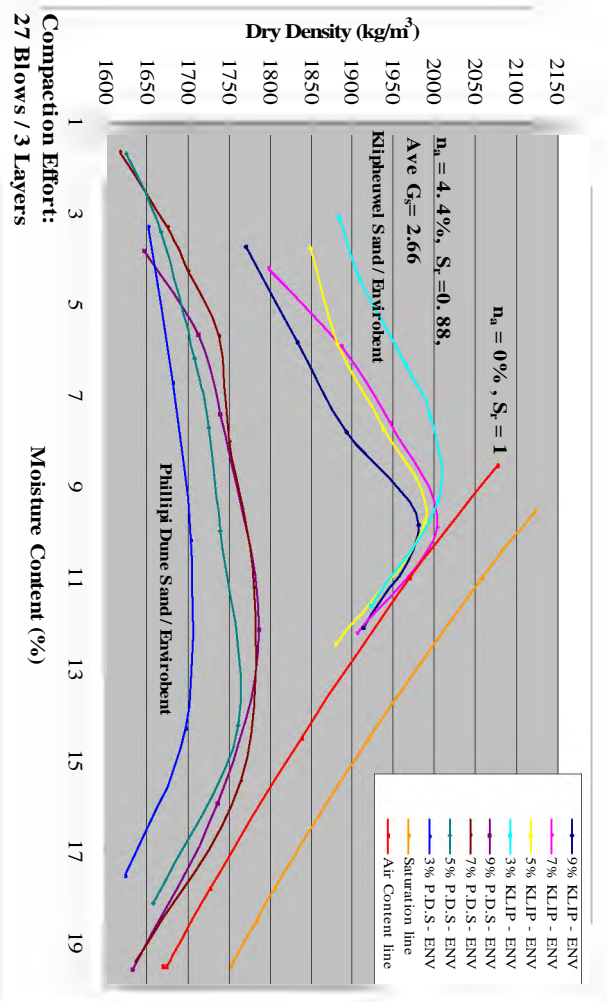
8.3 Summary of Compaction Results

A summary of the compaction results is given in Graphs 7 to 10. In Graphs 7 and 8, the effect of the sand type and Envirobent compacted with two different efforts on the dry density/moisture content behaviour is shown. Whilst, in Graphs 9 and 10, the effect of the sand type and Heidelberg Raw Bentonite is shown. Indications of the

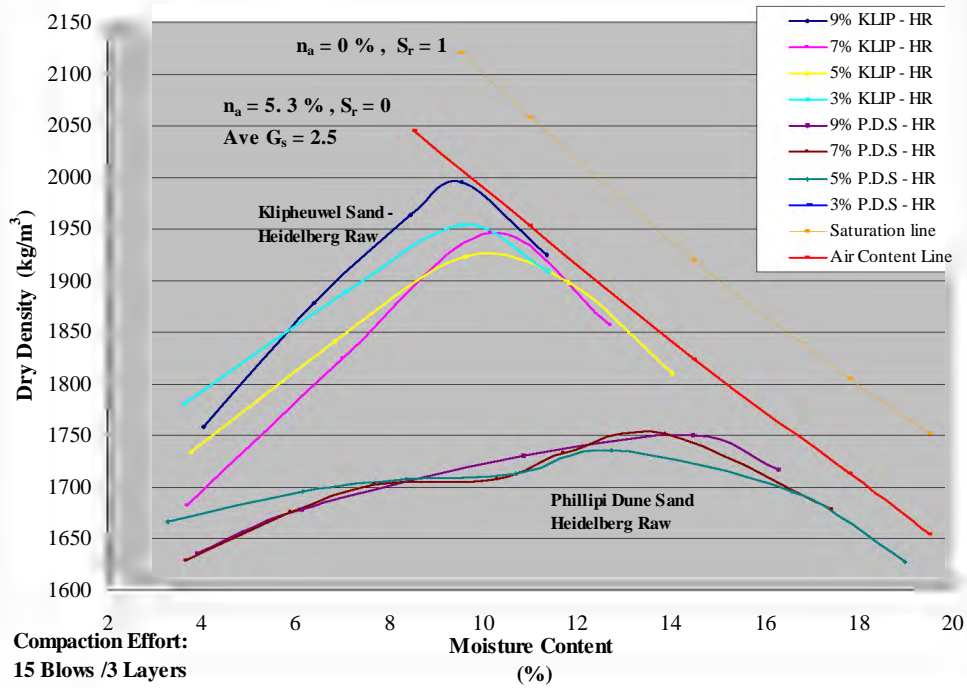
various degrees of the overall saturation of the mixes for an average specific gravity of the materials are also given. (PDS is an abbreviation of Philippi Dune sand and KLIP stands for Klipheuwel sand).



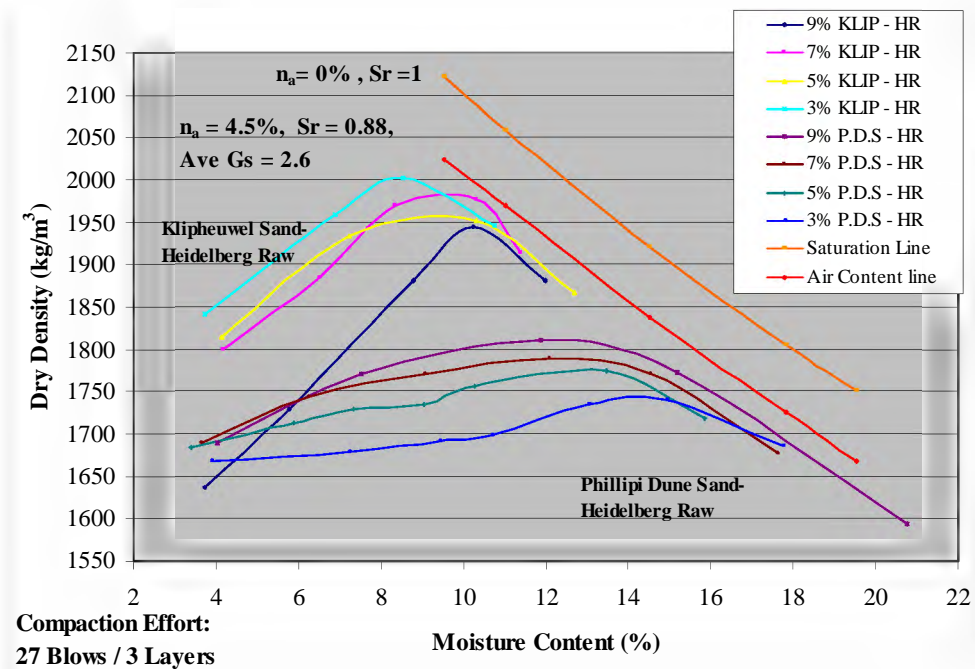
Graph 7: Effect of sand type on compaction of mixes with Envirobent



Graph 8: Effect of sand type on compaction of mixes with Envirobent



Graph 9: Effect of sand type on compaction of mixed with Heidelberg Raw Bentonite



Graph 10: Effect of sand type on compaction of mixes with Heidelberg Raw Bentonite

8.4 Discussion and Analysis

It is evident that the type and quality of bentonite that is used in sand/bentonite mixes affects the resulting fabric of the mix. The main objective of adding bentonite to the sand is to drastically reduce the amount of pores, the distribution of pore and size within a mix and thus possibly reduce the permeability of a material.

The compaction of sand/bentonite mix is unique. It is clear that the quantity of the bentonite and soil type affects the resulting maximum dry density and optimum moisture. A wide range of dry densities and moisture contents was achieved from the two compaction energy levels.

Summary Compaction of Mixes

Sand	Bentonite Type	Bentonite Content	Maximum Dry Density	Optimum Moisture Content
		%	Kg/m ³	%
Philippi Dune Sand	Envirobent	3	1690	13.6
Philippi Dune Sand	Envirobent	5	1690	15.4
Philippi Dune Sand	Envirobent	7	1715	14.5
Philippi Dune Sand	Envirobent	9	1750	12.0
Klipheuwel Sand	Envirobent	3	1934	10.6
Klipheuwel Sand	Envirobent	5	1958	10.5
Klipheuwel Sand	Envirobent	7	1933	10.2
Klipheuwel Sand	Envirobent	9	1921	10.0
Philippi Dune Sand	Heidelberg	3	1690	13.8
Philippi Dune Sand	Heidelberg	5	1735	12.8
Philippi Dune Sand	Heidelberg	7	1754	13.4
Philippi Dune Sand	Heidelberg	9	1750	14.3
Klipheuwel Sand	Heidelberg	3	1938	9.5
Klipheuwel Sand	Heidelberg	5	1934	10.1
Klipheuwel Sand	Heidelberg	7	1917	9.9
Klipheuwel Sand	Heidelberg	9	1698	9.8

Table 17: Summary of Compaction of Mixes at 15 blows per layer

Sand	Bentonite Type	Bentonite Content	Maximum Dry Density	Optimum Moisture Content
		%	Kg/m ³	%
Philippi Dune Sand	Envirobent	3	1706	12
Philippi Dune Sand	Envirobent	5	1764	13.3
Philippi Dune Sand	Envirobent	7	1780	12.7
Philippi Dune Sand	Envirobent	9	1785	12.0
Klipheuwel Sand	Envirobent	3	2005	9.2
Klipheuwel Sand	Envirobent	5	1826	13.8
Klipheuwel Sand	Envirobent	7	2004	9.8
Klipheuwel Sand	Envirobent	9	1980	9.9
Philippi Dune Sand	Heidelberg	3	1742	14.3
Philippi Dune Sand	Heidelberg	5	1775	13.0
Philippi Dune Sand	Heidelberg	7	1788	12.1
Philippi Dune Sand	Heidelberg	9	1809	11.8
Klipheuwel Sand	Heidelberg	3	1988	8.3
Klipheuwel Sand	Heidelberg	5	1986	9.9
Klipheuwel Sand	Heidelberg	7	1707	9.2
Klipheuwel Sand	Heidelberg	9	1947	8.8

Table 18: Summary of Compaction of Mixes at 27 blows per layer

9. Hydraulic Conductivity

9.1 Hydraulic Conductivity and Gradient

Hydraulic conductivity measurements in the laboratory should be made under conditions of hydraulic gradient, confinement pressure, density, fluid chemistry and temperature close to those found in the field. Unfortunately, depiction of field conditions is not always possible particularly with regards to hydraulic gradient, temperature and fluid chemistry. Hydraulic gradients found in waste containment barriers, are usually very low (0.33 to 1), because leachate generation is sporadic and highly depended on the thickness of the lining system, type of waste, climate and environmental conditions.

Temperature differences are also highly variable, due to the diverse chemical reactions and weather conditions. Permeate chemistry for laboratory testing is in general restricted to deaired tap water.

Therefore an attempt to simulate field conditions in the laboratory as well as research time frame is particularly challenging. (Chris Wise 2008). In this research, the applied hydraulic gradient was chosen to be in the order of 20 to 33. The temperatures in the laboratory averaged between 15°C to 21°C through out the testing period depending on the outside weather conditions.

9.2 Falling Head Permeability

Falling-head permeability test stands were developed at the Geotechnical Laboratory of the University of Cape Town, as shown in Photo 12. The flexible wall principle was applied as the 100mm diameter samples were encased in rubber membranes in triaxial cells. The tests were carried out according to the ASTM D5084.



Photo 12: Falling Head Permeability test apparatus

Two sets of equations are used to determine the coefficient of permeability, the inflow permeability, k_{in} and the outflow permeability, k_{out} .

De-aired water in standpipes is allowed to flow through the sample. The initial head $h = h_1$ at $t = t_1$ is recorded. After a period of time, $t = t_2$, the water level is measured $h = h_2$. The coefficient of permeability k_{in} through the sample is given by:

$$k_{in} = \frac{aL \ln\left(\frac{h_1}{h_2}\right)}{A(t_2 - t_1)} \quad (1)$$

Where $h_i =$ head level at time t_i

$A =$ cross-sectional area of specimen

$a =$ cross-sectional area of standpipe

$L =$ length of specimen

Using Darcy's law, the outflow (Q) coefficient of outflow k_{out} , after time thus $t = t_2$ is given by:

$$k_{out} = \frac{Q}{(iA)} \quad (2)$$

where A = cross sectional area of specimen

i = hydraulic gradient

Q = quantity of flow in time Δt

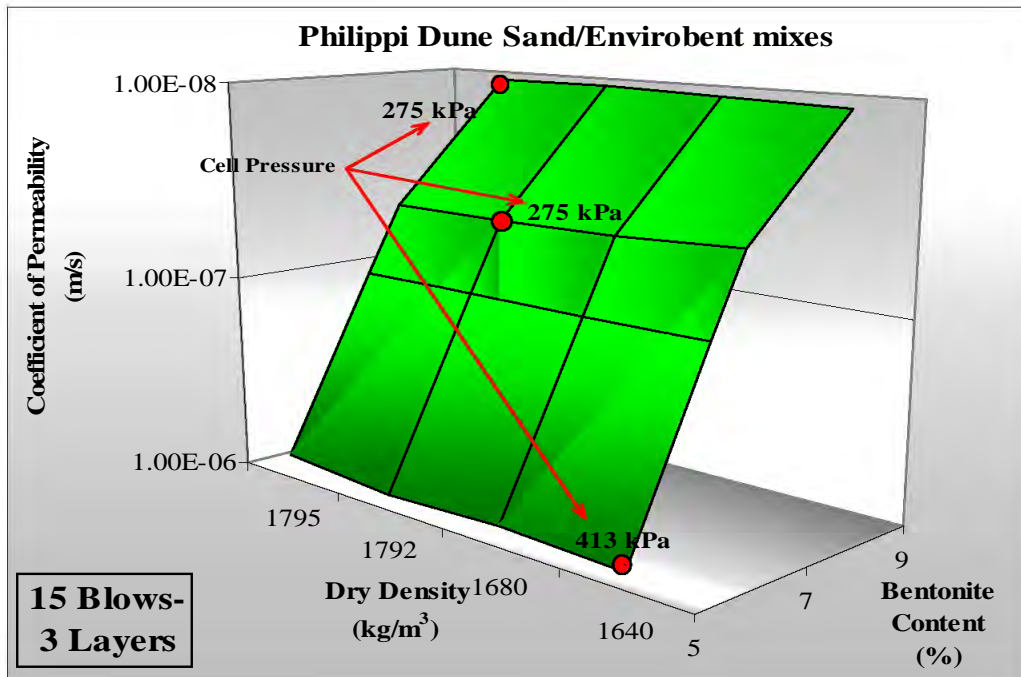
The two coefficients are then plotted against the in graphs representing coefficient of permeability of k_{in} and k_{out} , hence upon close conversion of these curves, the experimental coefficient of the mix is determined. A typical graph is shown in Appendix E.

9.3 Summary of Permeability Testing

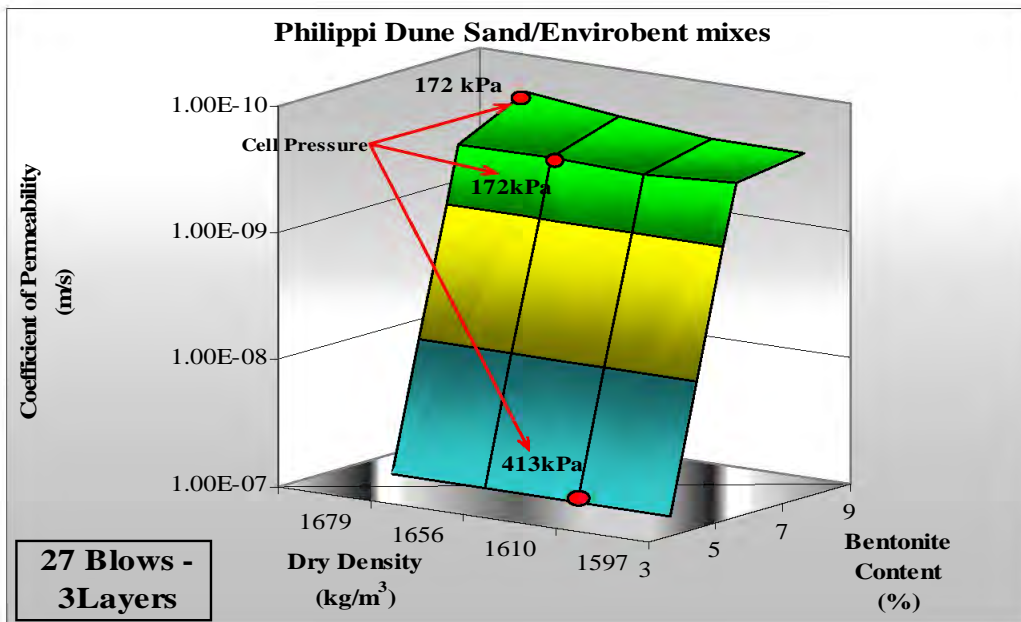
The results of the permeability testing of the investigated sand/bentonite mixes are presented in Graphs 11 to 18. The 3-D graphs address the bentonite content, the dry density and the coefficient of permeability. The surfaces were developed using the results of individual permeability tests i.e. the coefficients *ave* k_{in} and *ave* k_{out} . Each dot in the surface indicates a specific test at a particular dry density and bentonite content. The confinement pressure is added to show the behaviour of a mix at the respective all round pressure.

The idea is to give a pictorial behaviour of the coefficients of permeability as the bentonite content increases in a mix of a particular soil. In addition, the graphs allows for the reader to see the range dry densities achieved.

Philippi Dune Sand/ Envirobent mixes



Graph 11: Dry Density - Bentonite Content - Coefficient of Permeability of Philippi Dune Sand/Envirobent mixes



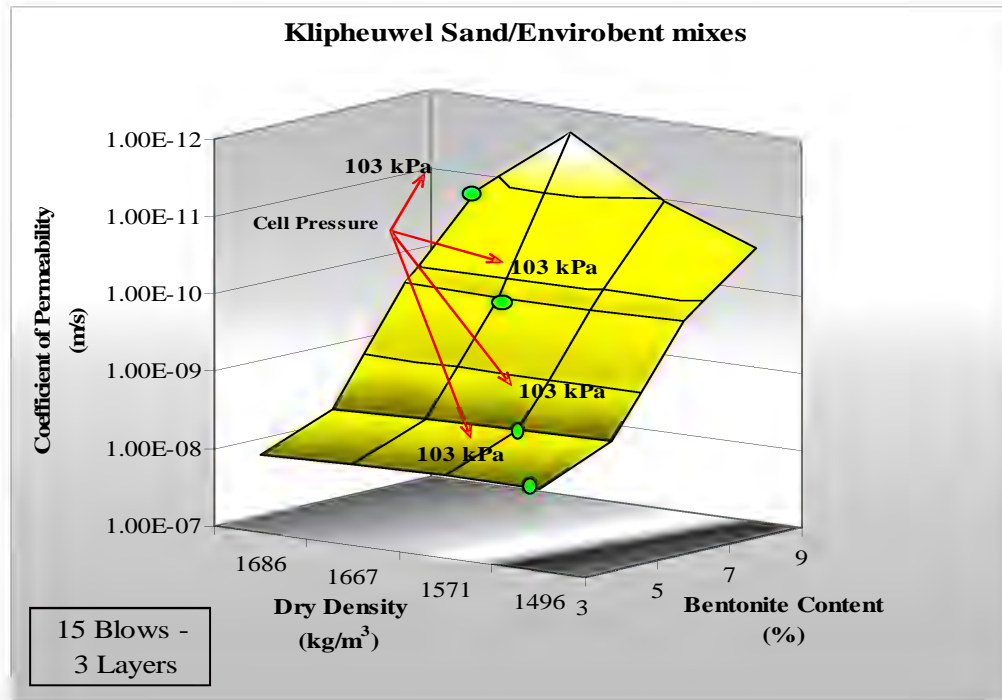
Graph 12: Dry Density - Bentonite Content - Coefficient of Permeability of Philippi Dune Sand/Envirobent mixes

In the Graphs 11 and 12, Philippi Dune Sand/Envirobent “surfaces” are presented. It was noticed that the 3% Envirobent mixes had insufficient bentonite to homogenise the matrix of the Dune sand hence they were discarded from the testing programme.

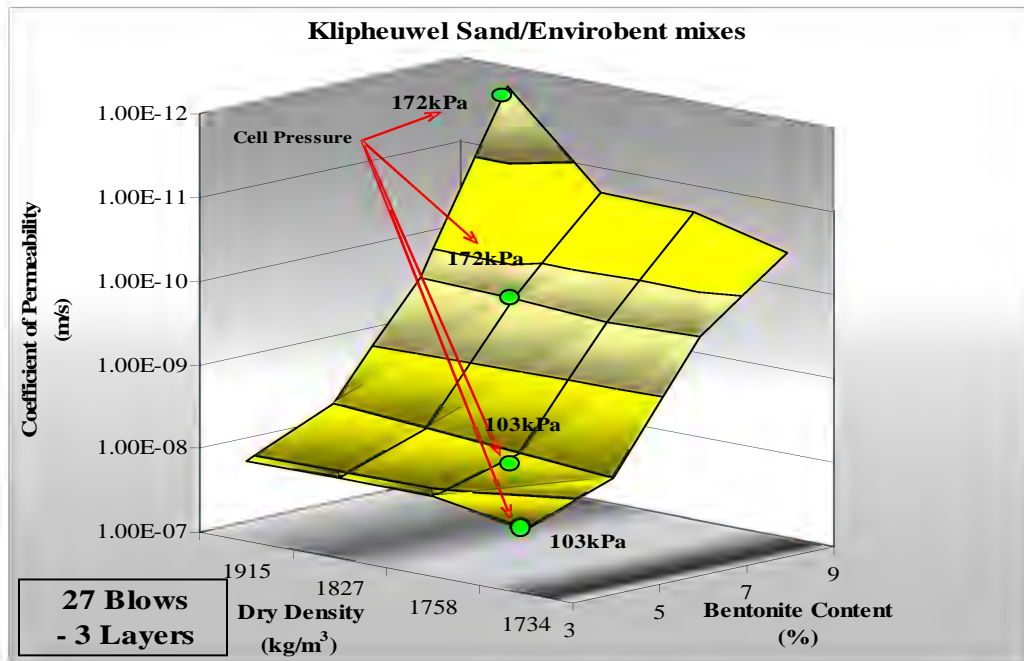
Both graphs show a steep decrease in the coefficient of permeability as the bentonite contents changes from 5% to 9%. The compaction effort affects the coefficient of permeability considerably as the range of coefficients of permeability in Graph 11 is higher than those in Graph 12. The confinement pressures are also higher in Graph 11 than those in Graph 12, but do not appear to affect the coefficient of permeability. As the bentonite contents increases the range of dry densities does not change as anticipated.

The geotechnical properties, such as grain size distribution, shape and texture of the Philippi Dune sand affects the compacted matrix of these mixes. This implies that the pore distribution and size within these samples are not sufficiently sealed by the bentonite. Therefore a decrease of the coefficient of permeability is highly dependant on an increase of bentonite content within a mix. However, due to the type of grains of Philippi Dune sand, a higher bentonite contents affect the structural integrity of the matrix of mix as its plasticity increases.

Klipheuwel Sand/ Envirobent mixes



Graph 13: Dry Density - Bentonite Content - Coefficient of Permeability of Klipheuwel Sand/Envirobent mixes

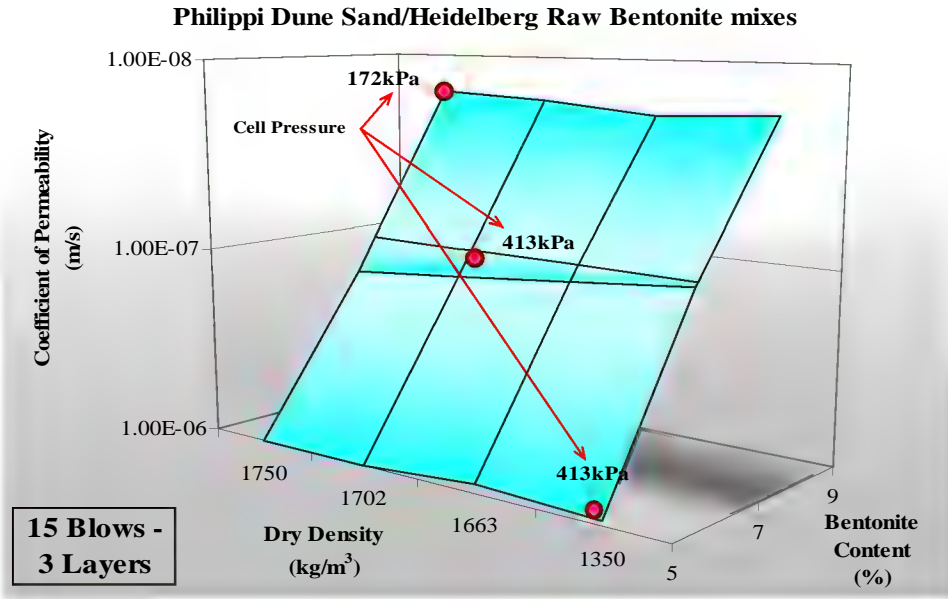


Graph 14: Dry Density - Bentonite Content - Coefficient of Permeability of Klipheuwel Sand/Envirobent mixes

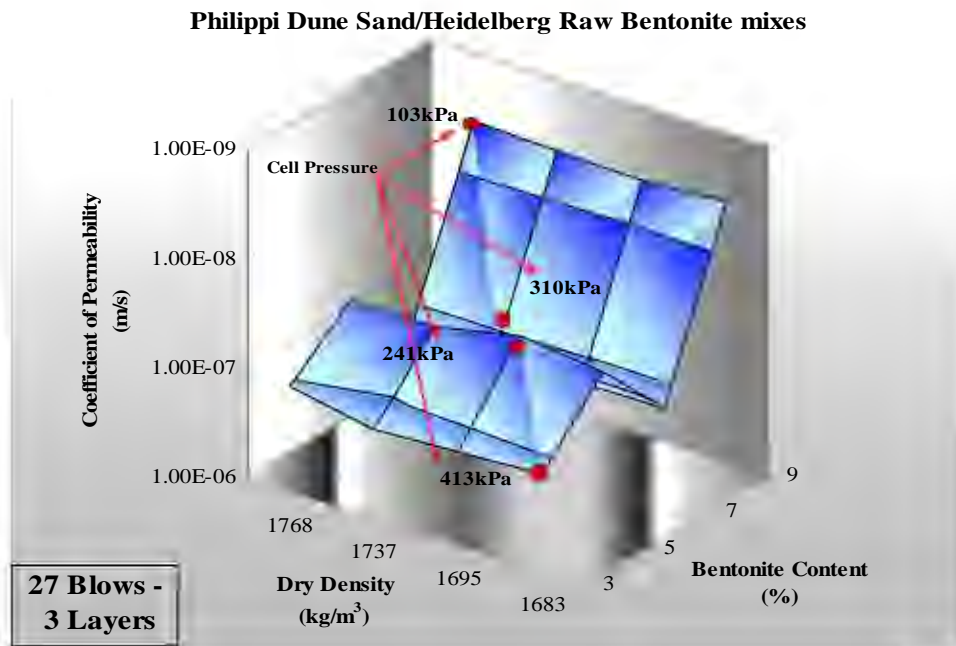
Klipheuwel/Envirobent mixes are presented in Graphs 13 and 14. Both graphs show a gradual decline in the coefficient of permeability as the bentonite content changes from 3% to 9%. The compaction effort does not affect coefficient of permeability as evidently displayed in the both graphs. Furthermore, the confinement pressures do not affect the coefficients of permeability as the bentonite content increase.

The geotechnical properties of Klipheuwel sand influence the coefficient of permeability of these mixes. Klipheuwel has sub-angular to irregular shaped particles and a considerable amount of silt sized particles in the range 20 μ m to 75 μ m. These properties assists in closing the voids and reduce the distribution of pores within a compacted matrix of the mix. As the bentonite contents increases, the remaining voids are sufficiently sealed hence lowering the coefficient of permeability. Furthermore, more as the bentonite content increases the range of dry densities also widens, partly contributed by the characteristic nature of the sand.

Philippi Dune Sand/ Heidelberg Raw Bentonite mixes



Graph 15: Dry Density - Bentonite Content - Coefficient of Permeability of Philippi Dune Sand/Heidelberg Raw Bentonite mixes



Graph 16: Dry Density - Bentonite Content - Coefficient of Permeability of Philippi Dune Sand/Heidelberg Raw Bentonite mixes

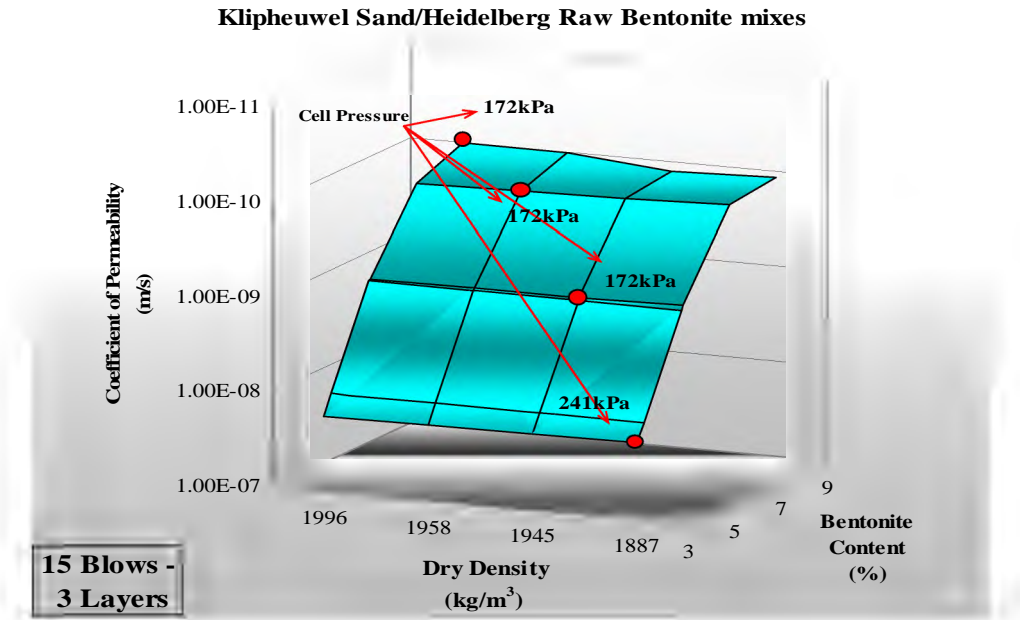
Philippi Dune Sand/Heidelberg Raw Bentonite mixes are present in Graphs 15 and 16. The Philippi Dune/3% Heidelberg Raw Bentonite sand test was discarded from the testing programme as fines were being flushed from the samples (piping) were experienced.

A steep decrease in the coefficient of permeability as the bentonite content changes from 5% to 9% is observed in Graph 15. The compaction effort is seen to influence the coefficients of these mixes..

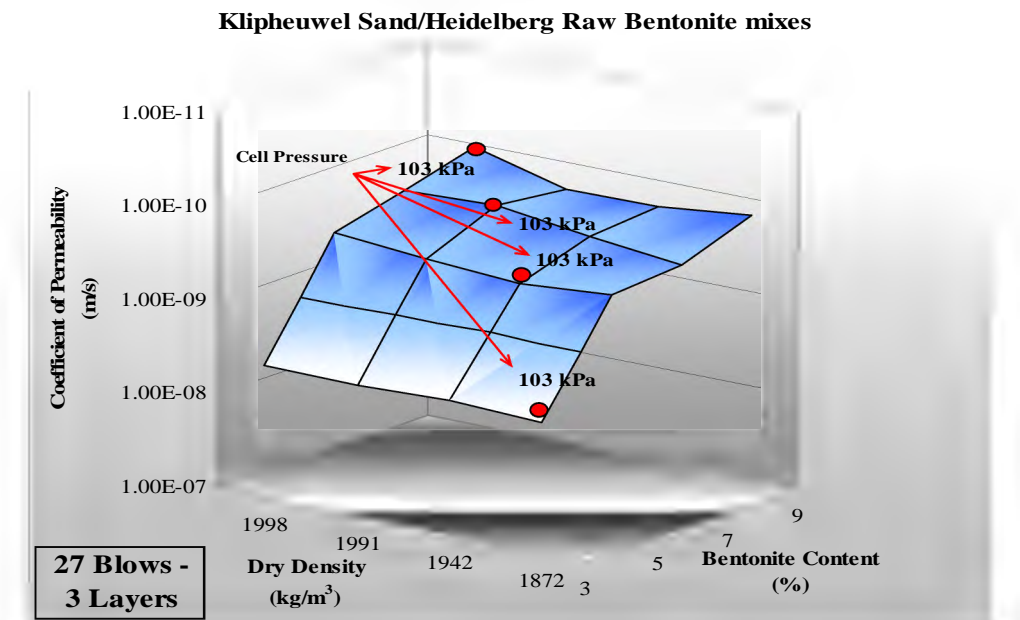
In Graph 16, a similar behaviour of the coefficients of permeability could have occurred but the permeability of the 7% sample increased considerably. The confinement pressure was higher than the 5% sample. It is noted that the dry densities of these samples were in the same order of magnitude.

A conceivable explanation is based on the geotechnical properties of the Dune Sand as described above. As the bentonite content increases, compactibility of the mixes become problematic as the particles shape and size determines void closure which lower the coefficient of permeability. Compton & Franceschini, (2006) and the XRF results indicate substantial quantities of carbonatious substances within the Philippi Dune sand. Therefore the varieties of distribution of pores are complicated by such substances.

Klipheuwel Sand/ Heidelberg Raw Bentonite mixes



Graph 17: Dry Density - Bentonite Content - Coefficient of Permeability of Klipheuwel sand/Heidelberg Raw Bentonite mixes



Graph 18: Dry Density - Bentonite Content - Coefficient of Permeability of Klipheuwel Sand/Heidelberg Raw Bentonite mixes

The permeability test results of Klipheuwel sand /Heidelberg Raw Bentonite mixes are present in Graphs 17 and 18. In both graphs, the compaction effort affects the coefficient of permeability of the mix. In Graph 17 the coefficient of permeability gradually decreases as the bentonite content increases. Also, the higher confinement pressure, i.e. 5 % samples, provides additional closure of voids which lower coefficient of permeability as anticipated.

In Graph 18, a uniform near horizontal surface is displayed. As the bentonite content increases the permeability also decreases with a constant all round pressure.

Heidelberg Raw Bentonite and Klipheuwel sand appears to be an ideal mixture for an impervious barrier. The Klipheuwel sand provides the structural frame work and matrix while the Bentonite fills the pores that were left behind during compaction and reduces drastically the coefficient of permeability of a mix.

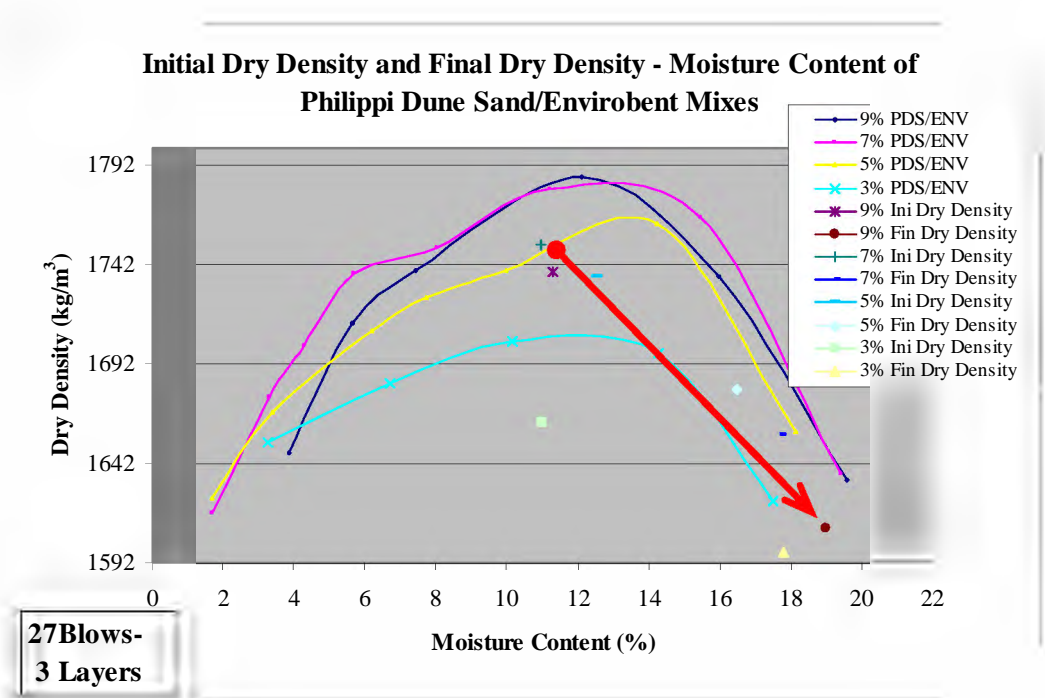
A consistent range of coefficients of permeability and a steady increase of dry densities (in the case of low and high compactive efforts) depends on the quality of the bentonite in terms of its morphological structure.

9.4 Discussion and Analysis

Hydration period of Sand/Bentonite mixes

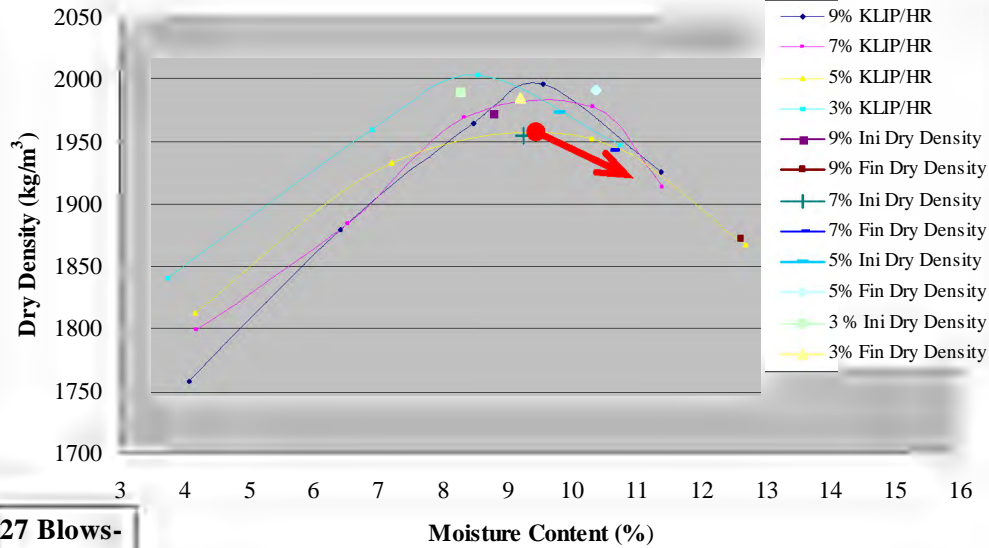
The hydration period of sand/bentonite mixes is variable. Depending on the bentonite content, confinement pressure and compaction, saturation usually takes 7 to 12 days to reach a steady state conditions. The criteria chosen for accessing complete hydration was based on monitoring certain aspects of a test. Firstly, the amount of trapped air bubbles within the lines leading to the sample was an initial indication that the sample has not reach saturation. Secondly, the fluctuation of the confinement pressure gauge around the chosen pressure. Monitoring of these data continued for roughly 4 days. Upon full hydration the pressure remained constant and air bubbles have disappeared.

In order to access the moisture content prior and after permeability testing an analysis of the moisture contents of selected sand/bentonite mixes (compacted with 27 blows/3layers) is presented in Graph 19 and 20. In Graph 19 a typical dry density/moisture content relationship of Philippi Dune Sand/Envirobent mixes shows that the permeability test samples experience a large increase of moisture (ave 7%), during the test period as indicated by the arrow. This reduces the dry density of the mixes.



Graph 19: Initial Dry Density and Final Dry Density - Moisture Content of Philippi Dune Sand/Envirobent mixes

Initial Dry Density and Final Dry Density - Moisture Content of Klipheuwel/Heidelberg Raw Mixes



**27 Blows-
3 Layers**

Graph 20: Initial Dry Density and Final Dry Density - Moisture Content of Klipheuwel Sand/Heidelberg Raw Bentonite mixes

For comparative reasons the same analysis was undertaken addressing the Klipheuwel Sand/Heidelberg Raw Bentonite with the same compaction effort. The results are shown in Graph 20. It is noticed that during permeability testing lesser quantities of water (ave 4%) were drawn into the sample as indicated by the arrow.

10. Conclusions

The aim of this research was to investigate the engineering behaviour and geo-mechanical properties of materials selected for the use of hydraulic barriers.

The objectives were to adopt exploratory investigative techniques to understand the geochemical properties and morphology of a commercially available treated local bentonite and a selected local bentonite. Furthermore, to study physico-mechanical properties and fabric of sands suitable for the selection of sand/bentonite mixes used in hydraulic barriers.

The objectives were also to determine the coefficient of permeability of different sand/bentonite mixes using the selected bentonites mixed with local sands of various densities subjected to a wide range confinement stresses.

The investigative techniques involved the use various departmental laboratories of the University of Cape Town. These laboratories were the Department of Physics, the Department of Chemical Engineering, the Department of Chemistry, the Department of Geological Sciences and the Geotechnical Laboratory of the Department of Civil Engineering. The conclusions of the research are divided into two sections i.e. Geochemical conclusions and Geotechnical conclusions and are given below.

Geochemical Conclusions

Philippi Dune Sand

Philippi Dune sand is primarily composed of Quartz particles which are smooth and regularly shaped due to its Aeolian deposition. There is a considerable amount of carbonatious substances such as shells within the sand. The X-ray fluorescence spectrometer also reveals a high loss of ignition indicating presence of combustible substances and high Silicon dioxide content. The potential cation exchange capacity is low (2-3 meg/100g) due to its high Quartz content.

Klipheuwel Sand

Klipheuwel sand is weathered a Cape Granite comprising of mainly consisting of Quartz. The sand is composed of sub-angular to irregular shaped particles with a considerable amount of finer particles in the range 20µm to 75µm. The surfaces of the particles are coarse to rough textured. The potential cation exchange capacity is low (5-9 meq/100g). The X-ray fluorescence spectrometer show high percentages of Silicon dioxide, due to its high Quartz content.

Envirobent

Envirobent is a product name of a sulphuric acid activated Calcium rich Montmorillonite clay mineral. Activation is the chemical treatment applied to certain types of clays to develop chemical and physico mechanical changes such as an increase in surface area and enhancing bleaching powers. Depending on the length of treatment, concentration of acid and type of Smectite the effects of acid activation are more significant in the morphology of layered structure of the clay (Komadel, 1999; Laird, 2006; Christidis et al. 1997; Babaki et al. 2007).

The X-ray diffractometer of Envirobent has identified the Illite as the main mineral within clay. The X-ray fluorescence spectrometer has also shown considerable changes in the chemical composition of the Envirobent compared to the original clay (Koppies) in findings published by Horn & Strydom, (2000). The potential cation exchange capacity of Envirobent is similar to that of the Illite (48 meq/100g) as opposed to Montmorillonite (100 meq/100g).

Transmission electron microscopy of Envirobent shows presences of non-expandable layers similar to micrographs of Illites found by Vali & Hesse (1990). Only secluded portions of the micrograph exhibited expandable layers as opposed to a uniform array of individual layers. The layers also appeared broken, discontinuous and dispersed. Transmission electron microscopy Hexal-Alkylammonium treated Envirobent appear blurred and presents very few visible and measurable basal spaces of individual layers.

Heidelberg Raw Bentonite

Heidelberg Raw Bentonite is an in-house name given to the second type of bentonite investigated in this research work. This bentonite was hand collected at the Heidelberg mine in May 2008. The Bentonite is mined by a subsidiary of the South African Minerals Resource Committee (SAMREC), called Cape Bentonite Mine

The diffraction pattern of the Heidelberg Raw bentonite (shown in Graph 6) has identified only one mineral i.e. Sodium Montmorillonite with the chemical formula $\text{Na}_{0.3}(\text{Al}, \text{Mg})_2\text{Si}_4\text{O}_{10}(\text{OH})_2 \cdot 4\text{H}_2\text{O}$, with a d -spacing of 13.6\AA and a diffraction angle of 6.49° .

The potential cation exchange capacity of Heidelberg Raw coincides with the cation exchange capacity value of 80 to 150 meq/100g published by Grim, (1969) and Mitchell, (1993). The Sodium cation alone is 100 meq/100g, hence suggesting that this element is the main exchangeable cation.

The X-ray florescence results of Heidelberg Raw Bentonite appear to be consistent with the soda-ash activated Drilling mud published by Horn & Strydom (2000) in Table 11.

Transmission electron microscopy of Heidelberg Raw Bentonite exhibit layers that are curvy suggesting flexibility and continuity of the layers. The clear fringes represent the expandable interlayers. Hexal-Alkylammonium treatment of Heidelberg Raw has an expanded basal spacing of 12.22\AA . This is an additional expansion of 1.44\AA from the original basal spacing of the bentonite. The extent of basal expansion depends on the Alkylammonium solution used.

Fabric of Sand/Bentonite mixes

The Scanning electron microscopy of Sand/Envirobent images show that sand particles rest in various locations within a mix. In the image found in Chapter 8 it is evident there could be a separation of the bentonite layers and the sand particles. Also most particles rested on the layers of the bentonite and appeared not to have integrated with the bentonite layers, whereas, in Sand/Heidelberg Raw Bentonite mixes seen (in

Chapter 8), the sand particles are embedded altogether in the continuous layers of the bentonite.

Geotechnical Conclusions

A flexible wall test setup in connection with the falling head principle was designed and implemented. The setup accommodated six permeameters running concurrently. The mixes were compacted at a relatively higher and relatively lower energy levels to cover a wide range of densities so as to simulate those obtained in major field works.

The design of a laboratory depicts range of the hydraulic gradients that can be applied to samples. Flexible wall permeability testing is considered to be of a laminar flow hence samples have to be tested across a wide range of hydraulic gradients to identify behavioural patterns of coefficients of permeability of mixes. The design of geotechnical laboratory of the University of Cape Town limits the ranges of gradients that samples could be subject to. Ideally high and low hydraulic gradient should be explored, but this was possible during this research.

Sand/Envirobent mixes

The coefficients of permeability of Philippi Dune sand/Envirobent mixes are considered as high. The lowest coefficient is in the order 1×10^{-9} m/s and the highest coefficient is in the order 1×10^{-6} m/s. The range of the achieved dry densities is not as wide as anticipated.

Low bentonite contents in Philippi Dune sands i.e. 3% to 5% exhibited experimental complications and are highly subject to piping. Furthermore, these samples cannot sustain high confinement stresses without inducing lateral failures.

It is concluded that the coefficient of permeability of Philippi Dune sand/Bentonite mixes is highly affected by the nature of the characteristics of the Philippi Dune sand, as opposed to an increase in the bentonite content. These characteristics include the grain size distribution, low achievable dry densities and inconsistent of particles such as shells within the soil mass.

In general Klipheuwel sand/Envirobent mixes have low coefficients of permeability. The coefficients are in the order 1×10^{-8} to 1×10^{-12} m/s. Furthermore a wider range of dry densities have been achieved. The coefficient of permeability of Klipheuwel

sand/Envirobent is not affected by the compaction effort as lower compaction energy mixes resulted in coefficients similar to those of high compaction energy mixes.

Although the confinement stresses for Klipheuwel sand/Envirobent mixes were not as high as Philippi Dune sand/Envirobent mixes. This is because the magnitude of the dry archived dry densities for Klipheuwel sand/Envirobent mixes were much higher than those of Philippi Dune sand/Bentonite mixes.

It is therefore concluded that the grains size distribution of Klipheuwel sand contributes immensely towards decreasing the void and distribution of pores within a compacted mix. This characteristic property is ideal for lowering the coefficient of permeability of Klipheuwel sand/Envirobent mixes

However, the grain size distribution of Envirobent also plays a major role in both Philippi Dune sand and Klipheuwel sand mixes. It is believed that if a finer grain size i.e. less than $63\mu\text{m}$ particles of Envirobent were used in these mixes higher coefficients could have resulted. This belief is supported by the given geochemical results discussed above.

It is recommended that in order to achieve low coefficients of permeability for Sand/Envirobent mixes higher i.e. greater than 9% bentonites percentages must be considered. The geotechnical properties of the selected sand should have similar properties as those of Klipheuwel sand as opposed to Philippi Dune sand.

Sand/Heidelberg mixes

Philippi Dune sand/Heidelberg Raw Bentonite mixes behaviour similarly as Philippi Dune sand/Envirobent mixes. Although a higher confinement stress was applied to these mixes, internal lateral failures occurred frequently which resulted in increases in the coefficient of permeability of samples. The range of coefficients of permeability was in the order 1×10^{-6} m/s to 1×10^{-9} m/s. However, a wider range of dry densities was achieved.

Klipheuwel sand /Heidelberg Raw Bentonite mixes show ideal behaviours of the coefficient of permeability as the bentonite content increase, i.e. the coefficient of permeability reduces as the bentonite content increases(within the tested range of percentage contents). There is also a significant difference in coefficient of permeability of mixes given the two compaction levels. It is believed that the quality of Heidelberg Raw Bentonite is responsible for these observations.

It is recommended that Klipheuwel sand /Heidelberg Raw mixes are ideally suited as mixes for impervious liners. Low coefficients of permeability can achieved from bentonite contents as low as 5 % Heidelberg Raw Bentonite, provided the geotechnical properties of the soil are similar or 'better' than those of Klipheuwel sand.

Conclusions

Lastly, the selection of sand/bentonite mixes for the use of hydraulic barriers solely depends on the geological qualities of bentonite and the grain size distribution of the soil. The design of sand/bentonite mixes should be based on the conditions surrounding its final use as an impervious liner.

Furthermore the compaction techniques adopted in field operation as opposed to those adopted in a laboratory affects the final distribution of the bentonite within the sand matrix. Field compactions are highly variable, therefore could comprise the global performance of a mix (Chapius, 1989).

From the testing knowledge gained from this research the coefficient of permeability of a mix depends also on the mixing capabilities of the machinery used. Emphasis on homogeneity must be attained at all times during sample preparation.

Ultimately, it is the client and hence the end user, i.e. the society, that benefit from a collective selection of technical information as outlined in this research for novel practices in the design and construction of a landfills.

References

1. Abichou, T., Benson, C.H. & Edil, T.B. (2002). *Micro-structure and hydraulic conductivity of simulated sand-bentonite mixtures*. Clays and Clay Minerals, Vol. 50, No 5, 537-545
2. Abichou, T., Benson, C.H., & Edil, T.B. (2000). *Foundry green sands as hydraulic barriers: laboratory study*. Journal of Geotechnical and Geoenvironmental Engineering, Vol. 126, 1174-1183
3. Allen, A. (2000). *Containment landfills: the myth of sustainability*. Engineering Geology, Vol. 60, 3-19
4. Agnello, V.N. (2004). *Bentonite, pyrophyllite and talc in the Republic of South Africa*, Directorate: Mineral Economics, 1-67
5. ASTM D5084. *Standard test method for measurement of hydraulic conductivity of saturated porous materials using a flexible wall permeameter*. [Online] Available: www.astm.org, 5th February 2007
6. Bakaki, H., Salem, A. & Jafarizad, A. (2008). *Kinetic model for the isothermal activation of bentonite by sulphuric acid*. Material Chemistry and Physics, Vol. 108, 263-268
7. Bremmer, C.N., Meskers, C.G., Weststrate, F.A., & van Ree, C.C.D.F. (1992). *Design aspects and permeability testing of natural clay and sand-bentonite liners*. Geotechnique 42, No.1, 49-56
8. Birch, G.F. (1975). *Sediments on the continental margin off the west coast of South Africa*. Bulletin No. 6 Marine Geoscience Group, Department of Geological Sciences, University of Cape Town, South Africa

9. Chapuis, R.P. & Pouliot, G. (1996). *Determination of bentonite content in soil-bentonite liner by X-ray diffraction*. Canadian Geotech Journal, Vol. 33, 760-769
10. Chapuis, R., Marcotte, D & Aubertin, M. (2006). *Discussion of network model for hydraulic conductivity of sand-bentonite mixtures*. École Polytechnique de Montréal, Québec, Canada
11. Chapuis, R. (1989). *Sand-bentonite liner: predicting permeability from laboratory tests*, École Polytechnique de Montréal, Québec, Canada
12. Czímerová, A., Bujdák, J. & Dohrmann, R. (2006). *Traditional and novel methods for estimating the layer charge of smectites*. Applied Clay Science. Vol. 34, 2-13
13. Compton, S.J & Franceschini, G. (2006). *Holocene Evolution of the sixteen mile beach complex, Western Cape, South Africa*. Journal of Coastal Research, Vol. 22, 1158-1166
14. Compton, S.J & Franceschini, G. (2004). *Aeolian and marine deposits of the Tabakbaai Quarry area, Western Cape, South Africa*. South African Journal of Geology, Vol. 107, 619-632
15. Compton, J.S. (2004). *The Rocks and Mountains of Cape Town*. Double Storey Books Crescent Wetton, Cape Town, South Africa
16. Cowland, J.W. & Leung, B.N. (1991). *A field trial of a bentonite landfill liner*. Waste Management & Research, Vol. 9, 277-291
17. DWAF (2008), Minimum requirements for waste disposal by landfill. 2nd Ed, Department of Water Affairs and Forestry

18. Divey, H. (2008), *AAS, Atomic adsorption spectrometer*. [Personnel Consultations]. Department of Chemical Engineering, University of Cape Town
19. Gates, W.P., Anderson, J.S., Raven, M.D. & Churchman, G.J. (2000). *Mineralogy of bentonite from Miles, Queensland, Australia and characterisation of its acid activation products*. Applied Clay Science, Vol. 20, 189-197
20. Garlanger, J.E., Cheung, F K A., & Tannous, Bishar S., *Quality control testing for a sand-bentonite liner*. Waste Disposal Practice, 489-499, Orlando. USA
21. Grim, R.E (1968). *Clay Mineralogy*. 2nd Ed, Mc Graw Book Company. New York
22. Güven, N. (1991). *On a definition of Illite/Smectite mixed-layer*. Clays and Clay minerals. Vol. 39, 661-662
23. Gustafsson, M. (2004). *Classification of key parameters of sand/bentonite mixtures for use as liners for sanitary landfill*. Journal of Geotechnical Engineering. Vol. 120, 691-698
24. Horn C.F.J & Strydom J.H. (2000), *Clay*. The mineral resources of South African 6th Ed. Council for Geosciences South Africa
25. Jaffers, M. (2008). *TEM, Transmission Electron Microscopy*, [Personnel Consultations]. Department of Physics, University of Cape Town
26. Komadel, P., Janek, M., Madejova J., Weekes, A., & Breen C. (1997). *Acidity and catalytic activity of mildly acid-treated Mg-rich montmorillonite and hectorite*. J.Chem. Soc., Faraday Trans, Vol. 23, 4207-4210

27. Kenney, T.C., van Veen, W.A., Swallow, M.A., & Sungila, M.A. (1992). *Hydraulic conductivity of compacted bentonite-sand mixtures*. Canadian Geotech Journal, Vol. 29, 364-374
28. Kleinhans, H. (2008). Cape Bentonite Mine manager, Heidelberg [Personnel Consultation]
29. Komadel, P., Bujdák, J., Madejová, V., Šucha, V. & Elsass, F. (1996). *Effect of non – swelling layers on the dissolution of reduced-charge montmorillonite in hydrochloric acid*. Clay Minerals, Vol. 31, 333-345
30. Komadel, P. (1999). *Structure and Chemical characteristics of modified clays*. Institute of Inorganic chemistry, Slovak Academy of Sciences, 3-18
31. Koerner, R. & Daniel, D. (2007). *Waste Containment Facilities 2nd Ed*, American Society of Civil Engineers, Texas, USA
32. Laird, D.A., Thompson, M.L., & Scott, A. D. (1989). *Technique for transmission electron microscopy and X-ray powder diffraction analyses of the same clay mineral specimen*. Clays and Clay Minerals, Vol. 37, No. 3, 280-282
33. Laird, D.A., Fenton T.E., & Scott, A.D. (1989). *Evaluation of the Alkylammonium method of determining layer charge*. Clays and Clay Minerals, Vol. 37, No. 1, 41-46
34. Laird, D.A., Fenton T.E., & Scott, A. D. (1987). *Interpretation of Alkylammonium characterisation of soil clays*. Soils Science Society American Journal, Vol. 51, 1659-1663
35. Laird, D.A. (2006) *Influence of layer charge on swelling of smectites*. Applied Clay Science, Vol. 34, 74-87

36. Laird, D. & Fleming, P. (2008). *Analysis of layer charge, cation and anion exchange capacities and synthesis of reduced charge clays*. Soil Science Society of America, Madison, USA Chapter 16, 485-508
37. Malusis, A.M., Shackelford, D.C., & Olsen, W.H. (2003). *Flow and transport through clay membrane barriers*. Engineering Geology Vol. 70, 235-248
38. Malan, J.A & Viljoen, J.H.A. (1990). *South Cape Excursion*. Geological Society of South Africa, 50-53
39. Noyan, H., Önal, M. & Sarikaya, Y. (2007). *The effect of sulphuric acid activation on the crystallinity, surface area, porosity, surface acidity and bleaching power of bentonite*. Food Chemistry, Vol. 105, 156-163
40. Önal, M. (2007). *Swelling and cation exchange capacity relationship for the samples obtained from a bentonite by acid activation and heat treatments*. Applied Clay Science, Vol. 37, 74-80
41. Ried, D. (2008). *XRF, X-Ray Florescence*, [Personnel Consultations]. Department of Geological Sciences, University of Cape Town
42. Ronel A. (2008). *XRD, X-Ray Diffraction*, [Personnel Consultations]. Department of Geological Sciences, University of Cape Town
43. Ruehlicke, G. & Kohler, E.E. (1981). *A simplified procedure for determining layer charge by the n - Alkylammonium method*. Clay Minerals, Vol. 16, 305-307
44. Sällfors, G. & Öberg-Högsta, A. (2002). *Determination of hydraulic conductivity of sand-bentonite mixture for engineering purposes*. Geotechnical and Geological Engineering, Vol. 20, 65-80
45. Sieas, P. (2008). *CEC, Cation exchange capacity preparations*, [Personnel Consultations]. Department of Geological Sciences, University of Cape Town

46. Smith, J. S. (1993). *Quartz*. Adopt-a-Mineral Project Example Paper. Department of Geological Sciences, University of Cape Town
47. Steward, D.I., Studds, P.G. and Cousens, T.W. (2003). *The factors controlling the engineering properties of bentonite-enhanced sand*. Applied Clay Science, Vol. 23, 97-110
48. Stout, P (2008). *XRF, X-Ray Florescence* [Personnel Consultations], Department of Geological Sciences, University of Cape Town
49. St. Husz, G. (2000). *Lithium chloride solution as an extraction agent for soils*, ÖKO- Datenservice Report, Leobersdorf, Austria
50. Spooner, A.J. & Giusti, L. (1999). *Geochemical interactions between landfill leachate and sodium bentonite*. The Geological Society of London. Vol. 157, 131-142
51. Thornton, S.F., Bright, M.I., Lerner, D.N. & Tellam, J.H. (1999). *The geochemical engineering of landfill liners for active containment*. The Geological Society of London. Vol. 157, 143-157
52. Tan, H.K. (1993). *Principle of Soil Chemistry*. Marcel Dekker, Inc, 2nd Ed., NY, USA
53. Vali, H. & Hesse, R. (1990). *Alkylammonium ion treatment of clay minerals in ultrathin section: A new method for HRTEM examination of expandable layers*. American Mineralogist, Vol. 75, 1443-1446
54. Vali, H., Hesse, R. & Martin, F.R. (1994). *A TEM-based definition of 2:1 layer silicates and their interstratified constituents*. American Mineralogist, Vol. 75, 644-653

55. Webber, T. & Williams, M. (1993) *Construction of low permeability soil-bentonite barrier caps and liner for landfills*. Pyramid Environmental, Highpoint, USA
56. Willis, J.P. (1999). *Instrumental parameter and data quality for routine major and trace element determinations by WDXRFs*. Department of Geological Science, University of Cape Town, South Africa
57. Waldron, M. (2008). *SEM, Scanning Electron Microscopy*, [Personnel Consultations]. Department of Physics, University of Cape Town
58. Wise, (2008), [Personal Communication], Jeffares and Green Consulting Engineers, Pinelands, Cape Town
59. Williams, D.G., Skipper, T.N., Smalley, V.M, & Soper, K.A. (1996). *Structure of Alkylammonium solutions in vermiculite clays*. Faraday Discuss, No. 104, 296-306
60. Website: Scintag Inc. *Basics of X-Ray Diffraction* [Online] Available: www.scintag.com. [25 October 2006]
61. Yildiz, N., Aktas, Z., Calimli, A. (2004). *Sulphuric acid activation of a Calcium Bentonite*. Particulate Science and Technology, No. 22, 21-33
62. Young Jo, H., Benson, H.C. & Edil, B.T. (2006). *Rate-limited cation exchange in thin bentonitic barrier layers*. Canadian Geotech Journal, Vol. 43 370-391

List of Appendices

- A. Typical data recording sheet for Permeability tests (Geotechnical Engineering Laboratory, University of Cape Town)
- B. Typical sand/bentonite mix calculation sheet (Geotechnical Engineering Laboratory, University of Cape Town)
- C. Mastersizer grain sheet analysis sheet (Department of Chemical Engineering, University of Cape Town)
- D. Typical X- Ray diffraction pattern result sheet (Department of Geological Sciences, University of Cape Town)
- E. Typical results of Coefficient of Permeability Graphs of Philippi Dune Sand/Envirobent mixes and Klipheuwel Sand/Heidelberg Raw Bentonite mixes